EXPLORING FLAVOR ENHANCER METABOLITES OF CHAYA LEAVES *Cnidoscolus* spp.

Mr. Nuti Hutasingh

จุฬาลงกรณ์มหาวิทยาลัย
CHULALONGKORN UNIVERSITY

A Dissertation Submitted in Partial Fulfillment of the Requirements
for the Degree of Doctor of Philosophy in Food Technology
Department of Food Technology
FACULTY OF SCIENCE
Chulalongkorn University
Academic Year 2022

การสำรวจเมแทบอไลต์ที่มีสมบัติเสริมกลิ่นรสของใบชายา *Cnidoscolus* spp.

นายนุติ หุตะสิงห

วิทยานิพนธ์นี้เป็นส่วนหนึ่งของการศึกษาตามหลักสูตรปริญญาวิทยาศาสตรดุษฎีบัณฑิต
สาขาวิชาเทคโนโลยีทางอาหาร ภาควิชาเทคโนโลยีทางอาหาร
คณะวิทยาศาสตร์ จุฬาลงกรณ์มหาวิทยาลัย
ปีการศึกษา 2565

Thesis Title	EXPLORING FLAVOR ENHANCER METABOLITES OF CHAYA LEAVES *Cnidoscolus* spp.
By	Mr. Nuti Hutasingh
Field of Study	Food Technology
Thesis Advisor	Professor UBONRATANA SIRIPATRAWAN, Ph.D.

Accepted by the FACULTY OF SCIENCE, Chulalongkorn University in Partial Fulfillment of the Requirement for the Doctor of Philosophy

-- Dean of the FACULTY OF SCIENCE

(Professor POLKIT SANGVANICH, Ph.D.)

DISSERTATION COMMITTEE

-- Chairman

(Assistant Professor Romanee Sanguandeekul, Ph.D.)

-- Thesis Advisor

(Professor UBONRATANA SIRIPATRAWAN, Ph.D.)

-- Examiner

(Associate Professor KANITHA TANANUWONG, Ph.D.)

-- Examiner

(Associate Professor CHALEEDA BOROMPICHAICHARTKUL, Ph.D.)

-- Examiner

(Assistant Professor NATTIDA CHOTECHUANG, Ph.D.)

จุฬาลงกรณ์มหาวิทยาลัย

CHULALONGKORN UNIVERSITY

นุติ หุตะสิงห : การสำรวจเมแทบอไลต์ที่มีสมบัติเสริมกลิ่นรสของใบชายา *Cnidoscolus* spp.. (
EXPLORING FLAVOR ENHANCER METABOLITES OF CHAYA LEAVES
Cnidoscolus spp.) อ.ที่ปรึกษาหลัก : ศ. ดร.อุบลรัตน์ สิริภัทราวรรณ

รสอูมามิให้รสชาติคล้ายน้ำต้มกระดูก มีสมบัติเสริมกลิ่นรสของอาหารโดยส่งผลให้การยอมรับอาหารโดยรวมดีขึ้น ดังนั้นรส
อูมามิจึงเป็นหนึ่งในปัจจัยสำคัญในการพัฒนาผลิตภัณฑ์อาหารคาวให้เป็นที่ยอมรับของผู้บริโภค แหล่งของรสอูมามิที่ใช้กันอย่างแพร่หลาย
ในอุตสาหกรรมอาหารคือโมโนโซเดียมกลูตาเมต (MSG) หรือผงชูรส อย่างไรก็ตามผู้บริโภคจำนวนมากมีทัศนคติเชิงลบต่อสารนี้
ดังนั้นการหาวัตถุดิบธรรมชาติที่ให้รสอูมามิ เพื่อทดแทนการใช้ผงชูรสจึงมีศักยภาพในเชิงพาณิชย์ ต้นชายา (*Cnidoscolus* spp.*)*
เป็นพืชยืนต้นที่โตเร็วและทนแล้ง ในปัจจุบันใบของต้นชายาถูกนำมาทำแห้งและจำหน่ายเพื่อใช้ในการเสริมรสอูมามิและชูรสชาติให้กับ
อาหาร แต่อย่างไรก็ตามยังไม่มีการรายงานถึงสารหลักที่ให้รสอูมามิในใบชายา ดังนั้นงานวิจัยนี้จึงมีวัตถุประสงค์เพื่อระบุสารที่ให้รสอูมามิ
และศึกษาผลของวิธีการทำแห้งต่อสารให้กลิ่นรสในใบชายา ในการสำรวจสารประกอบที่เกี่ยวข้องกับรสอูมามิในใบของชายาสองสปีชีส์
(*Cnidoscolus chayamansa* และ C. *aconitifolius*) ผู้วิจัยใช้วิธีการทางเมตาโบโลมิกส์แบบหลายแพลตฟอร์มโดยไม่
ระบุสารเป้าหมาย ลิ้นอิเล็กทรอนิกส์ และการคัดกรองด้วยการจำลองการจับกันของโมเลกุลเชิงคอมพิวเตอร์ พบว่าเมตาโบไลต์ชนิดต่าง ๆ
มีปริมาณที่แตกต่างกันระหว่างสปีชีส์และระยะการเจริญของใบ ผลการทดลองโดยลิ้นอิเล็กทรอนิกส์พบว่าใบระยะอ่อนมีความเข้มข้นของ
รสอูมามิสูงที่สุด รองลงมาคือใบระยะโตเต็มที่ และใบระยะแก่ตามลำดับ (p < 0.05) ผลการวิเคราะห์ด้วยสมการถดถอยกำลังสองน้อย
ที่สุดบางส่วนร่วมกับการจำลองการจับกันของโมเลกุลเชิงคอมพิวเตอร์พบสารในใบชายาที่ให้รสอูมามิที่ยังไม่มีการรายงานทั้งหมดห้าชนิด
ได้แก่ กรดควินิก, ไตรโกเนลลีน, อะลานิลไทโรซีน, ลิวซิลไกลซิลโพรลีน และลิวซิลแอสปาร์ติกลูตามีน และสารประกอบอูมามิที่มี
รายงานแล้ว ได้แก่ กรดกลูตามิก, กรดไพโรกลูตามิก และ 5'-อะดีโนซีนโมโนฟอสเฟต เมื่อยืนยันรสชาติของสารละลายของสารบริสุทธิ์
เหล่านั้นด้วยลิ้นอิเล็กทรอนิกส์พบว่าสารอูมามิที่ยังไม่เคยมีรายงานดังกล่าวเป็นสารให้รสอูมามิชนิดใหม่ มากไปกว่านั้นยังพบว่าลิวซิลไกล
ซิลโพรลีนมีสมบัติเสริมรสอูมามิแบบทวีคูณร่วมกันกับ MSG โดยทั่วไปแล้ว การทำแห้งส่งผลให้กลิ่นรสของวัตถุดิบอาหารมีการ
เปลี่ยนแปลง เมื่อประเมินผลของวิธีการทำแห้ง ได้แก่ การทำแห้งแบบแช่เยือกแข็ง (FD) การทำแห้งแบบสุญญากาศ การให้แห้งด้วย
ตู้อบลมร้อนที่อุณหภูมิ 50°C และ 120°C (OD120) และการคั่วในกระทะ (PR) ต่อการเปลี่ยนแปลงของสารประกอบที่ระเหย
ได้ และระเหยไม่ได้ด้วยวิธีการทางเมตาโบโลมิกส์ ความเข้มของรสอูมามิ และสมบัติต้านอนุมูลอิสระของใบชายาระยะอ่อนและใบระยะโต
เต็มที่ พบว่า 3-methylbutanal (กลิ่นคล้ายมอลต์) เป็นสารประกอบที่ระเหยได้ที่มีค่า relative odor active value
(rOAV) สูงที่สุดในทุกกลุ่มตัวอย่าง ในขณะที่ hexanal (กลิ่นคล้ายหญ้าตัดใหม่) และ 2-methylbutanal (กลิ่นคล้ายเมล็ด
กาแฟคั่ว) มีค่า rOAV สูงเป็นอันดับที่สองในกลุ่มตัวอย่างที่ทำแห้งด้วย FD และ PR ตามลำดับ ส่วนตัวอย่างที่ทำแห้งด้วย
OD120 และ PR มีปริมาณของกรดอะมิโนที่ให้รสอูมามิและ 5'-ไรโบนิวคลีโอไทด์ และความเข้มของรสอูมามิสูงที่สุด (p <
0.05) ในขณะที่ตัวอย่างที่ทำแห้งด้วย FD มีสมบัติต้านอนุมูลอิสระสูงสุด (p < 0.05) ผลการทดลองจากงานวิจัยนี้เป็นหลักฐานทาง
ทฤษฎีที่สำคัญสำหรับการผลิตและการประยุกต์ใช้ใบชายาเพื่อใช้เป็นเครื่องปรุงรสอูมามิจากแหล่งธรรมชาติในผลิตภัณฑ์อาหารต่อไป
นอกจากนี้การศึกษานี้ยังสามารถใช้เป็นต้นแบบเพื่อใช้ศึกษาสารให้รสอูมามิในวัตถุดิบอาหารอื่น ๆ ได้อีกด้วย

สาขาวิชา	เทคโนโลยีทางอาหาร	ลายมือชื่อนิสิต	....
ปีการศึกษา	2565	ลายมือชื่อ อ.ที่ปรึกษาหลัก	....

Nuti Hutasingh : EXPLORING FLAVOR ENHANCER METABOLITES OF CHAYA LEAVES *Cnidoscolus* spp.. Advisor: Prof. UBONRATANA SIRIPATRAWAN, Ph.D.

Umami, described as brothy and meat-like flavor, is one of the key factors in the successful savory food product development. It acts as a taste enhancer and improves overall acceptability. Monosodium glutamate (MSG) is the most common synthetic compound added to savory providing umami taste. Many consumers, however, have a negative attitude toward this substance. Thus, natural ingredients providing umami taste as a substitute for MSG could be beneficial for commercial purposes. Chaya (*Cnidoscolus* spp.) is a fast-growing and drought-resistant plant whose leaves have been widely used as a dried umami seasoning. However, the key umami substances in the leaves have not been reported. Therefore, this research aims to identify key umami compounds and to study the effects of drying methods on flavor-related substances of the chaya leaves. To explore umami-related compounds in the leaves of two species (*Cnidoscolus chayamansa* and C. *aconitifolius*), we used a multiplatform untargeted metabolomics approach, electronic tongue, and *in silico* screening. The profile of nonvolatile metabolites varied between leaves of the two species and between leaf maturity stages. Young leaves exhibited the highest umami taste intensity, followed by mature and old leaves ($p < 0.05$). Partial least squares regression and computational molecular docking analyzes revealed five potent umami substances (quinic acid, trigonelline, alanyl-tyrosine, leucyl-glycyl-proline, and leucyl-aspartyl-glutamine) and three known umami compounds (L-glutamic acid, pyroglutamic acid, and 5'-adenosine monophosphate). The five substances were validated as novel umami compounds using an electronic tongue assay; leucyl-glycyl-proline showed synergistic effects with monosodium glutamate, enhancing the umami taste. Thus, substances contributing to the taste of chaya leaves were successfully identified, and the leaf maturation stages possessing higher umami intensity (young and mature leaves) were selected for the next study. Drying, in general, results in changes of flavor of food ingredients. Hence, the effects of different drying methods [freeze drying (FD), vacuum drying, oven drying at 50°C and 120°C (OD120), and pan roasting (PR)] on volatile and nonvolatile metabolites, umami intensity, and antioxidant properties of the young and mature chaya leaf mixture were investigated. The predominant volatile compound among all samples are aldehydes. 3-methylbutanal (malt-like odor) had the highest relative odor activity value (rOAV), while hexanal (green grass-like odor) and 2-methylbutanal (coffee-like odor) had the second highest rOAV in the FD and PR samples, respectively. The OD120 and PR samples possessed the highest concentration of umami-tasting amino acids and 5'-ribonucleotides as well as the most intense umami taste ($p < 0.05$), whereas FD samples exhibited the highest antioxidant capacity ($p < 0.05$). Ultimately, the findings contribute to fundamental knowledge and theoretical evidence for the production and use of dried chaya leaves as a natural umami flavoring. In addition, this study can be used as a model to identify key umami substances in other food ingredients.

Field of Study:	Food Technology	Student's Signature	
Academic Year:	2022	Advisor's Signature	

ACKNOWLEDGEMENTS

First of all, I would like to express my sincere gratitude to my advisor Profesor Dr. Ubonrat Siripatrawan, for her continuous support of my doctoral studies and related research, her patience, motivation and immense knowledge. Her guidance has helped me throughout the research and writing of this thesis. I could not have imagined a better advisor and mentor for my doctoral studies.

In addition to my advisor, I would also like to thank the rest of my dissertation committee: Assistant Professor Dr. Romanee Sanguandeekul, Associate Professor Dr. Kanitha Tananuwong, Associate Professor Dr. Chaleeda Borompichaichartkul and Assistant Professor Dr. Natthida Chotechuang, for their insightful comments and encouragement, as well as the difficult questions that stimulated me to expand my research from different perspectives.

My sincere gratitude also goes to Professor Dr. Supaart Sirikantaramas, Department of Biochemistry, Faculty of Science, Chulalongkorn University who gave me the opportunity to join his research team and granted me access to the laboratory and research facilities. Without their valuable support, it would not have been possible to conduct this research.

Special thanks to Assistant Professor Dr. Nat Tansrisawad and his colleague Mrs. Apinya Tubtimrattana, Department of Forensic Medicine, Faculty of Medicine, Chulalongkorn University, King Chulalongkorn Memorial Hospital, The Thai Red Cross Society, Bangkok, Thailand, who gave access to their research department, invaluable advice, technical support, and patience during my research.

I thank my laboratory colleagues for the stimulating discussions and for all the wonderful memories we had during the last three years.

In particular, I would also like to acknowledge the Second Century Fund (C2F) and the 90th Anniversary of Chulalongkorn University Fund under the

Last but not least, I would like to thank my family for supporting me spiritually during the writing of this thesis and in my life in general.

Nuti Hutasingh

จุฬาลงกรณ์มหาวิทยาลัย
CHULALONGKORN UNIVERSITY

TABLE OF CONTENTS

Page

จุฬาลงกรณ์มหาวิทยาลัย

CHULALONGKORN UNIVERSITY

LIST OF TABLES

LIST OF FIGURES

LIST OF ABBREVIATIONS

3Y	Young leaves of *C. chayamansa* (three-lobed leaf)
3M	Mature leaves of *C. chayamansa* (three-lobed leaf)
3O	Old leaves of *C. chayamansa* (three-lobed leaf)
5Y	Young leaves of *C. aconitifolius* (five-lobed leaf)
5M	Mature leaves of *C. aconitifolius* (five-lobed leaf)
5O	Old leaves of *C. aconitifolius* (five-lobed leaf)
MSG	Monosodium glutamate
5'-AMP	5'-Adenosine monophosphate
5'-GMP	5'-Guanosine monophosphate
PCA	Principle component analysis
PLSR	Partial least square regression
UHPLC–qTOF/MS	Ultra-high performance liquid chromatography–quadrupole time-of-flight mass spectrometry
GC–MS	Gas chromatography–mass spectrometry
HCTUltra/LC–MS	High-capacity ultra-ion trap liquid chromatography mass spectrometry
HS-GC/MS	Headspace gas chromatography/mass spectrometry
EUC	Equivalent umami concentration
AY	Alanyl-tyrosine
LGP	Leucyl-glycyl-proline
LDQ	Leucyl-aspartyl-glutamine
VIP	Variable importance in projection
GSH	Glutathione
FD	Freeze drying
VD	Vacuum Drying
OD50	Oven drying at 50°C
OD120	Oven drying at 120°C
PR	Pan roasting
OAV	Odor active value
TPC	Total phenolic content
DPPH	1,1-Diphenyl-2-picrylhydrazyl
FRAP	Ferric Reducing Antioxidant Power Assay

CHAPTER I
INTRODUCTION

1.1 Background, motivation and linking of the study

Umami taste is one of the key factors in food product development, especially in savory. It provides a brothy and meaty-like flavor, acts as flavor enhancer. Umami is exemplified by the L-glutamic acid, which has been extensively used in the food supply as a sodium salt (monosodium glutamate, MSG). However, an increase of health-awareness trends triggers the consumer's negative attitude towards synthetic MSG and consequently, food manufacturing seeks natural source alternatives. Even though the natural umami ingredients such as mushroom extract, tomato paste, or yeast extract, are rich in umami substances, the addition of these ingredients could alter the overall flavor of the food due to their own distinct flavor and consequently, could possibly reduce the overall consumer acceptability (Dermiki et al., 2015).

Chaya (*Cnidoscolus* spp.) is a fast-growing and drought resistant medicinal plant native to central America and its leaf is consumed as a protein-rich vegetable. The previous study reported that Chaya leaf has a high protein content (5.7%-7.4% w/w, wet basis) which is 2-3 times higher than most edible green leafy vegetables (Kuti & Torres, 1996). In Thailand, the leaves are commonly dried and ground into fine powder as a natural MSG substitute used in savory dishes. Unlike other natural umami-rich plants and fungus, fresh chaya leaves have an outstanding sensory property of not having a strong and distinct flavor, so they can be easily added to a variety of dishes to enhance the overall taste without altering the original flavor of the dishes (ECHO community, 2006; USAID, 2013). However, after drying, the dried leaves possess distinct aroma. As far as we know, there is still no theoretical knowledge about the umami taste intensity, key umami compounds, and the aroma characteristics of chaya leaves.

As for umami-tasing compounds, in addition to L-glutamic acid, there are several compounds that have been reported the contribution of umami taste such as free

L-aspartic acid, ribonucleotides, organic acids and some small peptides containing acidic amino acids and etc. Umami perception can be synergistic or suppressive as affected by different umami substances. The synergistic effect between glutamic acid and inosinic acid (1:1) was reported by Bellisle (1999) as the mixture produced 7-fold greater umami intensity compared with the intensity from glutamic acid alone. Moreover, the molecular structure of substance also affected the umami perception. Xue et al. (2009) reported that umami peptide might exhibit less umami intensity than the free L-glutamic acid since the larger and more complex molecules inhibit the peptide from accessing the umami taste receptor and, which could reduce the umami taste. Examples of umami peptide are Asp-Glu-Ser, Glu-Gly-Ser and Ser-Glu-Glu annotated in fish protein hydrolysate (Zhang et al., 2017). Identifying the key umami compounds present in food ingredients is therefore crucial in comprehending their potential interactions with other food components and during food processing. Since chaya leave is high in protein content, the hypothesis is that the key umami compounds are free amino acids and short peptides. Finally, the identification of key umami substance that contribute to the umami taste of the chaya leaves and the successful application of a multiplatform metabolomics approach implemented *in silico* technique and electronic tongue to explored and identified novel umami substance for plant-based foods, was demonstrated. The study is presented in Chapter II, which was published in *Food Chemistry*.

Dried Chaya leaf powder, in Thailand, has been commercialized as umami seasoning powder and an alternative caffeine-free tea infusion. The common drying method used for manufacturing the dried leaf are pan roasting, oven-dried at low temperature (50-60 ºC) and oven-dried at high temperature (>100 ºC). Drying is a common way to extend the shelf life of food or plant samples and is beneficial in terms of logistical point of view. Several studies have shown that drying can affect the content of flavor components including volatile and non-volatile compounds which determine the product quality and consumer preference to a great extent (Zhang et al., 2021). Li et al. (2015) studied the effects of several drying methods on the taste-active compounds of *Pleurotus*

eryngii and found that hot air drying could increase the content of umami tasting components such as free amino acid due to protein degradation. While Shen et al. (2023) reported that freeze drying process provides *Oudemansiella raphanipes* the highest content of umami nucleotides, while oven drying rise cyclic sulfur-containing volatiles generated from nonenzymatic reaction. Based on our finding from the first study reporting that L-glutamic acid, 5'-adenosine monophosphate (5'-AMP) and other short peptides are key umami compounds in Chaya leaf, it is assumed that oven drying could promote the increasing of free amino acids, umami taste intensity and cyclic volatiles.

Thus, the effect of different drying methods on the volatile and nonvolatile metabolites concentration, umami taste intensity and antioxidant activities were comprehensively investigated and is presented in Chapter III as submitted manuscript to *Food Chemistry*.

Ultimately, this research will provide an insight regarding metabolites found in Chaya leaf including amino acid, sugar, organic acid, flavonoid, and flavor enhancer-related compounds, between cultivars and among maturation stages. Moreover, the impact of drying methods on umami-tasing compounds and volatiles could provide a theoretical insight and benefit to the food industry. All these findings could be a knowledge foundation promoting the development of superior savoury plant-based food products shifting towards natural claims.

1.2 Objectives of research

1) to explore and identify the key umami substances in Chaya leaves
2) to investigate the effect of different drying methods on volatile and nonvolatile metabolites, umami taste intensity and antioxidant in Chaya leaves.

1.3 Scope of the study

This research contains two sections.

1) The exploration of key umami substance was conducted with two chaya species: 3-lobed leaf (*Cnidoscolus chayamansa*) and 5-lobed leaf (*Cnidoscolus aconitifolius*) with three leaf maturation stages: Young (Y), mature (M), and old (O) leaf (3 x 2 treatment). Three analytical platforms were used to capture and relatively quantify the non-volatile metabolites, including GC–MS, ultra-high performance liquid chromatography–quadrupole time-of-flight mass spectrometry (UHPLC–qTOF/MS), and high-capacity ultra-ion trap LC–MS (HCTUltra/LC–MS). Umami taste intensity of the leaf samples were conducted using electronic tongue and the stability of candidate umami compounds on human umami taste receptor were predicted using in silico method (computational molecular docking).

2) The effects of five different drying methods including freeze drying, vacuum drying, oven drying at 50 °C, oven drying at 120 °C and pan roasting, on volatile and nonvolatile metabolite, umami taste intensity and antioxidant activities of chaya leaf were determined. The mixture of young and mature leaves of the 3-lobed leaf species (*Cnidoscolus chayamansa*) were used in this study. Two analytical platforms were used to capture and quantify the non-volatile metabolites, including GC–MS and UHPLC–qTOF/MS. Umami taste intensity of the leaf samples were conducted using electronic tongue.

1.4 Benefits of this study

1) The key and novel umami substances in Chaya leaf were explored. Thus, the parameter of corresponding food processing used to produce chaya leaf product could be adjusted according to the nature of each compound. For example, the heat treatment (e.g., blanching) could be adjusted to increase the concentration of umami substances (e.g., 5'-AMP and 5'-GMP) by the activation of phosphodiesterase enzyme.

2) A multiplatform metabolomics approach, combined with *in silico* techniques, was successfully applied to screen plant samples for umami compounds that can be utilized as novel ingredients for plant-based foods. The findings of this research can be applied to other food or food ingredients and have significant implications for the development of new and innovative food products.

3) The study investigated the effects of different drying methods on the flavor compounds present in Chaya leaf. The successful outcome of this research can lead to the development of dried Chaya leaf powder with high umami taste intensity, which can be used as a natural ingredient to enhance the acceptability of savory food products. Additionally, the findings of this study can provide theoretical evidence for the manufacturing of dried Chaya leaf and serve as a foundation for future research in this field.

CHAPTER II
MANUSCRIPT I

Metabolite Profiling and Identification of Novel Umami Compounds in the Chaya Leaves of Two Species using Multiplatform Metabolomics

Nuti HUTASINGH [a], Hathaichanok CHUNTAKARUK [b, c], Apinya TUBTIMRATTANA [d], Yanisa KETNGAMKUM [e], Putthamas PEWLONG [f], Narumon PHAONAKROP [g], Sittiruk ROYTRAKUL [g], Thanyada RUNGROTMONGKOL [b, c], Atchara PAEMANEE [e], Nat TANSRISAWAD [h], Ubonrat SIRIPATRAWAN [a, *], Supaart SIRIKANTARAMAS [f, *]

[a] Department of Food Technology, Faculty of Science, Chulalongkorn University, Bangkok, Thailand

[b] Center of Excellence in Biocatalyst and Sustainable Biotechnology, Department of Biochemistry, Faculty of Science, Chulalongkorn University, Bangkok, Thailand

[c] Program in Bioinformatics and Computational Biology, Graduate School, Chulalongkorn University, Bangkok 10330, Thailand

[d] Department of Forensic Medicine, King Chulalongkorn Memorial Hospital, The Thai Red Cross Society, Bangkok, Thailand

[e] National Omics Center, National Science and Technology Development Agency (NSTDA), Pathum Thani, Thailand

[f] Center of Excellence for Molecular Crop, Department of Biochemistry, Faculty of Science, Chulalongkorn University, Bangkok, Thailand

[g] National Center for Genetic Engineering and Biotechnology (BIOTEC), National Science and Technology Development Agency, Pathum Thani, Thailand

[h] Department of Forensic Medicine, Faculty of Medicine, Chulalongkorn University, Bangkok, Thailand

* Corresponding authors
Ubonrat SIRIPATRAWAN: Department of Food Technology, Faculty of Science, Chulalongkorn University, Bangkok, Thailand; email: Ubonratana.S@chula.ac.th
Supaart SIRIKANTARAMAS: Center of Excellence for Molecular Crop, Department of Biochemistry, Faculty of Science, Chulalongkorn University, Bangkok, Thailand; email: Supaart.s@chula.ac.th

_____

Cite: Hutasingh, N., Chuntakaruk, H., Tubtimrattana, A., Ketngamkum, Y., Pewlong, P., Phaonakrop, N., Roytrakul, S., Rungrotmongkol, T., Paemanee, A., Tansrisawad, N., Siripatrawan, U. & Sirikantaramas, S. (2023). Metabolite profiling and identification of novel umami compounds in the chaya leaves of two species using multiplatform metabolomics, *Food Chemistry,* 404, 134564. https://doi.org/10.1016/j.foodchem.2022.134564

Highlights

- Metabolite variation in two species of chaya leaves was described
- Young chaya leaves exhibited high umami taste intensity
- L-glutamic acid and 5′-adenosine monophosphate accumulated in young leaves
- Quinic acid, trigonelline, and other small peptides are novel umami compounds

Abstract

Chaya (*Cnidoscolus chayamansa* and *C. aconitifolius*) is a fast-growing medicinal plant, and its leaves exhibit a strong umami taste. Here metabolite variation and umami-related compounds in the leaves of two chaya species were determined using a multiplatform untargeted-metabolomics approach, electronic tongue, and *in silico* screening. Metabolite profiles varied between the leaves of the two species and among leaf maturation stages. Young leaves exhibited the highest umami taste intensity, followed by mature and old leaves. Partial least square regression and computational molecular docking analyses revealed five potent umami substances (quinic acid, trigonelline, alanyl–tyrosine, leucyl–glycyl–proline, and leucyl–aspartyl–glutamine) and three known umami compounds (L-glutamic acid, pyroglutamic acid, and 5′-adenosine monophosphate). The five substances were validated as novel umami compounds using electronic tongue assay; leucyl–glycyl–proline exhibited synergism with monosodium glutamate, thereby enhancing the umami taste. Thus, substances contributing to the taste of chaya leaves were successfully identified.

Chemical compounds

Formic acid (PubChem CID: 284), L-glutamic acid (PubChem CID: 33032), adenosine 5′-monophosphate (AMP) (PubChem CID: 6083), Puerarin (PubChem CID: 5281807), Alanyl–tyrosine (PubChem CID: 572319), Leucyl–aspartyl–glutamine (PubChem CID: 71464619), Leucyl–glycyl–

proline (PubChem CID: 439585), monosodium glutamate (PubChem CID: 23672308), Trigonelline (PubChem CID: 5570), quinic acid (PubChem CID: 6508), L-pyroglutamic acid (PubChem CID: 7405), Gallic acid (PubChem CID: 370)

2.1 Introduction

Umami, a savory and meaty flavor, is one of the basic five tastes, the others being sourness, sweetness, bitterness, and saltiness. Monosodium glutamate (MSG) and 5′-ribonucleotide are key umami compounds added to savory products to improve the sensory quality and overall acceptability of the latter (Dermiki et al., 2013). Despite these benefits, the addition of MSG to food products remains controversial in several cultures. Many consumers have a negative attitude toward MSG as a food additive based on reports that MSG causes headaches, sweating, abdominal pain, and urticaria within a few hours of consumption (Bawarskar et al., 2017). Hence, using natural taste-enhancing substances is a promising approach to improve the palatability of foods, as successfully demonstrated by several studies (Wang et al., 2019; Matter et al., 2018). However, to the best of our knowledge, there has been no research addressing the presence of taste-enhancing substances in leafy green vegetables.

Chaya or tree spinach (*Cnidoscolus* spp.) is native to Central America. It is a medicinal plant, and its leaves exhibit therapeutic effects against diabetes, rheumatism, gastrointestinal disorders, and inflammation (Moura et al., 2018). The chaya tree is commonly found in Thai households and is considered a protein-rich vegetable as its leaves contain two to three times more protein than most other edible leafy green vegetables (Kuti & Torres, 1999). Additional benefits of the plant include its rapid growth and drought resistance (Rodrigues et al., 2020). Although raw chaya leaves contain the toxic substance linamarin, a cyanogenic glycoside, the total cyanogen content of fresh leaves is 0.17–2.89 µg hydrogen cyanide (HCN)/g (Kuti & Konuru, 2006; Kongphapa et al., 2021), which is considerably lower than the accepted

safe level in food as recommended by the World Health Organization (10 μg HCN equivalents/g fresh weight). Accordingly, the maximum amount of raw leaves of this plant that can be consumed per day is ~ 3 g. Cooking and other heat treatments, including drying methods, can eliminate up to 99% of these glycosides (Kuti & Konuru, 2006; Kongphapa et al., 2021). In Thailand, two species of chaya have been found: *C. chayamansa*, a nonflowering species with three-lobed leaves, and *C. aconitifolius*, a flowering species with five-lobed leaves. Chaya leaves are used as natural flavor enhancers in numerous dishes as they provide an umami taste without altering the original flavor. However, whether umami compounds accumulate in chaya leaves remains unknown.

The presence of umami compounds in foods or food materials is usually detected using sensory-guided fractionation via preparative chromatography. However, only a few samples can be analyzed via this method as it is time- and labor-intensive (Shiga et al., 2014). Metabolomics is a powerful high-throughput approach enabling the identification of diverse metabolites in numerous samples. Gas chromatography–mass spectrometry (GC–MS) and liquid chromatography–mass spectrometry (LC–MS) are primarily used in combination to accurately, precisely, and completely identify phenotype-related metabolites (Zeki et al., 2020). Each platform can detect different metabolite subsets. GC–MS, combined with derivatization, can detect small polar metabolites in primary metabolism. Accordingly, it has been used to assess relationships between metabolites and food quality, such as identifying key taste compounds in foods coupled with sensory evaluation (Shiga et al., 2014).

Several studies have investigated the binding interactions between taste compounds and taste receptors (Yu et al., 2021). Molecular docking is an effective tool for predicting peptides imparting an umami taste, while computer-aided receptor–ligand-binding analyses can be used to investigate the mechanism of such binding. The umami taste receptor is a class C G-protein coupled receptor (GPCR) with an affinity to L-glutamate and small

peptides. It is a heterodimer comprising the taste receptor type 1 member 1 (T1R1) and taste receptor type 1 member 3 (T1R3) subunits (Yu et al., 2021). *In silico* techniques have been successfully applied to screen and evaluate the binding mechanism of interesting compounds to the umami taste receptor (T1R1/T1R3) (Amin et al., 2020; Yu et al., 2021).

The present study aimed to investigate the flavor-related metabolites that contribute to the umami taste of the leaves of two chaya species found in Thailand using multiplatform metabolomic profiling coupled with electronic tongue assay. Three analytical platforms were used, including GC–MS, ultra-high performance liquid chromatography–quadrupole time-of-flight mass spectrometry (UHPLC–qTOF/MS), and high-capacity ultra-ion trap LC–MS (HCTUltra/LC–MS) for metabolite profiling. To select the potent umami compounds, partial least square regression (PLSR) analyses were conducted using metabolite data and umami taste intensity. Moreover, molecular docking was performed to understand the interactions between the candidate umami substances and homology models of the ligand-binding domain of T1R1/T1R3. To the best of our knowledge, this study is the first to profile metabolites in the chaya leaf and discover its umami-related metabolites. The results of the present study offer novel insights into the compounds that contribute to the umami taste of chaya leaves. Additionally, successful application of a multiplatform metabolomics approach and *in silico* technique to screen plant samples for umami compounds, which can be exploited as novel ingredients for plant-based foods, was demonstrated.

2.2. Materials and methods

2.2.1 Chemicals and plant materials

All internal standards, authentic standards, and organic solvents for GC–MS, UHPLC–qTOF/MS, and HCTUltra/LC–MS were purchased from Sigma-Aldrich (St. Louis, MO, USA). The peptides alanyl–tyrosine (Ala–Tyr, AY),

leucyl–glycyl–proline (Leu–Gly–Pro, LGP), and leucyl–aspartyl–glutamine (Leu–Asp–Gln, LDQ) were synthesized via solid-phase synthesis (Bankpeptide Inc., Hefei, China) with more than 95% purity. Two species of 10-month-old chaya plants (*Cnidoscolus* spp.) approximately 150–170 cm tall (Figure A1, Appendix A) were collected from the Krathum Baen District, Samut Sakhorn Province, Thailand. Chaya leaves were collected at different stages of maturity, with four biological replicates per species. Young (Y), mature (M), and old (O) leaves of both the species were collected in October 2021, per the leaf order counted from the apical bud: $1^{st}–2^{nd}$, $4^{th}–6^{th}$, and $10^{th}–12^{th}$, respectively (Figure A2, Appendix A). In total, six leaf samples were used in this study: three-lobed *C. chayamansa* leaves (3Y, 3M, and 3O) and five-lobed *C. aconitifolius* leaves (5Y, 5M, and 5O). The leaves were immediately frozen in liquid nitrogen, freeze-dried for at least 48 h, and ground into a fine powder using mixer mills at 1000 Hz for 30 s.

2.2.2 Evaluation of umami taste intensity using an electronic tongue

Following the method of Hayashi et al. (2008) with some modifications, 2 g of dried chaya leaf samples were boiled with 200 mL of ultrapure water for 5 min, and the solutions were filtered immediately using a filter paper. Aliquots were then cooled to ambient temperature (~25°C) in an ice–water bath. Poly(vinylpolypyrrolidone) (2 g) was added to a 100 mL aliquot for polyphenol removal, which can interfere with the measurement of umami intensity. The mixtures were shaken every 20 min for 60 min and filtered through a filter paper. The collected filtrate was used for taste measurements.

To evaluate the umami taste intensity of potent umami compounds, such as quinic acid, trigonelline, AY, LGP, LDQ, L-glutamic acid, pyroglutamic acid, and 5′-adenosine monophosphate (5′-AMP), 1.5 mM of each compound was dissolved in 10 mM KCl (a tasteless solution). To evaluate the synergism among the potent umami compounds, binary mixtures were prepared from 0.75 mM MSG and 0.75 mM solutions of the potent umami compounds. The

potent umami solution was adjusted to a pH~7 using NaOH. The samples were measured using TS-5000Z taste sensing system (Intelligent Sensor Technology, Inc., Kanagawa, Japan) fitted with an umami taste sensor probe (SB2AAE) and a reference probe. The samples were analyzed using the probe, and the membrane electric potentials were stabilized in standard solutions. The sample measurements were averaged across four values. A standard curve demonstrating the relationship between the MSG concentration and umami taste intensity response was constructed to convert the umami intensity value obtained from the electronic tongue into MSG equivalents (Figure A3, Appendix A). The MSG equivalent of each sample was subsequently interpolated.

2.2.3 GC–MS analysis

Extraction was performed according to the method of Rosado-Souza et al. (2019), with minor modifications. Briefly, the extraction solvent comprised 50% methanol and 0.015 mg/mL $^{13}C_6$ sorbitol as an internal standard. Freeze-dried leaf powder (10 mg) was added to 800 µL of the extraction solvent. The samples were agitated at 500 rpm for 1 h at 25°C using a shaking incubator (Eppendorf, Germany). Then, 800 µL of chloroform was added to the samples and vortexed for 30 s followed by centrifugation at 3000 g for 3 min. Next, 200 µL of the supernatant was concentrated using a centrifuge vacuum concentrator at 25°C for 3 h till the solvent was completely evaporated. For derivatization, methoxyamine hydrochloride was solubilized with pyridine (20 mg/mL, 50 µL) and added to the freeze-dried sample, and oxime formation was performed at 30°C for 90 min. Subsequently, 100 µL N-methyl-N-(trimethylsilyl) trifluoroacetamide (MSTFA, GL Sciences, Japan) was added, and trimethylsilylation was performed at 37°C for 30 min.

Derivatized samples were analyzed via GC–MS. GCMS-QP2020 NX (Shimadzu Corp., Kyoto, Japan) equipped with an SH-Rxi-5Sil MS capillary column (0.25 µm df × 0.25 mm I.D. × 30 m) NX (Shimadzu Corp., Kyoto,

Japan) was used for compound separation and spectra identification. Helium gas was used as a carrier with 24.0 and 1 mL/min total and column flow rates, respectively. The derivatized samples were injected at 0.2 μL using the split mode, with a split ratio of 1:20. Mass spectra were obtained by electron ionization at 70 eV. The column oven temperature was set at 60°C (held for 3 min) and increased at a rate of 8°C/min till it reached 280°C. The injection, ion source, and interface temperatures were set at 250°C. The acquisition mode was SCAN mode (45–700 m/z). The scan speed was 2500 amu/s, event time was 0.30 s, and detector gain was 0.79 kV + 0.00 kV.

2.2.4 UHPLC–qTOF/MS analysis

The extraction procedure was performed according to the GC–MS analysis, but 0.2 ppm of puerarin in the extraction solvent was used as the internal standard. Then, 0.5 mL of the supernatant was filtered through a 0.22-μm microfilter before being placed in a glass vial.

The samples were separated in a C18(2) Luna column (100 mm × 2 mm × 2.5 μm) (Phenomenex, Torrance, CA, USA), with the column temperature maintained at 40°C. A mixture comprising solvents A (water and 0.1% formic acid) and B (acetonitrile and 0.1% formic acid) was used with a flow rate of 0.3 mL/min. gradients were started at 0% B for 5 min, then increased to 20% B over 3 min (held for 4 min), increased to 25% B over 1 min (held for 4 min), and increased to 50% B over 5 min, followed by a linear gradient to 95% B over 1 min (held for 7 min). The total acquisition time was 30 min. The injection volume was 1 μL, and the column temperature was maintained at 35°C throughout the analysis. Compounds were detected using qTOF/MS LCMS 9030 (Shimadzu Corp., Kyoto, Japan) equipped with an electrospray ionization source. The qTOF/MS scan and product ion scans were performed using the independent data acquisition mode. The MS conditions were as follows: positive-ion mode; collision energy, 35 eV; DL temperature, 250°C;

and a drying gas (N_2) flow of 10.0 L/min. The oven temperature was 40°C and mass spectra were acquired at 50–3000 m/z.

2.2.5 HCTUltra/LC–MS analysis

Dried chaya powder samples (100 mg) were added to 0.5% sodium dodecyl sulfate with a 1:1 volume ratio, vortexed for 60 min, and centrifuged at 10,000 *g* for 15 min. The supernatant was transferred into a new tube, mixed well with two volumes of cold acetone, and incubated overnight at −20°C. The mixture was centrifuged at 10,000 *g* for 15 min, and the supernatant was discarded. The pellet was protonated with 0.1% formic acid before injection into LC–MS/MS. The peptide samples were prepared for injection into Ultimate3000 Nano/Capillary LC System (Thermo Scientific, UK) coupled with HCTUltra/LC–MS system (Bruker Daltonics Ltd., Hamburg, Germany) equipped with a nanocaptive spray ion source. Briefly, 5 μL samples were enriched on a μ-Precolumn 300 μm I.D. × 5 mm C18 Pepmap 100, 5 μm, 100 A (Thermo Scientific, Loughborough, UK), separated on a 75 μm I.D. × 15 cm, and packed with Acclaim PepMap RSLC C18, 2 μm, 100 Å, nanoViper (Thermo Scientific, Loughborough, UK). The C18 column was enclosed with a thermostatted column oven and set to a temperature of 60°C. Solvents A and B were added to the analytical column, each containing 0.1% formic acid in water and 0.1% formic acid in 80% acetonitrile. A gradient of 5%–55% solvent B was used to elute the peptides at a constant flow rate of 0.30 μL/min for 30 min. Electrospray ionization was conducted at 1.6 kV using CaptiveSpray. Nitrogen was used as a drying gas with a flow rate of 50 l/h. Collision-induced-dissociation product ion mass spectra were obtained using nitrogen gas as the collision gas. Mass spectra and MS/MS were obtained in the positive-ion mode at 2 Hz at 150–2200 m/z. The collision energy was 10 eV.

2.2.6 Metabolome data processing

For GC–MS, peak identification was performed by matching the mass spectra with the NIST 17 database and confirmed using the retention indices of the eluted compounds based on a standard alkane mix (C10–C36) using LabSolutions GC–MS (ver. v.5.6) software. The retention indices of each compound were calculated based on the standard alkane mixture. Compounds were tentatively identified by comparing the retention indices and percentage of similarity of the mass spectra with the in-house reference library (>80%).

For UHPLC–qTOF untargeted-metabolomic analyses, raw data collected via mass spectrometry were converted into .mzml format using LabSolution software. MS-DIAL (RIKEN, v.4.16) and used for peak detection, MS^2 data deconvolution, peak alignment, MS/MS extraction, relative quantification, and metabolite annotation. Blank matrix samples were used for background subtraction in MS-DIAL. Database metabolites were initially annotated using a public metabolomics library (http://prime.psc.riken.jp/compms/msdial/main.html#MSP) containing 13,303 unique compounds. Finally, tentative and unknown peaks were further annotated with their elemental formulas and mass spectral fragmentation using MS-FINDER 2.0 (http://prime.psc.riken.jp/) (Lai et al., 2018). An MS tolerance of 0.01 Da and MS/MS tolerance of 0.05 Da were set as parameters for peak identification. The spectra were then normalized by adjusting the peak area with the puerarin concentration as an internal standard before further analyses.

For peptide quantification using HCTUltra/LC–MS, DeCyder MS Differential Analysis software (DeCyderMS, GE Healthcare) was used. The analyzed MS/MS data from DeCyderMS were submitted for a database search using Mascot software (Matrix Science, London, UK). Data were searched against the NCBI database for protein identification. Database interrogation comprised taxonomy (Euphorbiaceae), enzymes (no cleave), variable modifications (carbamidomethyl, oxidation of methionine residues), mass

values (monoisotopic), protein mass (unrestricted), peptide mass tolerance (1.2 Da), fragment mass tolerance (±0.6 Da), peptide charge state (1+, 2+, and 3+), and max missed cleavages. The peptide abundance in each sample was expressed as a log2 value, and the top 250 most abundant peptides were selected for PLSR. Before multivariate analysis, the analyzed metabolite matrices were exported to Microsoft Excel v.2020 (Microsoft Corp, USA) and normalized manually against the peak area of the internal standard.

2.2.7 Absolute quantification and equivalent umami concentration (EUC) calculation

The concentrations of L-glutamic acid and 5′-AMP in the samples assessed using electronic tongue assay were quantified. Standard curves were constructed from standard compounds (data not shown). The concentrations of L-glutamic acid and 5′-AMP used to construct the standard curve were between 0.00125 and 0.0125 mg/mL. Absolute quantification analysis was performed using a similar method, according to UHPLC–qTOF/MS methodology. Umami taste can be assessed based on the concentration of MSG measured using the EUC of the value (mg MSG/g), which corresponds to umami intensity. The synergistic effect between umami amino acids and 5′-nucleotides is represented by the following equation (Yamagushi, 1971):

$$Y = \Sigma a_i b_i + 1218\ (\Sigma a_i b_i)\ (\Sigma a_j b_j),$$

where Y is the EUC (%MSG equivalent), a_i (%) is the concentration of the respective umami amino acid (L-glutamic acid and L-aspartic acid), a_j (%) is the concentration of the respective umami 5′-nucleotide (5′-inosine monophosphate, 5′-guanosine monophosphate, 5′-xanthosine monophosphate, or 5′-AMP), b_i is the relative umami concentration for umami amino acids to MSG, and b_j is the relative umami concentration for umami 5′-nucleotides to 5′-inosine monophosphate.

2.2.8 Computational study of the binding of umami compounds to T1R1/T1R3

Molecular docking analysis was used to clarify the umami characteristics of the compounds (L-glutamic acid, quinic acid, pyroglutamic acid, trigonelline, 5′-AMP, phosphoric acid, biorobin, and rutin) and peptides (AY, LGP, LDQ, PLMEAL, GGLIIVML, MAIPCPPL, MIHVGKFSL, ACRQALSAINL, VDGLYGKNL, AFNPGHVHGF, and PPKVYFAL) using a T1R1/T1R3 model. In humans, the umami taste receptor is a GPCR with an affinity to L-glutamic acid. GPCR is a heterodimer comprising two chains with the "close–open" conformation reported in a study regarding the molecular docking of preferential agonist conformation, suggesting that T1R1 and T1R3 are in closed and open conformations, respectively (López Cascales et al., 2010). The three-dimensional (3D) structure of T1R1/T1R3 was predicted using AlphaFold2 software (https://deepmind.com/research/case-studies/alphafold) (Jumper et al., 2021) via the protein sequence of T1R1 (UniProtKB–Q7RTX1) and T1R3 (UniProtKB–Q7RTX0) (Uniprot consortium, 2021). Supplemental Figure A7, Appendix A shows the number of sequences per position, AlphaFold2 confidence measures, and all five models on the T1R1 and T1R3 targets. The highest percentages of correctly predicted interatomic distances were 86.46% and 87.62% for the predicted structure Model1 of T1R1 and T1R3, respectively. To build the human T1R1/T1R3 heterodimer for the docking study, Model1 of both proteins was superimposed on the crystal structure of the closed–open state of metabotropic glutamate receptor 1 (mGluR1)/L-glutamate complex (PDB: 1EWK (Kunishima et al., 2000)) using University of California at San Francisco (UCSF) Chimera package (https://www.cgl.ucsf.edu /chimera/) (Pettersen et al., 2004), and the crystal structure was then removed. The ionized states of T1R1/T1R3 and the peptides were configured at pH 7.0 using PROPKA3.1 (Olsson et al., 2011), whereas ChemAxon (Bhatt et al., 2019) was used to check the pKa value of the reference ligand bound to T1R1/T1R3, L-glutamic acid in its ionized form. L-glutamic acid (Nguyen et al., 2020) was docked into T1R1/T1R3 pocket sites for validating AutoDock VinaXB with the genetic algorithm (Eberhardt et

al., 2021) used in this study. The umami compounds and peptides were then individually docked into the binding site of the T1R1/T1R3 model (Figure A8, Appendix A). Their binding affinities were calculated and compared with L-glutamic acid. The 3D and 2D peptide–protein and ligand–protein binding interactions were visualized using UCSF Chimera package and Accelrys Discovery Studio 3.0 (Accelrys Inc.), respectively.

2.2.9 Statistical analysis

The umami taste intensity obtained via electronic tongue analyses is expressed as means ± standard deviation and was subjected to a one-way analysis of variance with Duncan's test using SPSS (25.0, IBM) software. For multivariate analyses, the normalized peak intensity of the metabolites from all analytical platforms was uploaded into multivariate software MetaboAnalyst 5.0 (Pang et al., 2021), which was subjected to cluster analyses, such as principal component analysis (PCA) and heat map analyses with Pareto scaling. PLSR was performed using SIMCA-P 14.1 (Umetrics, Umea, Sweden) to assess the relationships between umami taste intensity (response variable: y) and the concentrations of the annotated metabolites (explanatory variable: x). The number of PLS components was determined by computing the optimum number providing the lowest value of root mean square error of prediction with the SIMCA-P software algorithm. To investigate the contribution of metabolites to umami taste and select the candidate umami compounds, variable importance in projection (VIP) values were also calculated from the regression. All experiments were conducted with four biological replicates. At least three technical replicates were analyzed for the HCTUltra/LC–MS analysis and electronic tongue assay.

2.3 Results and Discussion

2.3.1 Electronic tongue analysis revealed umami response to be dependent on chaya leaf maturation

An electronic tongue surpasses subjective effects, unlike human sensory evaluation, and can be appropriately calibrated to achieve reliable consistency in the output (Kobayashi et al., 2010). Recently, studies have combined electronic tongue and sensory evaluations to assess the taste of food and pure compound solutions (Wang et al., 2021). The results of both the methods are highly consistent and correlated. Hence, the electronic tongue is a promising approach to evaluate tastes and could substitute sensory evaluations (Gao et al., 2021). First, the umami intensity in various chaya leaf extracts using the electronic tongue was evaluated. Based on Table 2.1, umami taste was significantly different across the leaf maturation stages ($p < 0.001$). The young leaves of both the species exhibited the highest umami response value, followed by the mature and old leaves. This result suggests that younger leaves near the apical bud highly accumulate umami substances.

Furthermore, when comparing the same maturation stage of the leaves of the two species, there were no significant differences in the umami response. The umami intensity of the young leaf was ~10, which is higher than that of the food products reported in other studies. Using the same evaluation method, the umami response of young chaya leaf powder solution (1 mg/mL) was higher than that of cooked pufferfish meat solution (1 mg/mL; umami intensity = 6.10) (Yang et al., 2019) and preserved egg yolk solution (1.4 mg/mL; umami intensity = 5.53) (Gao et al., 2021). This indicates that the chaya leaf extract investigated in this study has higher umami intensity than those animal-based extract evaluated by electronic tongue. In terms of the umami taste intensity of all the samples, 3Y and 5Y showed a %MSG equivalent concentration greater than the taste recognition threshold of MSG [1.38 mM or 0.02% (w/v)] (Webb et al., 2015). This indicates that in the aqueous extract of young and mature

chaya leaves (1 mg/mL), the umami taste can be recognized via the human gustatory sense. Consequently, multiplatform metabolomics, including UHPLC–MS/MS, GC–MS, and HCTUltra/LC–MS, were used to further identify the potent umami substances in chaya leaf.

Table 2.1 Mean value of umami intensity and monosodium glutamate (MSG) equivalent concentration of chaya leaf extract based on electronic tongue measurement (n = 4). The 3Y, 3M, and 3O samples are the young, mature, and old leaves of *Cnidoscolus chayamansa* (three-lobed leaves) and the 5Y, 5M, and 5O are the young, mature, and old leaves of *Cnidoscolus aconitifolius* (five-lobed leaves),

Sample	Umami intensity	MSG equivalent	
		mM*	%w/v
3Y	10.11 ± 0.08^a	8.93 ± 0.15^a	0.131 ± 0.001^a
3M	5.52 ± 0.06^c	1.16 ± 0.12^c	0.024 ± 0.000^b
3O	3.10 ± 0.06^e	0.40 ± 0.12^e	0.005 ± 0.001^e
5Y	10.37 ± 0.10^a	10.02 ± 0.19^a	0.147 ± 0.002^a
5M	7.40 ± 0.017^b	2.68 ± 0.03^b	0.039 ± 0.000^c
5O	3.95 ± 0.013^d	0.58 ± 0.03^d	0.009 ± 0.000^d

respectively.

*MSG equivalent (mM) is calculated from MSG concentration dependency equation obtained from the experiment:
y = 1.8573ln (x) + 5.4197; R^2 = 0.9812, where y is the umami taste intensity and x is the equivalent concentration of MSG (mM). Different superscript letters indicate the significant differences (p < 0.05) between each type of sample by Duncan's test. Statistical analyses were compared between all datasets (species and leaf maturation stages).

2.3.2 Metabolite profile of chaya leaves

Structurally distinct umami compounds have been discovered in foods. In addition to common umami compounds, such as L-glutamic acid, L-aspartic acid, and 5′-ribonucleotides, other substances related to umami taste include glycine, dipeptides, tripeptides, oligopeptides, and organic acids. To profile as many metabolites as possible, UHPLC–qTOF/MS was employed to capture both primary and secondary metabolites, such as free amino acids, organic acids, dipeptides, tripeptides, alkaloids, and flavonoids. GC–MS is more sensitive to primary metabolites, mainly hydrophilic compounds, which can be easily derivatized, such as free amino acids and sugars. Peptidomic analysis using HCTUltra/LC–MS was employed to separate and annotate peptides with more than five amino acids. Consequently, 118 metabolites, 104 metabolites, and 250 peptides were annotated using the UHPLC–qTOF/MS, GC–MS, and HCTUltra/LC–MS platforms, respectively. UHPLC–qTOF/MS and GC–MS annotated a total of 14 compounds exhibiting the same general trend. The relative levels of these compounds in the leaves of the two species at the three maturation stages demonstrated a positive correlation between UHPLC–qTOF/MS and GC–MS (Table A1, Appendix A), indicating the consistency and reliability of the results between the two platforms.

2.3.2.1 PCA demonstrated discrete metabolite profiles among the chaya leaf maturation stages of the two species

To obtain an overview of the differences in the metabolite profiles across the leaf maturation stages in the two species, an unsupervised PCA was implemented, constructed with the metabolite peak area acquired from the three analytical platforms (Figure 2.1). As shown in Figure 2.1A, the principal components principal components 1 and 2 comprised 53.2% and 16.5% of the variance, respectively, obtained from UHPLC–qTOF/MS. The young and old leaf samples of both the

species were located on the positive PC1, whereas the mature leaf samples were located on the negative PC1, indicating that the metabolite profiles of young and old leaves are more similar than that of mature leaves. Variables contributing to PC2 were responsible for species discrimination. In the 2D-PCA score plot, all clusters exhibited clear separation, indicating significant changes in the primary and secondary metabolites during leaf maturation and between the species. However, the metabolite data obtained from GC–MS (Figure 2.1B) was not fully distinguishable between the two species. The 3Y and 5Y clusters were clearly separated from the overlapped clusters of 3M, 5M, 3O, and 5O, indicating that metabolites in 3Y and 5Y were significantly different from those in mature and old leaves. As seen in Figure 2.1B, PC2 separated samples according to leaf maturation stage but not species. Thus, the metabolites annotated using GC–MS were related to the leaf maturation stages. As shown in Figure 2.1C, the five-lobed samples clustered together and were clearly separated from the three-lobed samples, revealing significant differences in the peptide profiles between the two species. Notably, PCA revealed a lower variation in five-lobed samples compared with the three-lobed samples because each biological replicate clustered close together. Overall, the metabolic variation between the leaf maturation stages was revealed via multimetabolomic platforms. Heat map analyses were further conducted to specify the metabolites contributing to the observed variation.
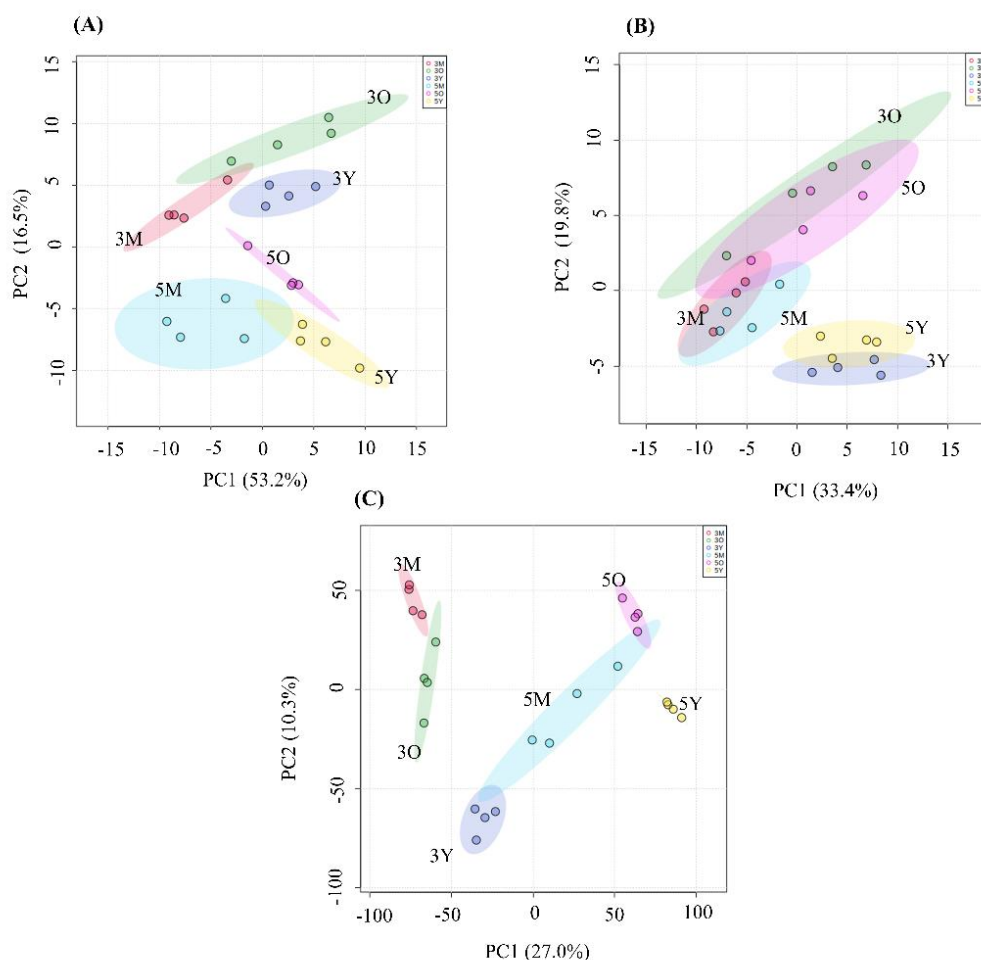
Figure 2.1 Principal component analysis plots of all samples acquired from ultra-high performance liquid chromatography–quadrupole time-of-flight mass spectrometry (A), gas chromatography–mass spectrometry data (B), and high-capacity ultra-ion trap/liquid chromatography–mass spectrometry (C). Each sample point represents a biological replicate (n = 4).

2.3.2.2 Heat map analysis illustrated changes in metabolite concentrations among the leaf samples

The top 50 metabolites or peptides annotated from each analytical platform (UHPLC–qTOF/MS (Figure 2.2a), GC–MS (Figure 2.2b), and HCTUltra/LC–MS (Figure A4, Appendix A) were selected based

on their relative abundance in the heatmap analysis to visualize their contents in all the samples at different leaf maturation stages and for each species (Figure 2.2). The heatmap was divided into classes according to the involvement of these metabolites in various metabolic pathways.

2.3.2.2.1 Free amino acids

The relative concentrations of 20 proteinogenic and nonproteinogenic amino acids were determined in this study. Generally, the concentration of free amino acids is high in younger leaves; it decreases when the leaves mature, and increases again in old leaves. The relatively high concentration of numerous amino acids in young leaves might be related to the highly active synthesis of protein components essential for plant growth. However, in old leaves hidden from the sunlight by ascending leaves, a shading effect could account for this observation. Li et al. (2017) reported that aromatic amino acids, such as phenylalanine, tryptophan, and tyrosine, show high accumulation as a result of the dark-induced response, and several amino acid biosynthetic genes were upregulated during leaf senescence. Regarding umami taste amino acids, the concentrations of L-glutamic and L-pyroglutamic acids peaked in younger leaves and significantly decreased with senescence (Figure 2.2A). This also aligns with previous research reporting that glutamic acid concentrations decrease in old leaves (Avila-Ospina et al., 2017). A previous report showed that while glutamate and aspartate decrease during leaf senescence, stress-related amino acids, such as GABA, branched-chain amino acids, and aromatic amino acids, accumulate at higher levels (Diaz et al., 2005). Apart from umami taste amino acids, other taste-related amino acids, such as L-phenylalanine and L-arginine, are also detected in high concentrations (Table A2, Appendix A) in chaya leaves. These amino acids have been reported to impart an umami taste in food. L-

phenylalanine elicits an umami taste in soy sauce at subthreshold concentrations (Zhao et al., 2016). In MSG solutions, the addition of L-arginine enhances the umami intensity (Lioe et al., 2006). In young and old chaya leaves, sweet-tasting amino acids, such as glycine and alanine, showed high accumulation (Figure 2.2B) and both synergistically increase the umami perception of MSG (Yang, et al., 2019).

2.3.2.2.2 Peptides

More than 50 peptides have been reported to exhibit an umami taste or have umami-enhancing properties in food and food ingredients. Most umami taste peptides are dipeptides and tripeptides; however, a few medium-chain peptides, such as octapeptides and undecapeptides, also exhibit this property (Zhang et al., 2018a). Based on the present study, short-chain peptides (less than four amino acids) and peptides with more than four amino acids could be detected using UHPLC–qTOF/MS (Figure 2.2A) and HTCUltra/LC–MS (Figure A4, Appendix A), respectively. Thus, combining these analytical platforms enables the identification of a wide range of potent umami peptides. Heatmap analysis revealed that young and old leaves possess a relatively higher concentration of most dipeptides, similar to the pattern observed for free amino acids. This might be due to differences in biosynthesis/proteolysis. In old leaves, senescence-associated proteolysis is essential for nutrient mobilization from old or stressed tissues (Diaz-Mendoza, et al., 2016). γ-Glutamyl-cysteinyl-glycine, known as glutathione (GSH), is a common γ-glutamyl peptide found in plants, which exhibits antioxidant activities against abiotic stresses. GSH provides "kokumi" sensations, such as mouthfulness, thickness, and continuity of the perception of food taste, by increasing the sensation of umami and saltiness (Goto et al., 2016). The concentration of GSH was three-fold higher in young and mature leaves of the

aconitifilus species (five-lobed leaf) compared with that in leaves of the *chayamansa* species (three-lobed leaves) (Figure 2.2A). Besides GSH, four γ-glutamyl peptides were identified in chaya leaves. γ-Glutamyl dipeptides are becoming more popular, given their desirable umami-enhancing and kokumi-imparting properties. All γ-glutamyl dipeptides found in chaya leaves were reported to increase the umami taste of MSG and NaCl solutions, with γ-glutamyl leucine exhibiting the strongest effect (Yang et al., 2021), as analyzed via sensory evaluation and electronic tongue analysis. These peptides were found to naturally exist at higher concentrations in young chaya leaves in this study.

2.3.2.2.3 Sugars

Among the eight annotated sugars, three monosaccharides (D-glucose, D-allose, and D-altrose) showed higher accumulation in the young and mature leaf, as shown in Figure 2.2B. Sucrose was detected to be the most abundant sugar in chaya leaves (Table A3, Appendix A), and its accumulation in mature leaves was two to three folds higher than that in young and old leaves of both the species (Figure 2.2). A similar observation was found in tobacco leaves, wherein the remobilization of sucrose from old senescing leaves into sink mature leaves occurs (Li et al., 2017). Another study reported the drastic accumulation of glucose, fructose, and sucrose during developmental leaf senescence (Wingler & Roitsch, 2008). Sugar content in plant cells is species-dependent and can be easily modulated via light, which affects the photosynthesis rate.

2.3.2.2.4 Nucleotides

5′-AMP was the only umami nucleotide detected in chaya leaves in the present study (Figure 2.2A). It is an important umami substance widely distributed in natural foods, especially seafood. Additionally, 5′-AMP can mask the perception of bitterness in seafood products and produce a pleasant and sweet taste. In plants, it is the main umami nucleotide in

ripe tomatoes (Oruna-Concha, 2007). The concentration of 5′-AMP in young chaya leaves is twice that of mature leaves, whereas it is undetectable in old leaves of both the species. This might be due to its degradation in senescing leaves, presumably for nutrient redistribution (Thomas, 2003). Degradation products from nucleic acids could be remobilized as nucleotides, purine or pyrimidine bases, or phosphates. For example, RNase activity is elevated during leaf senescence (Green, 1994), and the degradation of purine nucleotides occurs when 5′-AMP is converted to 5′-IMP under the action of 5′-AMP deaminase.

2.3.2.2.5 Other compounds

The concentrations of organic acids, alkaloids, flavonoids, cyanogenic glucoside, and glucosinolate varied among the different leaf maturation stages and between the species. Among the organic acids annotated in chaya leaves, malic and quinic acids were the most abundant metabolites, according to their relative mass intensities (Table S2 and S3). Malic acid was present at slightly higher concentrations in *aconitifolius* species (five-lobed) (Figure 2.2B), and quinic acid was highly accumulated in the young leaves of both the species (Figure 2.2). Although the quantitative analyses of these organic acids were not performed, they are known as flavor-related compounds. Malic acid imparts a sour taste and is present in many fruits, and quinic acid provides an astringent sensation (Peleg et al., 1998). However, there are no reports mentioning that malic and quinic acids possess umami tastes. Six alkaloids were annotated in chaya leaves. Among alkaloids, trigonelline was present at the highest abundance based on relative mass intensities (Table A2, Appendix A). It was highly accumulated (Figure 2.2A) in the young leaves of both the chaya species, consistent with another study reporting its content peaking in young coffee leaves (Zheng et al., 2004). Trigonelline is a flavor-related compound that contributes to the desirable roasted flavor in coffee beans and possesses several health benefits (Zhou et al., 2012).

Several flavonoids were also tentatively annotated in chaya leaves, such as biorobin (kaempferol 3-robinobioside), nicotiflorin (kaempferol-3-O-rutinoside), robinin (kaempferol-3-O-robinoside-7-O-rhamnoside), and clovin (quercetin 3-robinobioside-7-rhamnoside). A study has reported that kaempferol and quercetin were the most abundant flavonoid aglycones found in chaya leaves (Rodrigues et al., 2020). The concentration of these flavonoids varied accordingly. Biorobin was detected in 3Y at concentrations three to four times of that in 5Y, whereas nicotiflorin was doubled in concentration in the *aconitifilus* species. These variations suggest that the flavonoid levels in chaya leaves are species-dependent. Moura et al. (2018) reviewed over 70 *in vivo* and *in vitro* studies reporting the bioactive molecules in chaya leaves, and they concluded that their antidiabetic, antimicrobial, anti-inflammatory, and antiproliferative effects arise from their high flavonoid content. Recently, biorobin and nicotiflorin demonstrated strong binding affinity to potential severe acute respiratory syndrome coronavirus 2 infection targets, such as the viral and human angiotensin-converting enzyme 2 receptors (Andrianov et al., 2021). These findings highlight the potential medicinal application of chaya leaves in preventing coronavirus disease 2019. The results obtained in the present study will be helpful in further understanding the bioactive functions of chaya leaves at different leaf maturation stages and from different species. Linamarin is a cyanogenic glucoside found in chaya, produced mainly in the leaves (Gonzalez-Laredo et al., 2003). It shows the highest concentration in the mature leaves of both the species (Figure 2.2A). Cooking and other heat treatments, such as drying methods, could reduce its toxicity levels by hydrolyzing its glycosidic bond and allowing the release of hydrogen cyanide gas (Ross-Ibarra & Molina-Cruz, 2002). There has been no evidence thus far of intoxication due to chaya leaf consumption.
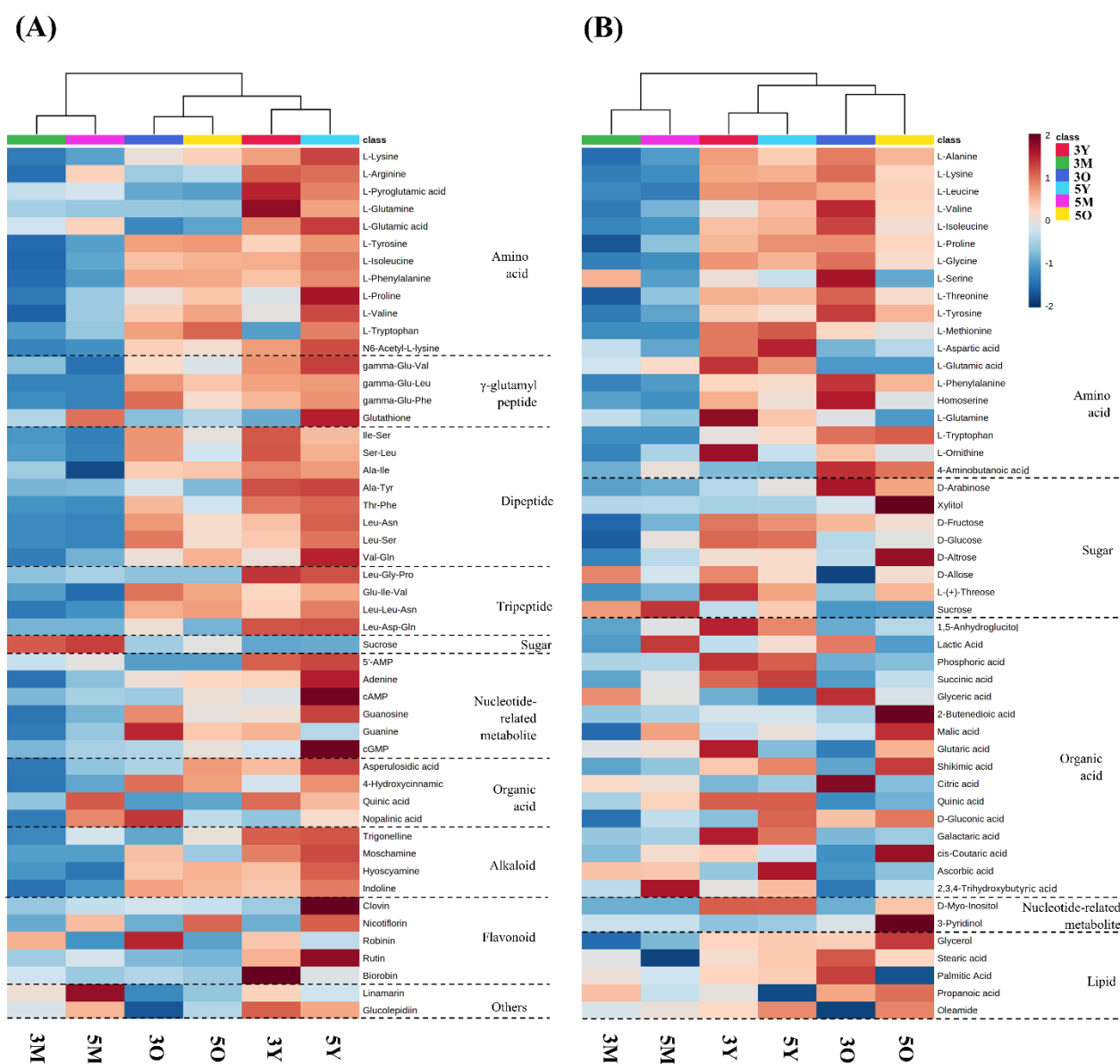
Figure 2.2 Heatmap visualization of the top 50 annotated metabolites based on the relative abundance from the ultra-high performance liquid chromatography–quadrupole time-of-flight mass spectrometry (A) and gas chromatography–mass spectrometry (B) platforms among chaya leaf samples (n = 4) at different leaf maturation stages and species. The color in the heatmap indicates the relative fold change of each metabolite between groups, with red and blue colors expressing higher or lower abundances, respectively.

2.3.3 PLSR correlation between metabolites and umami taste intensity identified candidate umami substances

To investigate the relationship between metabolite data and umami taste intensity across various chaya leaf samples, PLSR analysis was conducted with metabolite data obtained from the three analytical platforms as explanatory variables (x) and the umami taste intensity obtained from electronic tongue assay as the response variable (y).

2.3.3.1 Model diagnostics

We conducted a two-step PLSR model diagnostic cross-validation and permutation test to achieve the best-fit model for the study data. For cross-validation, the model evaluation parameters (R^2Y and Q^2) were obtained after seven cycles of interactive verification (Table A4, Appendix A). The validation of the PLS model was performed by evaluating the correlation index. The R^2X parameter describes the optimization of the analytical model representing the total variation in the explained variable (x). The R^2Y parameter describes variation in the response variable (y). The Q^2 parameter represents the model's predictive ability. Generally, an R^2Y and Q^2 values of 0.65 and 0.5 or higher, respectively, indicate adequate quantitative prediction abilities (Williams & Norris, 1987). The Q^2 and R^2Y values obtained from all the models in the present study were between 0.8 and 0.9, indicating that the model prediction quality was stable and reliable. To assess the risk of overfitting, 200 permutation tests were performed. Commonly, the y-axis intercept of Q^2 should be lower than 0.05, and the permutated data on the left should be lower than the original data on the right (Triba et al., 2005). In the present study, both the criteria were met, as shown in Figure A5, Appendix A, indicating that all PLSR models were valid and exhibited a low risk of overfitting.

2.3.3.2 Selection of umami compound candidates using biplot and VIP analyses

The young leaf samples (3Y and 5Y) in all the analytical platforms were located on the positive side of the biplot, which is close to the umami response. This relationship between the stage of the leaf samples and umami taste reflects a higher accumulation of metabolites, engendering the high value of umami taste intensity in young leaves. Young leaf samples from both the species exhibited a better separation from mature and old leaves in the supervised PLSR compared with that in the unsupervised PCA (Figure 2.1). Biplots obtained from PLS analysis visualized the association of metabolites (x), umami response (y), and chaya leaf samples (observations). As shown in Figure 2.3, the metabolites and umami taste located in the same quadrant signifies a positive correlation between them, and the displacement of the metabolites from the umami taste indicates their contribution (Zhu et al., 2017). To statistically evaluate the contribution of each metabolite to umami taste, a VIP analysis was conducted. VIP is an index of the effect of each explanatory variable on the response variable in the model and is used to select important metabolites in metabolomics-based research. In PLSR, any compounds with VIP values >1 were considered significant explanatory variables for predicting the response variable. Here potential umami metabolites having VIP values >1.5 were selected, as shown in Table 2.2; 19 umami compound candidates strongly correlated with umami taste, with L-glutamic acid and 5′-AMP exhibiting the highest VIP values. They are generally accepted as umami amino acids and nucleotides in foods, respectively. L-pyroglutamic acid, a cyclic form of L-glutamic acid, showed the third-highest VIP value and reportedly imparts an umami taste to potatoes (Zhang & Peterson, 2018). This further confirms the reliability and quality of the model used in this study. Interestingly, the other compounds in Table 2.2, including small peptides, organic acids,

inorganic acids, and flavonoids with a high VIP value, have not been reported to be associated with umami taste. Glutamic acid and nucleotides are mainly thought to contribute to umami taste. However, novel umami compounds, such as small peptides (Zhang et al., 2017) and amino acid derivatives (Shiga et al., 2014), have recently been reported. Thus, whether the umami taste of chaya leaves arises from L-glutamic acid and 5′-AMP was investigated.
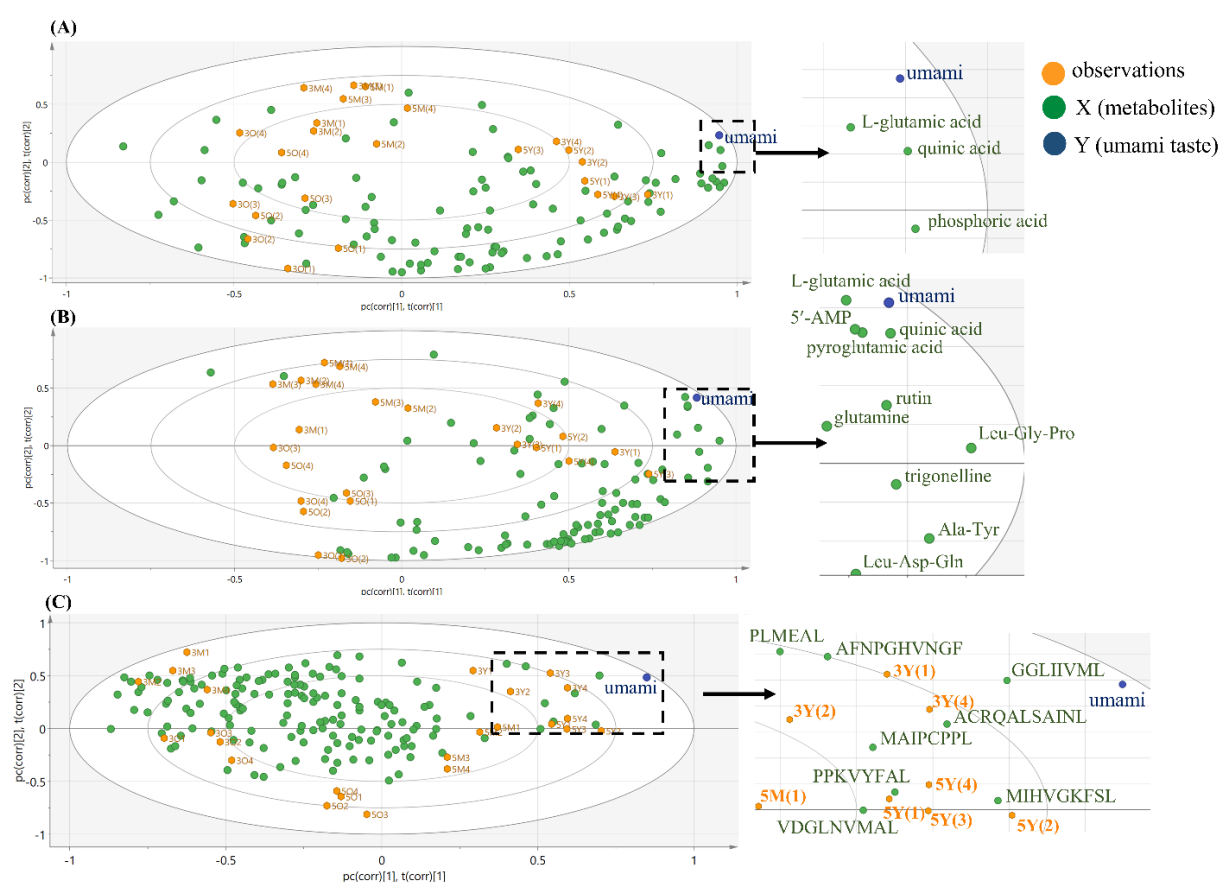
Figure 2.3 Correlation biplot from partial least square regression analysis of umami taste (Y-variables) of chaya leaves and relative metabolite concentrations (X-variables) annotated by ultra-high performance liquid chromatography–quadrupole time-of-flight mass spectrometry (A), gas chromatography–mass spectrometry (B), and high-capacity ultra-ion trap/liquid chromatography–mass spectrometry (C).

Table 2.2 Potential umami compounds selected by variable importance in the projection > 1.5

Compound	Retention time (min)	Adduct	m/z	VIP[a]	Error (ppm)	Score	Mass fragment
UHPLC–qTOF/MS							
pyroglutamic acid	1.04	[M+H]+	130.0491	1.99	5.9631	-	130.0491, 102.0546, 84.0046, 74.0046, 56.0483
L-glutamic acid	1.08	[M+H]+	148.0603	2.05	0.9126	-	138.0541, 120.0432, 92.0848, 65.0382
trigonelline	1.11	[M+H]+	138.0562	1.80	9.0852	-	138.0541, 120.0432, 92.0848, 65.0382
quinic acid	1.17	[M+H]+	193.0716	1.95	8.1463	-	121.0286,111.0430,95.0477, 83.0484, 77.0385,65.0382
Ala–Tyr	2.45	[M+H]+	253.1189	2.26	2.4457	-	182.1,166.0851, 144.0822, 120.0813, 103.0526, 93.0687, 77.0385
5′-AMP	3.07	[M+H]+	348.0695	2.02	2.4805	-	136.0619, 119.0359, 97.0288
Leu–Asp–Gln	3.63	[M+H]+	375.1890	1.61	4.2076	-	200.1394, 183.1144, 120.0813 155.164, 130.0491, 84.0446
Leu–Gly–Pro	9.36	[M+H]+	286.1743	1.88	6.4267	-	229.1512, 187.1068, 173.0954, 169.1324, 155.0821, 127.0854, 86.0955, 70.064
rutin	12.01	[M+H]+	611.1605	1.95	1.0879	-	465.1044, 345.062 303.0495, 257.0478 129.0546
biorobin	13.33	[M+H]+	595.1641	1.51	2.7715	-	449.1074, 287.055, 129.0546
GC-MS							
phosphoric acid	10.81	[M]+	241.00[b]	1.55	-	85%[c]	241.00, 163.05, 133.05, 70.10

quinic acid	21.44	[M]+	345.15[b]	1.76	-	83%[c]	345.15, 255.10, 147.05,73.05
glutamic acid	18.24	[M]+	363.25[b]	1.90	-	93%[c]	363.25, 348.15, 246.00, 147.05, 128.15, 84.00, 73.50
HCTUltra/LC–MS							
ACRQALSAINL	13.55	[M+H]+	1160.3840	1.65	-	2.1[d]	1088.5881, 701.4192, 630.3821, 613.3556, 517.2980, 413.2395, 331.1547
AFNPGHVNGF	13.68	[M+H]+	1060.2121	1.60	-	11.0[d]	988.4635, 841.3951, 727.3522, 494.7354, 421.2012, 223.1077
PPKVYFAL	13.80	[M+H]+	931.8955	1.58	-	7.2[d]	323.2078, 732.4079, 803.4450
MIHVGKFSL	14.13	[M+H]+	1031.6685	1.62	-	18.2[d]	787.4461, 770.4196, 650.3872, 551.3188, 534.2922, 366.2023, 348.1918
PLMEAL	14.45	[M+H]+	688.3046	1.90	-	17.6[d]	558.2592, 487.2221, 358.1795, 211.1441
MAIPCPPL	16.94	[M+H]+	840.5633	1.59	-	15.3[d]	639.3534, 526.2694, 429.2166, 326.2074
GGLIIVML	18.45	[M+H]+	814.8220	1.78	-	27.9[d]	701.4630, 588.3789, 475.2949, 362.2108
VDGLYGKNL	24.36	[M+H]+	978.2133	1.52	-	12.1[d]	764.4301, 594.3246, 431.2613

[a]Variable importance in the projection

[b]The highest fragment mass of peak detected by GC-MS

[c]Percentage of similarity compared with the mass spectrum in the library

[d]Mascot score

2.3.4 Absolute quantification and EUC analysis

As L-glutamic acid and 5′-AMP were the only established umami compounds identified in the present study. EUC values were calculated from the absolute concentration of these two compounds determined by the standard curves of each compound. Consequently, the 3Y samples showed the highest EUC value of 0.011% MSG equivalent (0.63 mM), which was still much lower than the MSG recognition threshold [1.38 mM or 0.02% (w/v)] (Figure A6, Appendix A). Conversely, the taste intensity results obtained from the electronic tongue assay (Section 2.3.1) showed that the umami intensity in the young leaf samples calculated as %MSG equivalent is greater than the taste threshold of MSG. Therefore, assessing the EUC value based on the concentrations of L-glutamic acid and 5′-AMP did not completely represent the umami taste in the complex matrix, as other compounds imparting umami taste have not yet been considered. Thus, the umami response at a suprathreshold concentration of MSG in the young leaves might be due to synergism with other compounds that positively correlated with the umami response (Table 2.2). To investigate the other potent umami substances, molecular docking analysis was conducted to evaluate the stability of and the interaction between these substances and the human umami receptor.

2.3.5 Molecular docking of candidate umami substances with the T1R1/T1R3 umami receptor

Because the 3D structure of the human T1R1/T1R3 has not been established, a neural network-based model, Alphafold2 (Jumper et al., 2021), was employed in the present study to construct the T1R1 and T1R3 modeled structures using protein sequences from UniProtKB (Q7RTX1 and Q7RTX0). The predicted local distance difference test measures the percentage of correctly predicted interatomic distances of the T1R1 and T1R3. It evaluates how well interatomic distances in a reference protein structure are reproduced in the second structure to measure local confidence (100% being the highest). The predicted

structure of the best T1R1 and T1R3 models were 86.46% and 87.62%, respectively (Figure A7, Appendix A), suggesting that these two models are likely reliable. Then, the superimposition of the 3D predicted structures and mGluR1 template was performed to obtain the human T1R1/T1R3 model (Figure A8, Appendix A) for docking studies. The interactions between either L-glutamic acid or the candidate umami ligands with T1R1/T1R3 were investigated by molecular docking using AutoDock VinaXB. In Figure 2.4A, the seven candidate umami ligands (quinic acid, pyroglutamic acid, trigonelline, 5′-AMP, AY, LGP, and LDQ) demonstrated binding energies lower than glutamic acid for T1R1/T1R3, indicating a stronger interaction. Conversely, other candidates, such as biorobin, rutin, and long-chain peptides with more than five amino acids, had higher binding energies than glutamic acid. These results align with previous research showing that the length of a peptide chain affects the umami taste intensity. Generally, peptides with molecular weights less than 1000 Da exhibit higher umami intensity and short dipeptides and tripeptides account for more than half of the identified umami peptides (Zhang et al., 2017). Due to relatively smaller molecular size of these peptides, they could enter the receptor cavity. Yu et al. (2021) also reported that peptides with more than four amino acids or sizable molecular compounds exhibited difficulty in entering the binding cavity of T1R1 due to the very small size of the cavity, obstructing the access of large molecules. Accordingly, via sensory evaluation and electronic tongue analysis, 5′-AMP was reported to show a higher umami taste intensity than L-glutamic acid at an equivalent concentration (Wang et al., 2021), and pyroglutamic acid was observed to be a key umami compound in potatoes (Zhang & Peterson, 2018). Hence, the seven umami ligand candidates positively correlated with umami taste and could stably bind with the umami heterodimer receptor *in silico*. Notably, the binding of the potential candidates was stabilized by hydrogen bonds with the 10 T1R1 residues, i.e., H71, D147, T149, A170, S172, D218, R277, Q278, E301, and S385. Furthermore, there were 10 H-bond formations between candidates with T1R3 residues, i.e., H145, S147, E148, G168, A169, S170, Y218, V277, E301, and Q389. Conversely, only three hydrogen bonds

with the T1R1/T1R3 catalytic residues T149, S172, and E301 (T1R1) and S147, G168, and S170 (T1R3) were detected with the reference ligand (Figure 2.4B). The 2D binding interaction of umami ligands with the active site residues is shown in Figure A9, Appendix A. This finding indicates that these effective umami ligands can play an essential role in umami flavor. To confirm whether these potent umami candidates exhibit umami taste intensity, the sensory evaluation of these pure compounds was further investigated via electronic tongue analysis.
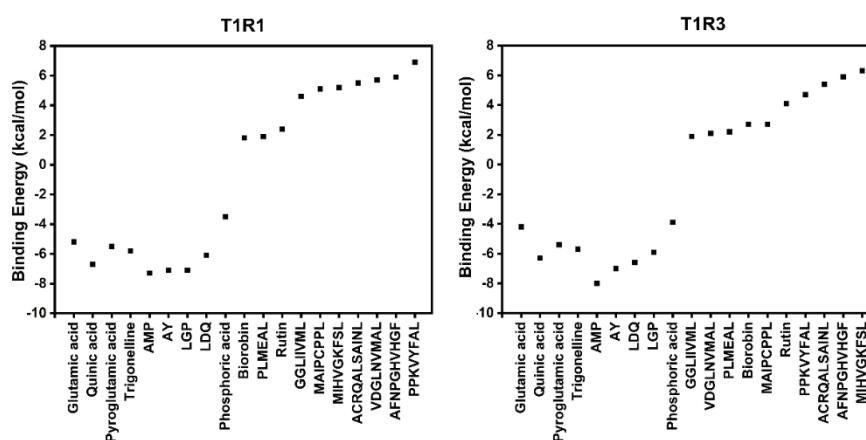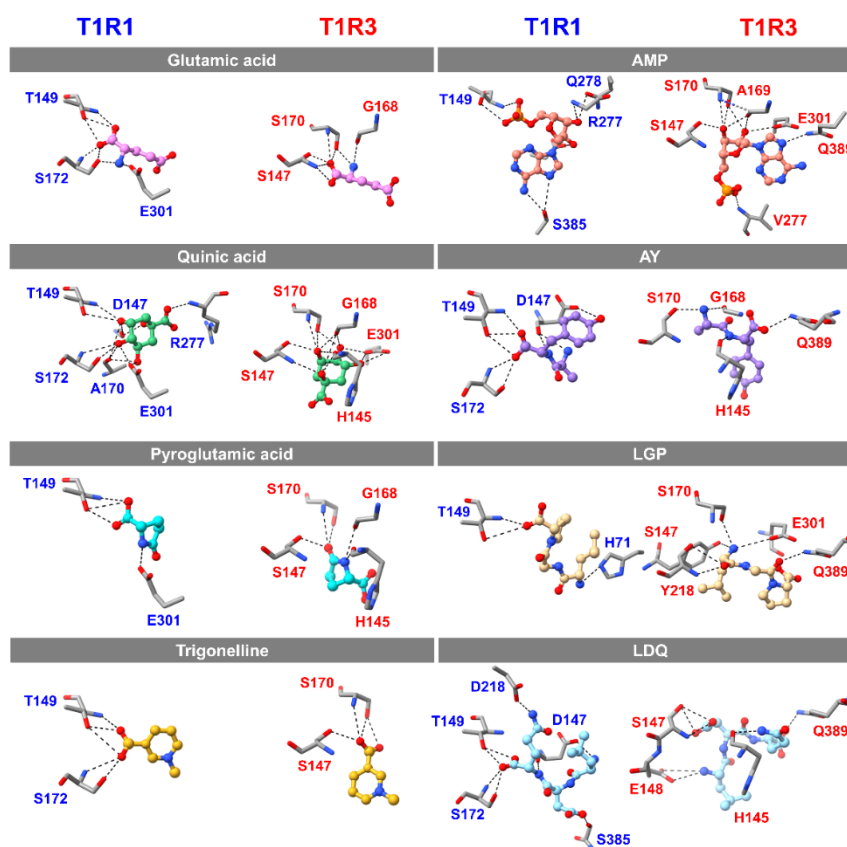
Figure 2.4 Dot plots showing the binding affinity (kcal/mol) of candidate umami substances with taste receptor type 1 member 1 (left) and taste receptor type 1 member 3 (right) (A). The 3D orientation and binding interaction of umami ligands with the active site residues of the closed conformation of taste receptor type 1 member 1 (left) and the open conformation of taste receptor type 1 member 3 (right).

The dashed line represents hydrogen bonds between ligands and taste receptor type 1 member 1/taste receptor type 1 member 3 residues (B).

2.3.6 Umami taste intensity of potent umami compounds and their synergism with MSG as evaluated using electronic tongue assay

The umami taste intensity of MSG and 5′-AMP (positive controls) were 2.67 and 3.74, respectively (Table A5, Appendix A). These results also align with previous research reporting that a 5′-AMP solution exhibited a significantly higher umami taste intensity than that of MSG (0.5 and 1.0 g/L) ($p < 0.05$) as evaluated by sensory evaluation and another model of an electronic tongue (Wang et al., 2021). Interestingly, the potent umami compounds exhibited an umami taste but with lower intensity than the positive controls at a similar molarity. Nonetheless, this result verified that the potent umami compounds screened using PLSR and molecular docking have umami taste and can be considered novel umami compounds.

Furthermore, an experiment to investigate the synergism among these novel umami compounds was performed. In Table A6, Appendix A, the novel umami compounds and MSG were mixed to achieve the final concentration of 1.5 mM. It was assumed that the relationship between the concentration and taste response within this range was linear, and the expected umami response of the binary mixture was summed from the intensity of each compound; hence, as the MSG concentration doubled, the umami taste intensity increased by a factor of two. Thus, the actual umami intensity of most samples was higher than the expected intensity. This might be due to the synergism between the compounds and MSG. Notably, LGP exhibited the weakest umami intensity among the peptides (Table A5, Appendix A), but the copresence of LGP and MSG showed the highest intensity (Table A6, Appendix A). This suggests that synergism occurs between LGP and MSG. In comparison, 5′-AMP showed weak synergism with MSG, which is concordant with previous research demonstrating that 5′-AMP had the least synergism with MSG among umami taste nucleotides (Yamagushi et al., 1971). To the best of our knowledge,

quinic acid, trigonelline, AY, LGP, and LDQ have not been associated with umami taste. Thus, this is the first study reporting that these compounds possess an umami property and exhibit synergism with MSG.

2.4 Conclusion

This study explored the compounds and peptides contributing to the umami taste of chaya leaves using a multiplatform metabolomics approach, including UHPLC–qTOF/MS, GC–MS, and HCTUltra/LC–MS, combined with electronic tongue assay and molecular docking approaches. The annotated metabolites, including amino acids, sugars, nucleotides, organic acids, flavonoids, alkaloids, and peptides, showed different concentrations among chaya species and maturation stages of leaves. Regardless of the species, young leaves exhibited the highest umami taste intensity, followed by mature and old leaves. VIP values obtained from PLSR demonstrated that 19 candidate umami compounds were highly correlated with umami taste. By investigating the binding mechanism of these candidates with the umami heterodimer receptor T1R1/T1R3 via molecular docking, 5′-AMP, quinic acid, pyroglutamic acid, trigonelline, AY, LGP, and LDQ were found to stably bind to the receptor. These compounds possessed umami properties, and LGP exhibited synergism with MSG, as analyzed using the electronic tongue assay. It was demonstrated that applying multianalytical platforms with *in silico* techniques and sensory evaluation is advantageous for identifying a wide range of metabolites and exploring novel umami compounds.

Credit authorship contribution statement

Nuti Hutasingh: Conceptualization, Methodology, Investigation, Writing – original draft. **Hathaichanok Chuntakaruk**: Methodology, Investigation. **Apinya Tubtimrattana**: Methodology, Investigation. **Yanisa Ketngamkum:** Methodology, Investigation. **Putthamas Pewlong**: Methodology, Investigation. **Narumon Phaonakrop**: Methodology, Investigation. **Sittiruk Roytrakul**: Data curation,

Writing – review & editing. **Thanyada Rungrotmongkol:** Data curation, Writing – review & editing. **Atchara Paemanee:** Data curation, Writing – review & editing. **Nat Tansrisawad**: Data curation, Writing – review & editing. **Ubonrat Siripatrawan**: Funding acquisition, Project administration, Conceptualization, Data curation, Supervision, Writing – review & editing. **Supaart Sirikantaramas:** Funding acquisition, Project administration, Conceptualization, Data curation, Supervision, Writing – review & editing.

Declaration of competing interests

The authors declare that they have no known competing financial interests or personal relationships that influenced the work reported in this paper.

CHAPTER III
MANUSCRIPT II

Unraveling the Effects of Drying Techniques on Chaya Leaves: Metabolomics

Analysis of Nonvolatile and Volatile Metabolites, Umami Taste,

and Antioxidant Capacity

Nuti HUTASINGH [a], Apinya TUBTIMRATTANA [b],

Pornkanok PONGMAPORN [c], Putthamas PEWLONG [d],

Atchara PAEMANEE [c], Nat TANSRISAWAD [e],

Ubonrat SIRIPATRAWAN [a, *], Supaart SIRIKANTARAMAS [d, *]

[a] *Department of Food Technology, Faculty of Science, Chulalongkorn University, Bangkok, Thailand*

[b] *Department of Forensic Medicine, Faculty of Medicine Chulalongkorn University, King Chulalongkorn Memorial Hospital, The Thai Red Cross Society, Bangkok, Thailand*

[c] *National Omics Center, National Science and Technology Development Agency (NSTDA), Pathum Thani, Thailand*

[d] *Center of Excellence for Molecular Crop, Department of Biochemistry, Faculty of Science, Chulalongkorn University, Bangkok, Thailand*

[e] *Department of Forensic Medicine, Faculty of Medicine, Chulalongkorn University, Bangkok, Thailand*

* Corresponding authors

Ubonrat SIRIPATRAWAN: Department of Food Technology, Faculty of Science, Chulalongkorn University, Bangkok, Thailand; email: Ubonratana.S@chula.ac.th

Supaart SIRIKANTARAMAS: Center of Excellence for Molecular Crop, Department of Biochemistry, Faculty of Science, Chulalongkorn University, Bangkok, Thailand; email: Supaart.s@chula.ac.th

Highlights

- The volatile profile of chaya leaves were investigated for the first time
- 3-Methylbutanal (malt-like odor) is the key volatile in dried chaya leaves
- Oven drying (120°C) enhances 5′-ribonucleotide content 3-fold in dried chaya leaves
- Umami taste was most pronounced in oven-dried (120°C) and pan-roasted samples
- Freeze-dried chaya leaves exhibited the highest antioxidant activity levels

Keywords: chaya leaves, drying methods, metabolome, umami taste, antioxidant properties, aroma characteristics

Abstract

Chaya (*Cnidoscolus chayamansa*) leaves are known for their strong umami taste and used as a dried seasoning. This study aimed to assess the impact of different drying methods [freeze drying (FD), vacuum drying, oven drying at 50°C and 120°C (OD120) and pan roasting (PR)] on the metabolome, umami intensity, and antioxidant properties of chaya leaves using mass spectrometry. The predominant volatile compound among all samples, 3-methylbutanal, exhibited the highest relative odor activity value (rOAV), imparting a malt-like odor, while hexanal (green grass-like odor) and 2-methylbutanal (coffee-like odor) are the second highest rOAV in the FD and PR samples, respectively. OD120 and PR samples possessed the highest levels of umami-tasting amino acids and 5'-ribonucleotides as well as the most intense umami taste, whereas FD samples exhibited the highest antioxidant capacity. These findings enhance our understanding of the aroma characteristics, umami taste, and antioxidant potential of processed chaya leaves.

Chemical compounds

Formic acid (PubChem CID: 284); Puerarin (PubChem CID: 5281807); 3-Methyl-2-heptanone (PubChem CID: 92927); Monosodium glutamate (PubChem CID:

23672308); Polyvinylpolypyrrolidone (PubChem CID: 131751496); Trolox (PubChem CID: 40634), DPPH radical (PubChem CID: 15911); Sodium acetate trihydrate (PubChem CID: 23665404); Acetic acid (DPPH CID: 176).

3.1 Introduction

Chaya (*Cnidoscolus* spp.) is a highly nutritious edible leaf native to Central America. In Thailand, it is commonly dried and marketed as a natural seasoning powder or monosodium glutamate (MSG) substitute in savory products and caffeine-free tea. Hutasingh et al. (2023) recently reported on the remarkable umami taste properties of chaya. Umami is a crucial factor in the development of successful food products as it contributes a savory and meaty flavor, thereby enhancing overall food acceptability. The distinct taste quality is primarily attributed to the presence of free amino acids, such as glutamic acid and aspartic acid, as well as 5'-nucleotides, including 5'-adenosine monophosphate (5'-AMP), 5'-guanosine monophosphate (5'-GMP), and 5'-inosine monophosphate. In our previous study, we identified glutamic acid, 5'-AMP, and short peptides as the key umami compounds in chaya leaves. Beyond their umami taste quality, chaya leaves are renowned for their medicinal properties, exerting therapeutic effects against diabetes, rheumatism, gastrointestinal disorders, and inflammation (Moura et al., 2018).

Unlike other natural umami ingredients, such as mushrooms, tomatoes, cheese, and yeast extract, fresh chaya leaves lack a strong or distinctive flavor, allowing them to effectively enhance the overall flavor of various dishes without overpowering their original flavors. However, upon drying, the leaves acquire a distinct aroma perceptible to humans. Surprisingly, the aroma characteristics of dried chaya leaves have yet to be thoroughly examined. Therefore, the present study represents the first attempt to investigate the aroma characteristics and key aroma compounds of these leaves.

Drying is a traditional preservation method that extends the shelf life of food by reducing water activity, resulting in the inhibition of spoilage microorganisms, slowing down of enzyme activity, and preservation of nutrients. Zhang et al. (2021) showed that drying techniques can affect the composition of flavor compounds, both volatile and nonvolatile, thereby influencing product quality and consumer preference. Specifically, drying methods have been found to significantly alter umami taste components and even facilitate the formation of new taste components. Li et al. (2015) compared the effects of several drying methods on the taste-active compounds of king oyster mushrooms (*Pleurotus eryngii*) and found that oven drying and freeze drying (FD) increased the content of umami-tasting components. Similarly, Tian et al. (2016) reported that vacuum drying (VD) improved the quality of dried shiitake mushrooms while effectively preserving their flavor components.

Each drying method has distinct advantages and limitations. For example, FD is often used to preserve the bioactive compounds of plant materials such as antioxidants owing to its low-temperature usage. However, the FD process is time-consuming, taking several days to achieve the desired moisture content. VD has been successfully used in many food applications to safeguard volatile compounds against oxidation by limiting oxygen exposure during drying and offers faster drying compared with FD (Tian et al., 2016). However, VD has been shown to result in lower levels of umami-tasting amino acids and 5'-ribonucleotides in *Cordyceps militaris* samples compared with other drying methods (Zhang et al., 2022). The high energy consumption and low production efficiency of FD and VD constrain their widespread use (Xu et al., 2020). Therefore, the traditional and cost-effective method of OD is more widely used for drying plant materials, but the elevated temperature and presence of oxygen during OD can lead to significant degradation of bioactive compounds (Xu et al., 2020). However, Wen et al. (2022) reported a significant increase in umami-tasting free amino acids and 5'-ribonucleotides in mushrooms (*Lentinula edodes*) dried using OD at 50ºC. Pan roasting (PR),

also known as pan-firing, uses much higher drying temperatures (>150ºC) and achieves rapid drying times, and it has been found to enhance the content of umami-tasting amino acids in green tea (Lin et al., 2022). Nonetheless, PR is labor-intensive, as the plant material requires continuous stirring, and there is a risk of burning.

In Thailand, PR and OD are commonly used drying methods for chaya leaves owing to their convenience and cost-effectiveness. These methods are believed to enhance the overall flavor, including aroma and taste, of the leaf. The present study aimed to investigate the impact of different drying methods on the aroma characteristics of chaya leaves using headspace gas chromatography/mass spectrometry (HS-GC/MS) and relative odor active values (rOAV). Additionally, nonvolatile metabolites associated with umami taste and flavor precursors were analyzed using ultra-high performance liquid chromatography–quadrupole time-of-flight mass spectrometry (UHPLC–qTOF/MS), whereas umami taste intensity was evaluated using an electronic tongue. Furthermore, comprehensive analysis of antioxidant activities was conducted. Therefore, the hypothesis for this study is that different drying methods affect the aroma characteristics, umami taste components, and antioxidant properties of chaya leaves.

The findings of this study provide valuable insights into the effects of various drying methods on compounds that contribute to the umami taste and aroma profile of chaya leaves, which are considered an alternative source of umami compounds. Using volatilomics and metabolomics approaches, this research offers novel perspectives. Ultimately, the study's findings contribute fundamental knowledge and theoretical evidence for the production of dried chaya leaves, benefiting manufacturers in the field.

3.2 Materials and Methods

3.2.1 Chemicals, plant materials, and sample collection

All internal standards, organic solvents for HS-GC/MS and UHPLC–qTOF/MS, and reagents for determining total phenolic content (TPC) and antioxidant activities were purchased from Sigma-Aldrich (St. Louis, MO, USA). Chaya leaves (*Cnidoscolus chayamansa*) were collected from four one-year-old plants (approximately 150–170 cm tall) in January 2023 from Wangthonglang district, Bangkok, Thailand. Young leaves (1st–3rd leaf order from the apical bud) and mature leaves (4th–6th leaf order) were handpicked and pooled, representing commonly harvested maturation stages. Four replicates of leaves were used. In total, approximately 40 grams of the leaf's mixture were used per replicate. The leaves were rinsed twice with filtered water, gently pad-dried with paper towel to prevent damage, and stored in dry and odorless cold storage at 4°C for 1 day prior to drying.

3.2.2 Drying of plant materials and aqueous extract preparation

Five different methods were used to assess their effects: FD, VD, OD at 50°C (OD50) and 120°C (OD120), and PR. For FD, samples were prefrozen at −20°C for 4 h, followed by freeze drying at −30°C and 0.5 mbar for 30 h using a freeze dryer (5EC, Grisrianthong, Samutsakorn, Thailand). VD was performed in a vacuum oven (15VD, Grisrianthong, Samutsakorn Thailand) at 0.18 mBar and 50°C for 18 h. OD50 and OD120 were performed in a hot-air oven (YXD-4D, Kitchenmall, Shanghai, China) at air velocities of 0.5 m/s, with drying time of 48 h at 50°C and 30 min at 120°C, respectively. PR involved roasting the leaves for 15 min on a dry metal pan over a gas stove, maintaining a controlled surface temperature of 150°C while stirring constantly. Each batch of drying was approximately 40 grams of fresh leaves. The drying process was considered complete when the final moisture content

was <5% (w/w) determined using a moisture analyzer (HE53, Mettler Toledo, Greifensee, Switzerland). The dried leaf samples were illustrated in Figure B1 and were stored in aluminum pouches before being ground into fine powder using mixer mills (MM 400, Retsch GmbH, Haan, Germany) at 1000 Hz for 30 s.

For the aqueous extract preparation, a modified method based on that of Hayashi et al. (2008) was followed. A 1% (w/v) chaya leaf aqueous extract was prepared by boiling 2 g of dried chaya leaves with 200 mL of ultrapure water for 5 min. The solution was immediately filtered using filter paper, cooled to ambient temperature (~25°C) in an ice-water bath, and stored frozen in amber glass bottles for further analysis. This aqueous extract was used in the processes described in sections 3.2.6 and 3.2.7.

3.2.3 HS-GC/MS analysis

Analysis was done on the GCMS-QP2020 NX and HS-20 Trap system (Shimadzu Co., Japan) equipped with an SH-Rxi-5Sil MS column (0.25 μm df × 0.25 mm ID × 30 m length). 0.3 g of dried chaya powder was weighed in 20 mL headspace vials and sealed with a special PTFE-silicon spacer. To enable semi-quantitative analysis, 5 μL of 1000 ppm 3-methyl-2-heptanone was added to each sample as an internal standard. The absorbent trap dimension was 2 mm (ID) × 100 mm and the trap was filled with Tenax TA (amount not specified). Parameters for the HS-20 Trap for extracting volatiles in the "trap" mode (dynamic headspace) were as follows: sample line temp. 150°C; transfer line temp. 150 °C; trap cooling temp. -10 °C; trap desorption temp. 220°C; trap oven temp. 80°C; shaking level 3; equilibration time 15 min.; multi-injection count 10; pressurizing gas pressure 80 kPa; load time 0.5 min; load equilib. time 0.1 min; injection time 0.5 min; and GC cycle time 40 min. Parameters for the GC were as follows: column flow 1 mL/min of helium (99.9%); injection mode splitless; and column oven temp. program started at 35°C (held for 4 min), increased to 180°C at a rate of 15°C/min and finally

increased to 250°C at a rate of 40°C/min (held for 5 min.). Parameters for the mass spectrometer were as follows: ion source temp. 230°C; interface temp. 250°C; detector gain 0.87 kV; event time 0.3 sec.; scan acquisition mode; scan speed 1428 u/sec; mass scan range m/z 29-400. Compound identification was performed by comparing the mass spectra with the NIST 17 and the FFNSC 3 databases, considering spectra with >80% similarity as annotated. The retention index values of each component were calculated using an n-alkane solution (C7 to C30) under the same conditions. The annotated volatile compounds were further characterized by comparing measured and published retention index values along with the similarity index. Finally, the relative concentration of each component was determined using the following equation (Seo & Beak, 2009):

Relative concentration (ppb) =

$$\frac{1000 \times \text{peak area of compound} \times \text{weight of internal standard (µg)}}{\text{peak area of internal standard} \times \text{weight of the sample (g)}}$$

3.2.4 Calculation of relative odor active values

To consider the contribution of volatile compounds to the overall aroma, their odor active values (OAV) were calculated (Table B3, Appendix B). Based on the work of Gemert (2011), the OAV represents the ratio of the compounds' relative concentration to its odor threshold concentration. The relative contribution of each volatile component to the overall aroma was evaluated by calculating the percentage ratio of the OAV of an individual compound to the compound with the highest OAV in each treatment. This ratio, known as the relative odor active value (rOAV), was calculated using the following equation:

$$\text{rOAV} = \frac{C_i \times T_{max}}{C_{max} \times T_i} \times 100,$$

where C_i represents the relative concentration of the volatile compound (ppb); T_i is the aroma threshold of the compound in water (ppb); and C_{max} and T_{max} represent the relative concentration (ppb) and aroma threshold (ppb) of the compound with the highest OAV, respectively. A higher rOAV indicates a greater contribution of the component to the overall flavor of the sample. Compounds with rOAV ≥ 1 are considered key aroma compounds, whereas those with 0.1 ≤ rOAV < 1 are believed to be important modifiers of the overall aroma (Yi et al., 2021 & Sun et al., 2022).

3.2.5 UHPLC–qTOF/MS analysis

For the extraction process, ultrapure water containing 2 ppm of puerarin as an internal standard was used as the extraction solvent. Ten milligrams of leaf powder were mixed with one milliliter of the extraction solvent and boiled at 100°C using a shaking incubator (Eppendorf Thermomixer® C, Eppendorf, USA). After cooling to room temperature, 800 µL of dichloromethane was added to the samples, which were vortexed for 30 s and then centrifuged at 3000 g for 3 min. The upper phase (0.5 mL) was then filtered through a 0.22 µm microfilter and transferred to a glass vial. Nonvolatile nontargeted metabolomic analysis was performed following the method described by Hutasingh et al. (2023).

Raw mass spectrometry data were converted into .mzml format using LabSolution software. MS-DIAL (RIKEN, v.4.16) and used for peak detection, MS^2 data deconvolution, peak alignment, MS/MS extraction, relative quantification, and metabolite annotation. Background subtraction in MS-DIAL was performed using blank matrix samples. Initially, database metabolites were annotated using a public metabolomics library (http://prime.psc.riken.jp/compms/msdial/main.html#MSP) containing 13,303

unique compounds. Tentative and unknown peaks were further annotated with their elemental formulas and mass spectral fragmentation using MS-FINDER 2.0 (http://prime.psc.riken.jp/) (Lai et al., 2018). Peak identification parameters included an MS tolerance of 0.01 Da and MS/MS tolerance of 0.05 Da. The spectra were normalized by adjusting the peak area with the puerarin concentration as the internal standard before conducting subsequent analyses.

3.2.6 Evaluation of umami taste intensity using an electronic tongue

To remove polyphenols that could affect umami intensity measurements, poly(vinylpolypyrrolidone) (2 g) was added to a 100 mL aliquot following the method of Hayashi et al. (2008). The mixtures were shaken every 20 min for 60 min and filtered through filter paper. The collected filtrate was used for taste measurements.

Umami taste intensity of the samples was evaluated using the TS-5000Z taste sensing system (Intelligent Sensor Technology, Inc., Kanagawa, Japan) equipped with an umami taste sensor probe (SB2AAE) and a reference probe. The samples were analyzed with the probe, and the membrane electric potentials were stabilized in standard solutions. The measurements for each sample were averaged over four values. A standard curve relating the MSG concentration to the umami taste intensity response was constructed to convert the electronic tongue's umami intensity value into MSG equivalents (Figure A3, Appendix A). The MSG equivalent of each sample was then determined via interpolation.

3.2.7 Evaluation of TPC content and antioxidant activities

TPC was determined using the Folin–Ciocalteu technique adapted from the method of Swain and Hillis (1959). In a plastic vial, 40 μL of extract and 80 μL of 10% Folin–Ciocalteu reagent were mixed thoroughly using a Vortex mixer. After a 5-minute reaction, 320 μL of 3.5% Na_2CO_3 solution was added and mixed well. The solution was incubated in the dark at room temperature

(~25°C) for 2 h. The absorbance was measured at 725 nm using a microplate reader, and the results were expressed in gallic acid equivalents (mg/100 g fresh mass) using a gallic acid standard curve (0–0.1 mg/mL).

The 1,1-diphenyl-2-picrylhydrazyl (DPPH) radical scavenging activity was determined following a method described by Brand-Williams et al. (1995) with some modifications. A stock solution was prepared by dissolving 24 mg of DPPH in 100 mL of methanol, which was stored at −20°C. The working solution was prepared by mixing 10 mL of the stock solution with 45 mL of methanol to obtain an absorbance of 1.10 ± 0.02 units at 515 nm according to a microplate reader. In a dark environment, 360 μL of the working solution was mixed with 40 μL of the extract and incubated for 1 h. DPPH values (A_{515}) were reported as μmol Trolox equivalent (TE) per g dry matter based on a standard curve of authentic Trolox (50–1700 μM).

A ferric ion reducing antioxidant power (FRAP) assay was performed according to the method described by Benzie and Strain (1996) with some modifications. The FRAP working solution was freshly prepared by mixing 300 mM acetate buffer (3.1 g of sodium acetate trihydrate and 16 mL of acetic acid; pH 3.6), 10 mM 2,4,6-tripyridyl-s-triazine in 40 mM HCl, and 20 mM $FeCl_3 \cdot 6H_2O$ in a 10:1:1 ratio. The solution was warmed at 37°C before use. In a 96-well plate, 40 μL of the extract was mixed with 360 μL of the FRAP working solution and incubated at room temperature for 30 min in the dark. FRAP values (A_{593}) were reported as μmol TE per g dry weight based on a standard curve of authentic Trolox (50–1700 μM).

3.2.8 Statistical analysis

The umami taste intensity data obtained from electronic tongue analyses and the relative concentration of umami-related compounds were presented as means ± standard deviations and statistically analyzed using one-way ANOVA

with Duncan's test in SPSS 25.0 (IBM). Differences were considered to be significant at $p < 0.05$. For multivariate analyses, the relative concentration of metabolites was imported into MetaboAnalyst 5.0 (multivariate software) and subjected to cluster analyses, including principal component analysis (PCA) and heat map analyses with Pareto scaling. Partial least square (PLS) analysis was performed using SIMCA-P 14.1 (Umetrics, Umea, Sweden) to assess the relationships between the response variables, including umami taste intensity, TPC, and antioxidant activities (DPPH and FRAP assay results), and the explanatory variable, i.e., the concentrations of annotated metabolites. The optimal number of PLS components was determined based on the lowest root mean square error of prediction using the SIMCA-P algorithm. All experiments were conducted with four replicates.

3.3 Results and Discussion

3.3.1 Volatilomics analysis via HS-GC/MS

3.3.1.1 Distinct volatile metabolite profiles revealed by PCA across different drying methods

The drying methods employed in this study could be categorized into two groups. FD, VD, and OD50 were characterized as low-temperature–long-time processes involving drying for several hours, whereas OD120 and PR were classified as high-temperature–short-time processes, with samples being dried in <1 h to achieve a target final moisture content of <5% (w/w) wet basis.

PCA was performed on the relative content of 53 volatiles (Figure 3.1A) to provide an overview of the similarities in the volatile profiles across the drying methods. Principal components 1 (PC1) and 2 (PC2) accounted for 35.7% and 15.9% of the total variation, respectively. In

the PCA score plot, the clusters representing OD50 and VD showed close proximity and some overlap, indicating a degree of similarity in the volatile metabolite profiles of these two drying treatments. Conversely, OD120 and PR were positioned at the positive end of PC1, whereas FD, VD, and OD50 were located on the opposite side, indicating discrimination in the volatile profiles of chaya leaves subjected to high-temperature–short-time and low-temperature–long-time drying processes. Notably, the OD120 sample exhibited greater variance, occupying a larger area in the plot and spanning both the positive and negative sides of PC1, suggesting that the volatile profile of OD120 shares similarities with both high-temperature–short-time and low-temperature–long-time drying treatments.

3.3.1.2 Dominance of aldehydes as the primary volatiles in dried chaya leaves

The HS-GC/MS total ion chromatograms of the dried chaya leaf samples are presented in Figure B2, Appendix B. A total of 53 volatile compounds were annotated in these samples, categorized as 6 alcohols, 10 aldehydes, 10 ketones, 6 aromatic hydrocarbons, 7 heterocyclic compounds, 3 ethers and 11 others (Table B1, Appendix B). The relative concentrations of these compounds were expressed in µg/kg or ppb (Table B2, Appendix B). Notably, the total concentration of all flavor substances varied among the samples processed using different drying methods, with the OD120 sample exhibiting the highest relative content of total volatiles (Figure 3.1B). According to the HS-GC/MS data, aldehydes were found to be the prominent volatiles in the dried samples. Among them, the OD120 sample had the highest peak intensity of aldehydes (17,972 µg/kg), followed by the OD50 sample (17,210 µg/kg) (Table B2, Appendix B). This finding is consistent with previous research on dried *Cordyceps*, where oven-dried samples showed the highest concentration of aldehydes compared with samples

dried using other methods (Zhang et al., 2022). The formation of aldehydes during drying process can be attributed to the degradation and/or oxidation of unsaturated fatty acids (Zhang et al., 2021) and certain drying temperatures that promote their production through nonenzymatic or Maillard reactions, including the formation of Strecker aldehydes (generated by Strecker degradation) (Liu et al., 2015). Among the aldehydes, 3-methylbutanal exhibited the highest relative concentration across all samples, ranging from 4364.8 to 7928.1 µg/kg (Table B2, Appendix B). This aldehyde is one of the key volatiles in dried green tea providing malty and nutty aroma characteristics (Ho et al., 2015).

3.3.1.3 Changes in volatile metabolite concentrations among drying methods illustrated by heatmap analysis

The relative concentrations of annotated volatile metabolites were visualized on a heat map (Figure 3.1C) to observe the overall changes in chaya leaves under different drying methods. The heatmap clearly showed that the high-temperature–short-time drying methods (OD120 and PR) led to higher accumulation of volatiles compared with the low-temperature–long-time methods (FD, VD, and PR). The formation of these volatile compounds during the drying process is discussed in detail below.

3.3.1.3.1 Aldehydes

The dried chaya leaf samples contained an abundance of Strecker branched-chain aldehydes, namely 2-methylbutanal and 3-methylbutanal, which contribute to malt-like and roasted cocoa-like odors, respectively. These aldehydes were found at approximately a 2-fold higher concentration in OD50 and OD120 samples compared with FD samples (Table B2, Appendix B). They are formed through the

Maillard reaction involving free amino acids, such as leucine and isoleucine, as precursors (Smit et al., 2009). Notably, the relative contents of these amino acids were much lower in the PR sample compared with the other samples, which is further discussed in section 3.3.2.

Interestingly, in the PR sample, the concentration of 3-methylbutanal was expected to be the highest due to the high drying temperature promoting the Maillard reaction. However, its concentration was similar to that in the FD sample. This could be implied that the compound could be formed via nonenzymatic reaction and then decrease later. The increasing and decreasing tendency of 3-methylbutanal during PR was also reported by Flaig et al. (2020). This discrepancy was attributed to the evaporation of Strecker aldehydes during PR due to relatively high drying temperature. Therefore, the formation of these branched-chain aldehydes is dependent on the drying temperature and method employed. However, the concentration of 2-methylbutanal significantly increased in the PR sample ($p < 0.05$), although the underlying mechanism for this opposite trend of the compounds remains unknown. Additionally, other aldehydes commonly found in leafy green vegetables, such as hexanal and 2-hexenal, which provide a fresh-cut green grass aroma, were 1.5–3.0-fold more concentrated in FD samples compared with the other samples (Table B2, Appendix B). This suggests that the low-temperature process used in FD better preserves these volatile compounds. These C-6 aldehydes are key odorants in green tea and are derived from lipids primarily through lipoxygenase-mediated lipid oxidation (Ho et al., 2015). In this study, hexanal could possibly result from post-harvesting before the drying process such as washing, mixing, and cooling.

3.3.1.3.2 Heterocyclic and aromatic compounds

Heterocyclic compounds were found at higher concentrations in the PR sample (Figure 3.1C), although they were mostly undetectable in the samples from other drying methods. These nitrogen-containing heterocyclic compounds typically possess a roasted odor, which is generated through high heat treatment and is commonly found in roasted and toasted foods. Amino acids, such as glycine, valine, phenylalanine, methionine, and alanine, act as aroma precursors for these roasted-aroma compounds, as they react with reducing sugars to produce volatile compounds with pyrazine, pyrrole, or furan structures (Guo et al., 2021).

Aromatic compounds, such as toluene, ethylbenzene, and o-xylene, were also accumulated in samples subjected to high-temperature–short-time drying treatments (OD120 and PR; Figure 3.1B). This finding is consistent with the research of Ye et al., (2021), who observed an increase in the concentration of volatile aromatic compounds, including toluene and naphthalene, of up to 2–3-fold in dried black tea when the drying temperature was elevated. This can be attributed to the promotion of the Maillard reaction at higher temperatures, which leads to the production of aromatic compounds (Scalone et al., 2015).

3.3.1.3.3 Alcohols

As shown in Figure 3.1B, the FD sample showed the highest concentration of alcohols, including (R, R)-butane-2,3-diol, (Z)-3-hexen-1-ol, 1-penten-3-ol, 2-butyl-1-octanol, and 1-hexadecanol (Table S2). The lower temperature during the FD process allows for the preservation of alcohol content, as alcohols are prone to degradation and evaporation at higher temperatures through enzymatic and nonenzymatic reactions (Guo et al., 2018). This finding is consistent

with the study of Zhang et al. (2021), who observed a decrease in alcohol content when using higher drying temperatures. However, odor thresholds are higher in alcoholic odorants than in aldehyde compounds and may contribute less to the overall aroma of chaya leaves.

3.3.1.3.4 Ketones

Ketones in dried food products are formed through thermal oxidation/degradation of fatty acids, amino acid degradation, or microbial oxidation (Spurvey et al., 1998). Among the dried chaya leaf samples, 2,3-butanedione, which imparts a nutty and buttery aroma, was only detected in the FD sample. In contrast, 2-heptanone, with a sweet and fruity aroma, was present in all samples except FD, and its concentration increased in the OD120 and PR samples. Furthermore, 6-methyl-5-hepten-2-one (methylheptenone), a key volatile ketone in Chinese yellow tea that provides a sweet and fruity aroma (Hong et al., 2023), was detected in all samples, with the highest concentration observed in OD120 and PR.

(A)
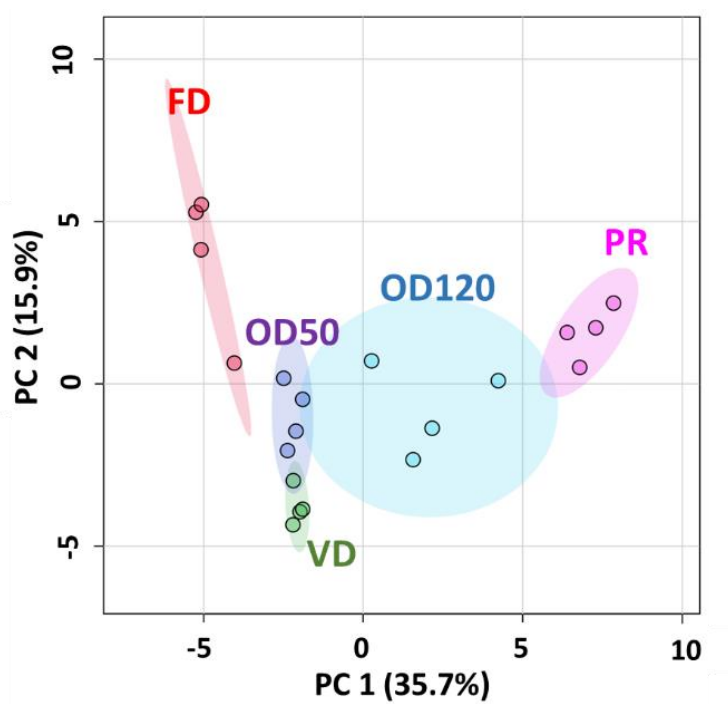
(B)
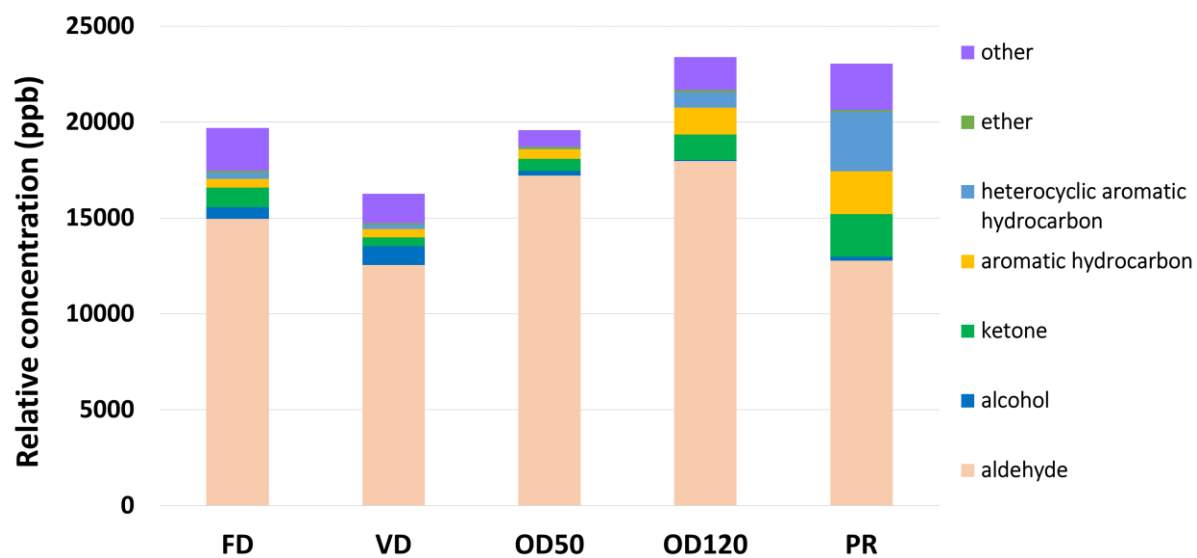
(C)
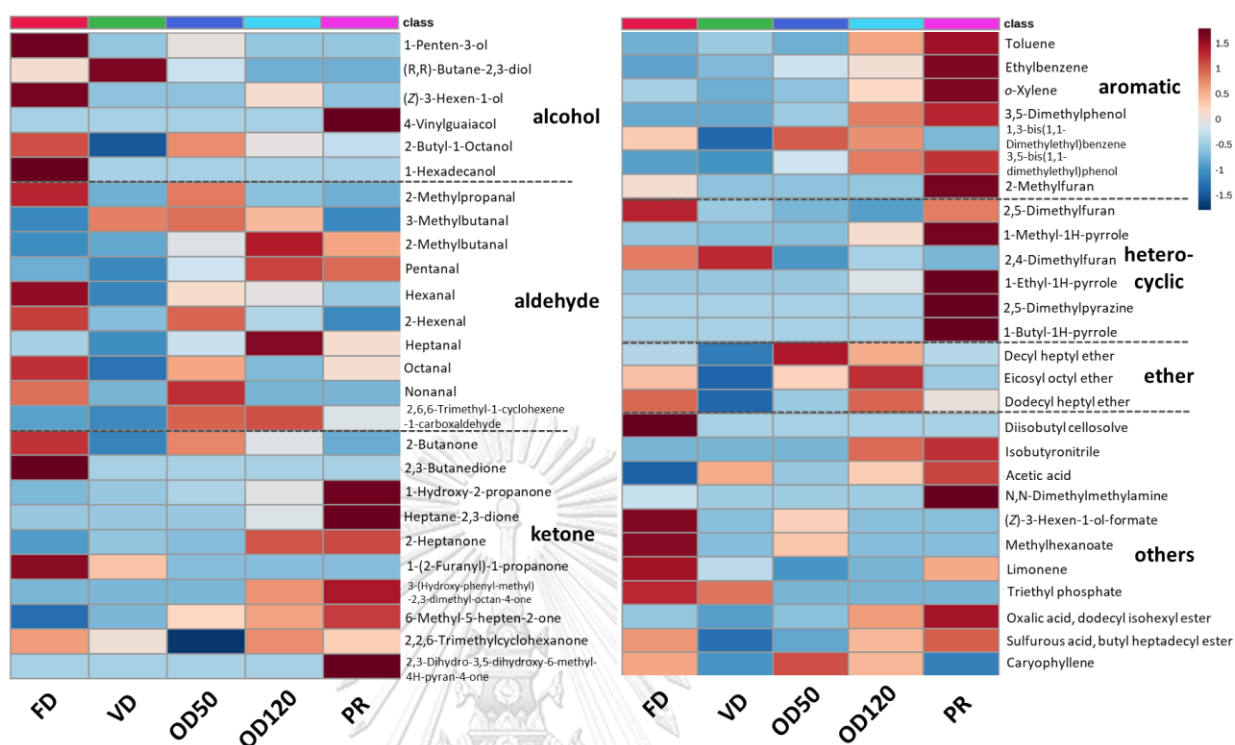
Figure 3.1 Analysis of chaya leaf volatile metabolites by HS-GC/MS. Plot of principal component analysis scores for all samples obtained from HS-GC/MS data. Each sample point represents a biological replicate (n = 4) (A). Mean value of relative concentration (ppb) of volatiles in chaya leaves prepared using different drying methods (n = 4) (B). Heatmap visualization of annotated volatile metabolites based on relative concentration data from HS-GC/MS. The color in the heatmap represents significance of differences (p < 0.05) between mean values of the relative concentration of each metabolite between drying treatments, with red and blue indicating higher and lower abundances, respectively (C).

3.3.1.4 Key aroma compounds in dried chaya leaves were revealed via rOAV analysis

To identify the volatile compounds contributing to the overall aroma of chaya leaf samples dried using different methods, 14 volatiles with rOAV ≥ 0.1 were considered (Table 3.1). Among all samples, aldehydes exhibited the highest rOAV, characterized by low odor

thresholds and unique aromas. The key aroma compounds in dried chaya leaves, with rOAV ≥ 1, were 3-methylbutanal, 2-methylbutanal, 2-methylpropanal, pentanal, hexanal, 2-hexanal, octanal, nonanal, and 4-vinylguaiacol. Notably, 3-methylbutanal, with an rOAV of 100, had the highest OAV among all samples. The OAV of 3-methylbutanal were in the range of two to five thousand, while the other volatile has OAV less than a thousand (Table B3, Appendix B). This could be implied that the main aroma characteristic of dried chaya leaves regardless of drying method is malt-like aroma. 2-Methylbutanal, a cocoa and coffee-like volatile, has the second highest rOAV in OD120 and PR samples. This indicates that the samples subjected to high-temperature–short-time drying treatment (OD120 and PR) may provide cocoa or coffee-like odor characteristics. However, in FD samples, the second highest rOAV hexanal possessing grassy green odor, respectively. Overall, dried chaya leaf may have malty-like aroma as dominant aroma characteristics, with a green grass–like aroma detected in FD samples and more pronounced coffee- and cocoa-like characteristics in OD120 and PR sample. Interestingly, the key aroma compounds identified in chaya leaves, such as 2-methylbutanal, 3-methylbutanal and hexanal, resemble those reported for dried green tea (Flaig et al., 2020).

Table 3.1 Relative odor activity values (rOAV) of key aroma active compounds of chaya leaves dried using different drying methods.

Compound	Category	Aroma description	Thresholda (ppb)	rOAV				
				FD	VD	OD50	OD120	PR
4-Vinylguaiacol	alcohol	clove-like roasted peanut odor	0.4	0.0	0.0	0.0	0.0	11.2
2-Methylpropanal	aldehyde	aldehydic, pungent, floral odor	4.0	9.2	0.0	3.9	0.5	0.0
3-Methylbutanal	aldehyde	Malty, nutty, almond, cocoa	0.15	100.0	100.0	100.0	100.0	100.0
2-Methylbutanal	aldehyde	cocoa or coffee-like	12.5	6.3	4.2	6.1	11.3	14.4
Pentanal	aldehyde	fermented bready	12	2.1	1.0	1.5	2.6	4.1
Hexanal	aldehyde	grassy green	4.5	11.4	3.0	4.5	4.8	6.7
2-Hexenal	aldehyde	fresh green odor	30	1.71	0.3	0.9	0.4	0.3
Heptanal	aldehyde	fruity to greasy odor	30	0.41	0.2	0.3	0.6	0.6
Octanal	aldehyde	fruit-like odor	0.7	8.2	1.6	3.7	2.4	5.7
Nonanal	aldehyde	rose-orange odor	1.4	9.01	0.0	5.8	0.0	0.0
2,6,6-Trimethyl-1-cyclohexene-1-carboxaldehyde	aldehyde	tropical odor	5	0.2	0.1	0.2	0.2	0.2
2,3-Butanedione	ketone	strong chlorine-like	20	0.75	0.0	0.0	0.0	0.0
6-Methyl-5-hepten-2-one	ketone	citrus, fruity	50	0.1	<0.1	0.1	0.1	0.2
Limonene	terpene	orange-like	10	0.2	<0.1	0.0	<0.1	0.1

[a] Thresholds of volatile compounds were obtained from Gemert (2011).

3.3.2 Metabolomic analysis via UHPLC–qTOF/MS

3.3.2.1 PCA reveals distinct nonvolatile metabolite profiles among drying methods

Using UHPLC–qTOF/MS, a comprehensive range of nonvolatile metabolites was captured. In total, 64 annotated metabolites were used to construct an unsupervised PCA (Figure 3.2A; Table B4, Appendix B). PC1 and PC2 accounted for 75.0% and 9.1% of the variance, respectively. In PC1, the PR and OD120 samples were positioned on the positive axis and clearly separated from the FD, VD, and OD50 samples located on the negative axis, indicating that the nonvolatile metabolites of OD120 and PR samples, which were dried using high-temperature–short-time methods, exhibit greater similarity compared with samples dried under low-temperature–long-time condition. Overall, distinct clusters exhibited clear separation, highlighting significant differences in nonvolatile metabolites among the different drying methods.

3.3.2.2 Heat map analysis illustrated changes in nonvolatile metabolite concentrations among drying methods

As shown in Figure 3.2B, the heatmap was constructed to illustrate the relative concentration of each metabolite among samples. Generally, the concentration of free amino acids, peptides, and nucleotide-related metabolites exhibited significant decreases in concentration in both OD120 and PR samples compared with the samples from other drying methods. However, the concentration of organic acids, flavonoids, sugars, and other compounds varied among the different drying methods.

3.3.2.2.1 Free amino acids

Sixteen taste-related amino acids were annotated in chaya leaves, including five sweet amino acids (proline, alanine, serine, threonine, and tryptophan), eight bitter amino acids (valine, leucine, isoleucine, methionine, phenylalanine, arginine, lysine, and tyrosine), and two umami amino acids (aspartic acid and glutamic acid). Among these, phenylalanine had the highest relative concentration compared with the other amino acids (Table B5, Appendix B). However, in OD120 and PR samples, the concentration of phenylalanine and other bitter-tasting amino acids significantly decreased (by approximately 2–10-fold). The decrease could be attributed to the high reactivity of bitter amino acids in the Maillard reaction, as reported previously Liu et al. (2015).

In contrast, the abundance of umami-tasting amino acids (glutamic acid and aspartic acid) in OD120 and PR samples was similar to that in the FD sample but markedly higher (~2-fold) than that in the VD and OD50 samples. This suggests that the umami taste intensity of OD120 and PR samples may not be affected by the high-temperature–short-time drying treatment. However, the drying conditions of VD and OD50 led to a significant decrease in the content of glutamic acid and aspartic acid (by approximately 4-fold). This decrease could be attributed to the activation of the glutamate dehydrogenase (GDH) enzyme at certain drying temperatures, leading to the conversion of glutamic acid to α-ketoglutaric, which is involved in carbohydrate metabolism during plant stress. Li et al. (2021b) found that heat stress increased the expression levels of both GDH-regulated genes (PhGDH1 and PhGDH2) in red algae ($p < 0.05$). Initially, gene expression levels rapidly increased and remained high throughout the stress, but a further increase in stress intensity led to decreased expression levels, possibly due to cell damage caused by high temperatures. Similarly, in green lettuce (*Brassica juncea* L.), heat

stress at 42ºC activated the GDH enzyme, resulting in the deamination of glutamic acid to form α-ketoglutaric and ammonium, leading to a decrease in glutamic acid content (Goel & Singh, 2015). A similar observation was made for glutamine content, which showed a decreasing trend in VD and OD50 samples, as both glutamate and glutamine are involved in the GS/GOGAT cycle for nitrogen assimilation.

The decreasing trend of umami-tasing amino acid levels observed in samples subjected to the low-temperature–long-time drying methods has also been reported. Zhang et al. (2022) observed a significant decrease ($p < 0.05$) in glutamic acid and aspartic acid concentration in dried cordyceps following the VD process.

3.3.2.2.2 Peptides

In total, 25 small peptides were annotated including γ-glutamyl peptides, dipeptides, and tripeptides. γ-Glutamyl dipeptides known for their desirable kokumi-imparting properties (mouthfulness and flavor continuity). Among the annotated peptides, γ-glutamylvaline was the most abundant. This kokumi peptide was also found to be abundant in our previous study using 70% methanolic extract (Hutasingh, et al., 2023). Glutathione or γ-L-glutamyl-L-cysteinylglycine, a natural antioxidant found in plants, was only detected in the FD sample. This is because glutathione is highly sensitive to heat and unstable in aqueous solutions (Masayoshi et al., 1980). Consequently, the oxidized form of glutathione showed an increasing trend in the OD50, OD120, and PR samples of which the presence of oxygen and heat triggered the formation of the compound. As shown in Figure 3.2B, dipeptides were the predominant peptides in dried chaya leaves. However, their abundance significantly decreased or disappeared when subjected to harsher drying conditions (OD120 and PR) as they could be consumed

by the nonenzymatic reaction (Zhang et al., 2016b). Furthermore, most of the peptides identified in our previous study (Hutasingh et al., 2023) were also found in the current study, indicating that peptides can be extracted using both methanol and water.

3.3.2.2.3 Nucleotide-related metabolites

In mushroom, 5'-ribonucleotide is a crucial umami-tasting compound that contributes to strong umami taste (Wen et al., 2022). In our previous study, we identified 5'-AMP as one of the key umami compounds in chaya leaves (Hutasingh et al., 2023). Given the heat sensitivity of most nucleotide-related metabolites, it was important to focus on changes in their abundance in this study.

In samples subjected to high-temperature drying process (OD120 and PR), significant decreases were observed in nucleotide substances, such as adenosine, adenine, guanosine, and guanine. Nucleotides can also degrade into other substances through oxidation (Wen et al., 2022). We observed that VD samples had the highest abundance of most nucleotides (Figure 3.2B), possibly due to the limited oxygen content under the vacuum conditions. Among all nonvolatile metabolites annotated in the dried chaya leaf samples, adenosine had the highest relative abundance (Table B5, Appendix B). Adenosine has been reported to enhance sweet taste through A2B receptors in taste buds without affecting umami taste responses (Dando et al., 2012). Thus, the high concentration of adenosine found in chaya aqueous extract could provide a pleasant, sweet taste to food.

Surprisingly, the umami-tasting nucleotide 5'-AMP exhibited a markedly higher concentration in OD120 and PR samples (2–3-fold higher) compared with the FD sample, whereas 5'-GMP content peaked in the OD120 sample (Table B5, Appendix B). Similar findings

were reported by Raigond et al. (2015) who found the 143.4% increase in a total of 5'-AMP and 5'-GMP content in cooked potatoes compared with raw potatoes. This could be attributed to the activation of cytoplasmic phosphodiesterase enzymes at higher temperatures, leading to the splitting of cyclic adenosine monophosphate (cAMP) and cyclic guanosine monophosphate (cGMP) into their umami-tasing components, 5'-AMP and 5'-GMP, respectively. The optimum temperature for phosphodiesterases in plants is around 65°C–70°C (Hua & Huang, 2010). Therefore, during the drying process of OD120 and PR, it is possible that at the early state of drying, where temperature was not too high to inactivate the enzymes and amount of free water was sufficient for enzymatic reactions, resulting in increased 5'-AMP and 5'-GMP content, with decreased cAMP and cGMP content as shown in the heatmap (Figure 3.2B). In contrast, the concentration of these umami nucleotides reached its lowest level when chaya leaves were dried using VD and OD50 methods, as the long-time thermal drying processes led to the degradation of 5'-nucleotides (Li et al., 2021a), and the drying temperature was below the optimum temperature of phosphodiesterases, inhibiting the formation of 5'-AMP and 5'-GMP from their precursors, cyclic nucleotides.

3.3.2.2.4 Sugars

The sugar content, including sucrose and gentiobiose, a disaccharide composed of two D-glucose molecules linked via beta (1, 6) linkage, peaked in the PR sample. This can be attributed to the harsh drying conditions under PR (150°C), which promote the dimerization of glucose molecules into gentiobiose through caramelization (Sugisawa, et al., 1966). OD120 and PR samples showed higher sucrose accumulation, as the extreme heat used to dry these samples increased their sucrose content (Figure 3.2B). Sucrose serves as a major protective sugar in plant cells and is accumulated in the late stage of

the drying process, likely resulting from the metabolic conversion of monosaccharides as part of the plant cell's protective mechanism (Ghasempour et al., 1998).

3.3.2.2.5 Organic acids

In our previous study, we found that quinic acid is a novel umami compound imparting umami taste in chaya leaves (Hutasingh et al., 2023). In OD50, OD120 and PR samples, the abundance of quinic acid increased by 1.5-fold compared with that in FD samples. This trend of increased quinic acid content could be due to thermal process was also observed in coffee bean roasting. Dawidowicz & Typek (2017) reported that the increase in quinic acid concentration was due to thermal decomposition of chlorogenic acid. Chlorogenic acid are ester phytochemicals formed between cinnamic acid derivatives and quinic acids. Although chlorogenic acid was not detected in chaya leaf in this study, this compound was described by Ramos-Gómez et al. (2016) as one of the major organic acids found in chaya leaf . Moreover, the 3-hydroxycinnamic acid, a nonflavonoid phenolic compound, also annotated in Chaya leaves at high relative concentration in VD samples (Figure 3.2B). Thus, it is possible that chlorogenic acid could be degraded, leading to an increase in quinic acid in OD120 and PR samples. Furthermore, we speculate that L-ascorbic acid or vitamin C, a heat-sensitive antioxidant, was only detected in FD samples owing to its thermal degradation in other drying treatments and the 3-hydroxycinnamic acid has a significant rise in VD samples ($p < 0.05$) caused by the thermal degradation of the parental molecules and consequently, be preserved by the limited of oxygen. This may explain the significant increase in antioxidant activity and total phenolic content in FD and VD samples, as discussed in section 3.3.4.

In our previous study, we found that quinic acid is a novel umami compound imparting umami taste in chaya leaves (Hutasingh et al., 2023). In OD50, OD120 and PR samples, the abundance of quinic acid increased by 1.5-fold compared with that in FD samples. This trend of increased quinic acid content could be due to thermal process was also observed in coffee bean roasting. Dawidowicz & Typek (2017) reported that the increase in quinic acid concentration was due to thermal decomposition of chlorogenic acid. Although chlorogenic acid was not detected in chaya leaf in this study, this compound was described by Ramos-Gómez et al. (2016) as one of the major organic acids found in chaya leaf. Thus, it is possible that chlorogenic acid could be degraded, leading to an increase in quinic acid in OD120 and PR samples. Furthermore, we speculate that L-ascorbic acid or vitamin C, a heat-sensitive antioxidant, was only detected in FD samples owing to its thermal degradation in other drying treatments. This may explain the significant increase in antioxidant activity in the FD sample, as discussed in section 3.3.4.

3.3.2.2.6 Flavonoids

Four flavanol glycosides, namely rutin (quercetin-3-O-rutinoside), robinin (kaempferol-3-O-robinoside-7-O-rhamnoside), biorobin (kaempferol-3-robinobioside), and nicotiflorin (kaempferol-3-O-rutinoside), were annotated in all the dried chaya leaves, consistent with our previous findings (Hutasingh et al., 2023). Overall, the flavonoid content showed minimal variation among the dried samples (Figure 3.2B; Table B5, Appendix B), except for a decrease of approximately 2-fold in rutin and robinin in the OD50 and PR samples, respectively. The differential responses of flavonoid compounds to heating methods may be attributed to their specific reactivity during the various heating processes. Notably, the PR sample contained the lowest concentration of robinin, the most abundant flavonoid identified

in dried chaya leaves (Table B5, Appendix B), compared with the samples from other drying treatments, suggesting that high temperatures can lead to the degradation of flavonoid content through thermal degradation and oxidation. Lemus-Mondaca et al. (2015) reported that higher drying temperature (>50°C) caused a significant loss of flavonoids as the heat breaks down cellular constituents accelerating the release and degradation of flavonoids.

(A)
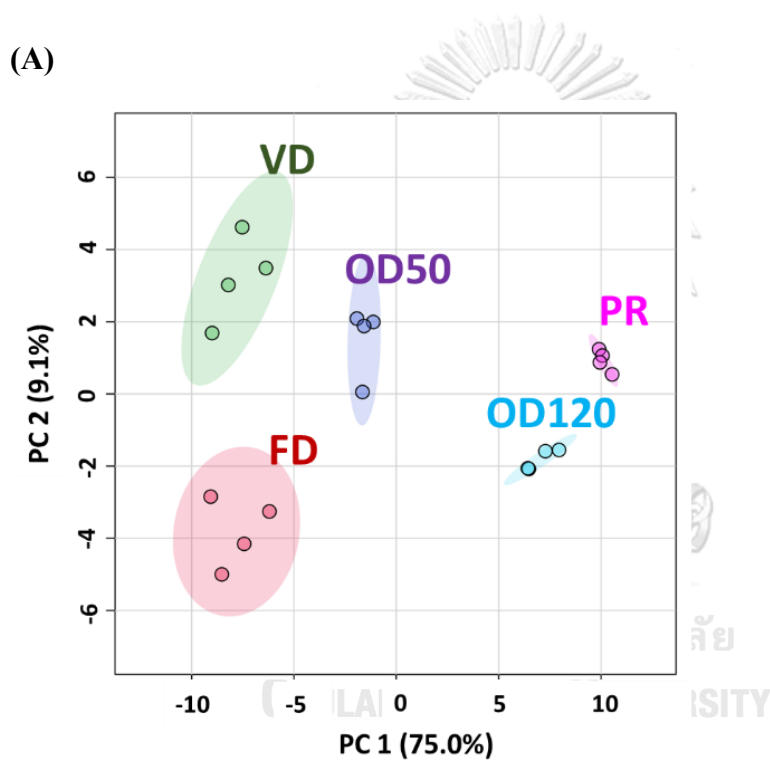
(B)
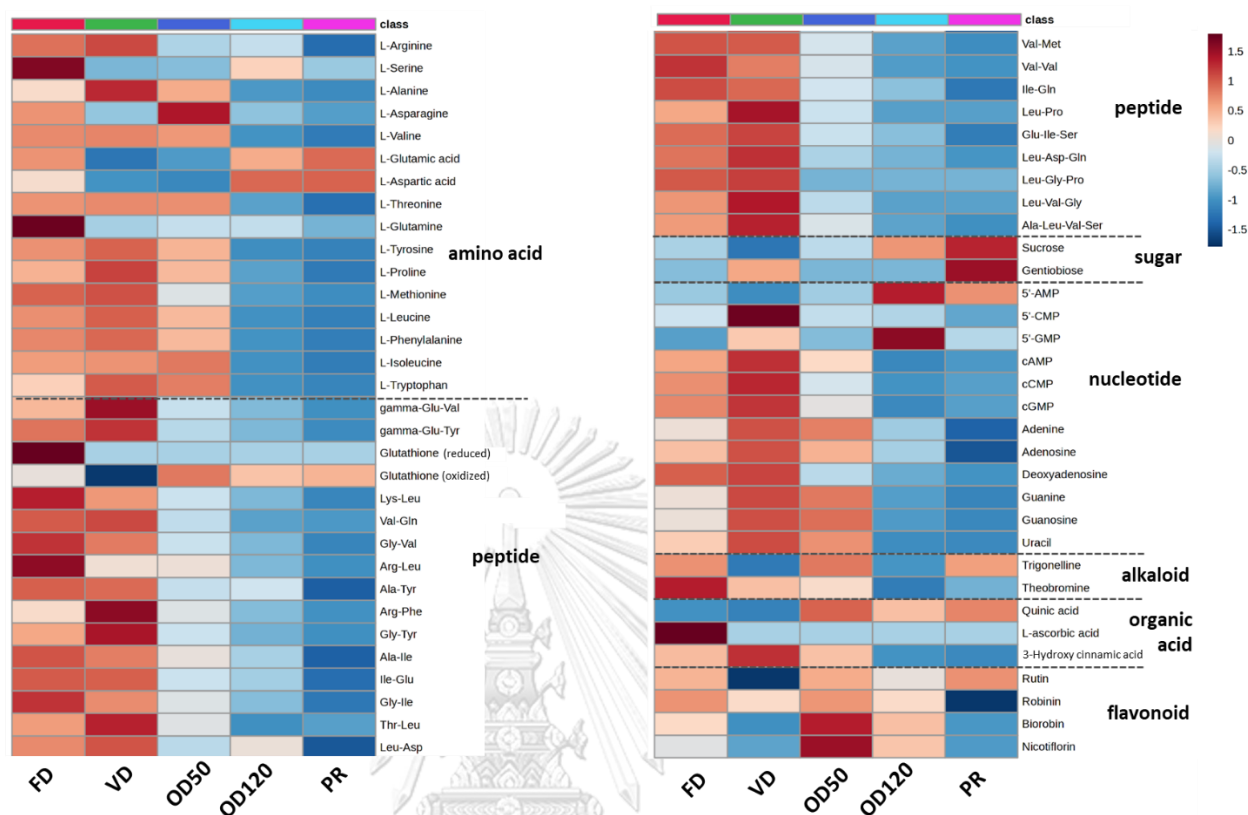
Figure 3.2 Analysis of chaya leaf metabolites using UHPLC–qTOF/MS. Plot of principal component analysis scores for all samples obtained from UHPLC–qTOF/MS data. Each sample point represents a biological replicate (n = 4) (A). Heatmap visualization of annotated metabolites based on normalized peak area data from UHPLC–qTOF/MS (B). The color in the heatmap represents significance of differences ($p < 0.05$) between mean values of the normalized peak area of each metabolite between drying treatments, with red and blue indicating higher and lower abundances, respectively.

3.3.3 Umami intensity elevation in OD120 and PR samples revealed by electronic tongue analysis

Electronic tongue analysis has been employed in various food studies owing to its strong correlation with human sensory evaluation, high sensitivity, and objectivity (Gao et al., 2021). Figure 3.3 shows the relationship between the normalized peak area of umami-related compounds in dried chaya leaves, as determined via UHPLC–qTOF/MS, and umami taste intensity measured using an electronic tongue. Umami taste intensity ranged from 5.2 to 7.0, depending on the drying method used, with significantly higher levels observed in OD120 and PR samples. This suggests that the substantial increase in umami-tasting nucleotides, such as 5'-AMP and 5'-GMP, in combination with existing umami amino acids, synergistically enhances the umami taste of chaya leaves. In our previous research, the umami taste intensity of a 1% (w/v) aqueous extract of freeze-dried young and mature chaya leaves was evaluated using an electronic tongue and found to be approximately 10 and 5, corresponding to approximately 0.13% and 0.02% (w/w) of MSG, respectively (Hutasingh et al., 2023). These values were above the reported umami taste detection threshold [1.38 mM or 0.02% (w/v)] (Webb et al., 2015) and could potentially be perceived by humans. In the present study, a mixture of young and mature *C. chayamansa* leaves was used to prepare the 1% (w/v) aqueous extract for umami taste intensity determination. The obtained umami intensities were then converted to %MSG equivalents using a standard curve (Figure B3, Appendix B). The umami taste intensity of the aqueous extract corresponded to 0.02%–0.04% (w/v) MSG. These values were slightly lower than those reported in our previous study (Hutasingh et al., 2023), as the inclusion of mature leaves in the mixture resulted in a slight reduction in umami taste intensity. The highest umami taste intensities were observed in the OD120 sample (6.92) and PR sample (6.70), equivalent to approximately 0.04% (w/v) MSG.
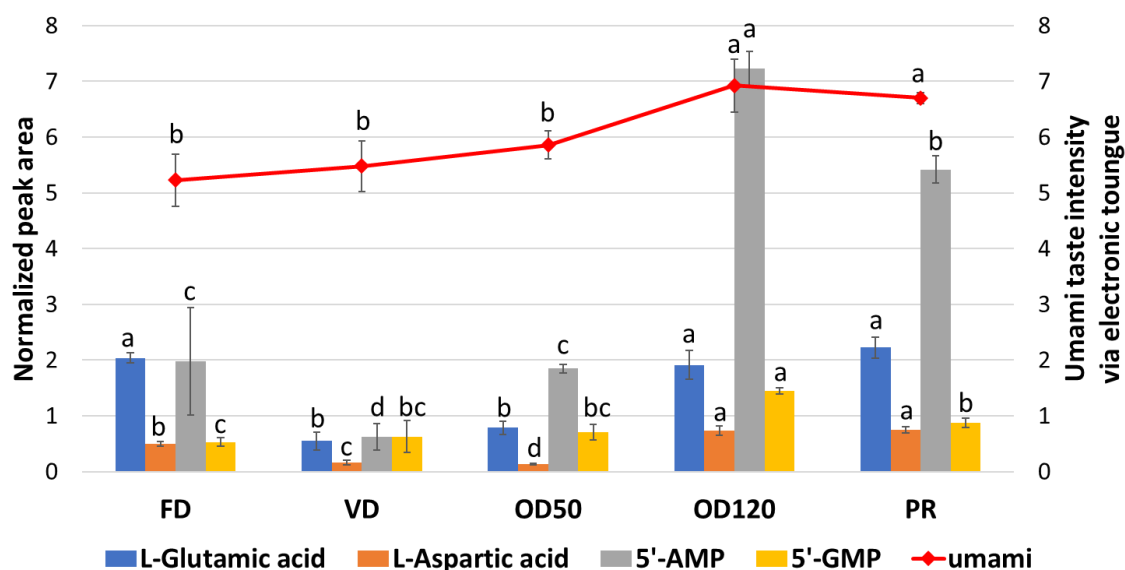
Different letters (a–d) among the drying methods indicate significant differences in each compound's concentration/umami taste intensity, as determined via ANOVA and Duncan's test ($p < 0.05$).

Figure 3.3 Umami-related compounds and umami intensity in chaya leaf aqueous extracts. Mean values of normalized peak areas of umami-tasting compounds (primary y-axis) in chaya leaf aqueous extracts and their corresponding umami intensity values (n = 4) (secondary y-axis).

3.3.4 Effect of drying method on TPC and antioxidant activities of dried chaya leaves

Drying chaya leaves is a common practice to produce shelf-stable products, such as tea infusion and seasoning powder. However, thermal drying can lead to the degradation and oxidation of phenolic compounds and a reduction in antioxidant through enzymatic- and non-enzymatic oxidation, enzymatic degradation and/or heat decomposition (Chan et al., 2009). Therefore, the TPC and antioxidant capacity were analyzed to assess the quality of chaya leaves dried using different methods.

Figure 3.4 shows the results of TPC and antioxidant activity analysis in dried chaya leaves. The FD sample exhibited the highest TPC (156.11 ± 4.55 mg gallic acid eq./g dry weight) and antioxidant capacity, as determined through both DPPH (691.50 ± 39.37 μmol Trolox eq./g dry weight) and FRAP (513.75

± 29.53 µmol Trolox eq./g dry weight) assays. FD, performed at a lower temperature compared with the other drying methods, minimized the loss of TPC and antioxidant compounds through thermal degradation. Moreover, it is spotted the higher abundance of amino acid and peptide in FD and VD samples (Figure 3.2B). Zou et al., (2016) reported that free amino acids (cysteine, cystine, histidine, methionine, tryptophan and tyrosine) and peptides could display antioxidant activities and could provide a positive result to TPC. For example, tryptophan containing peptide could exert antioxidant activities as the indole ring serves as an active hydrogen donor of the indole radical influencing the antioxidant activity of the total peptides (Tian et al., 2015). This could interfere with the TPC test and provide positive error as the reducing power of such amino acids and peptides were detected.

The OD50 sample exhibited significant lower ($p < 0.05$) antioxidant activities for both assays and slightly lower TPC than that in OD120 and PR samples. Although the heat used in OD50 was moderate, the longer drying time of two days exposed the leaf sample to oxygen under atmospheric conditions, leading to the degradation of antioxidant compounds via enzymatic degradation, especially when there are adequate amount of free water at the beginning of drying period (Chan et al., 2009). Similar findings were reported by Sun et al. (2015) for citrus slices dried at relatively low temperatures (20°C–25°C) over 48 h, resulting in larger deterioration of TPC and antioxidant activities compared with other drying methods.

The VD sample, dried at a temperature similar to the OD50 sample, exhibited significantly higher TPC and antioxidant activities via DPPH assay compared with the OD50 sample ($p < 0.05$). The vacuum process limited the oxygen content, resulting in less deterioration of antioxidant compounds by oxidation. OD120 and PR samples exhibited the second highest antioxidant activities in both DPPH and FRAP assays. These drying treatments accelerated moisture reduction, allowing the sample to reach the desired moisture content (< 5% w/w) in less than 1 h. By this, the degradative enzyme activities are limited

due to the low water activity and the levels of antioxidant activities remained (Hassain et al., 2010).

Correlations between TPC and antioxidant activities for different drying processes were analyzed (Table B6, Appendix B). The antioxidant activities exhibited a very strong positive correlation between the DPPH and FRAP assays (r = 0.99), which aligns with previous research (Xu et al., 2011). These results are consistent with the shared reducing mechanisms of the two assays, involving the transfer of electrons from an antioxidant to reduce an oxidant. However, the correlations between TPC and DPPH (r = 0.54) and FRAP (r = 0.44) were moderate. Phenolic compounds, such as polyphenols and flavonoids, mainly contribute to plant antioxidants; however, we identified reducing free amino acid, peptides, ascorbic acid and glutathione having higher concentration in the FD sample. These substances are not phenolic compounds but known to exhibit strong antioxidant activity. (Bartoli et al., 2009). This could explain why the FD sample exhibited the highest antioxidant activity among the different drying treatments but not in terms of TPC.

(A)
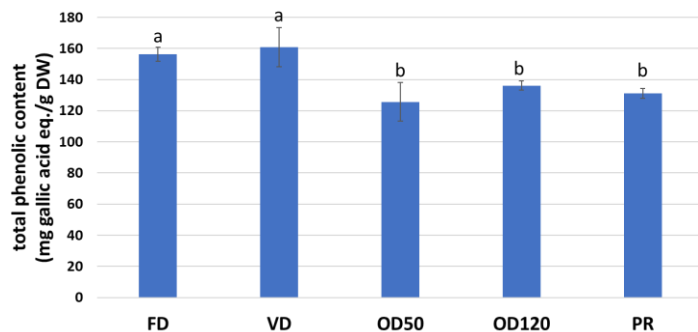
(B)
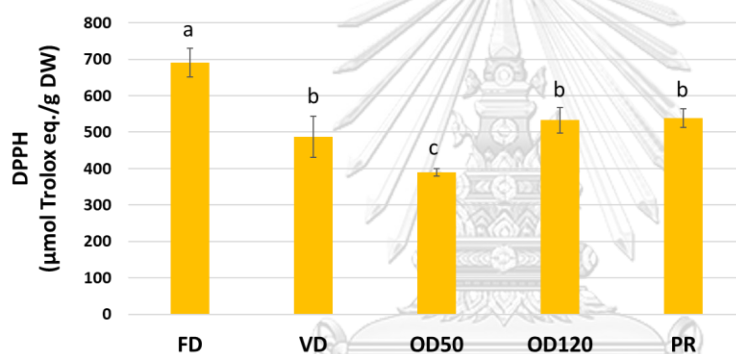
(C)
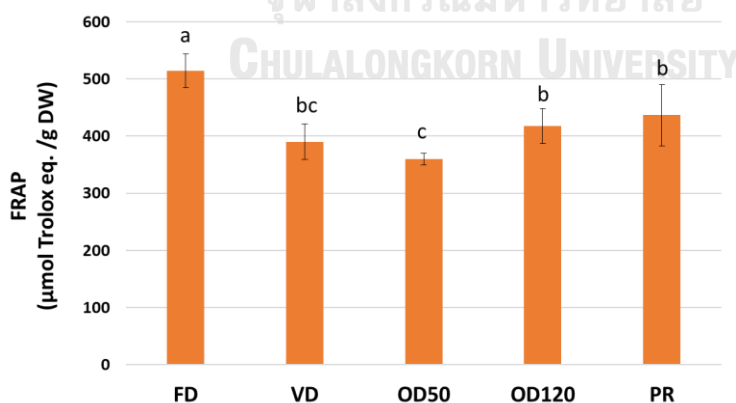
Figure 3.4 Total phenolic content and antioxidant activity of chaya leaf aqueous extracts under different drying methods. Comparison of total phenolic content (A) and antioxidant activity analyzed using either the DPPH assay (B) or FRAP assay (C), in chaya leaf aqueous extract subjected to various drying treatments. Different letters (a–

c) among the different drying methods indicate significant differences, as determined using ANOVA and Duncan's test ($p < 0.05$). The results are presented as means ± standard deviations (n = 4).

3.3.5 PLS biplot analysis illustrates the overall relationship between nonvolatile metabolite concentrations, umami intensity, TPC, and antioxidant activities

To visualize the overall relationship between drying methods, nonvolatile metabolite concentrations, umami taste intensity, and antioxidant activities of chaya leaves, a PLS biplot was constructed (Figure 3.5). The first component of PLS divided the low-temperature–long-time drying treatments (FD and VD) to the left side of the biplot and the high-temperature–short-time drying treatments (OD120 and PR) to the right side, with the OD50 treatment located in the center, close to the y-intercept. This clear separation of samples indicates that nonvolatile metabolite concentrations were influenced by different drying methods.

Umami taste was positioned on the right part of the biplot, close to the periphery, indicating significant variation in umami intensity among the samples, which was highly influenced by changes in metabolite abundance. Additionally, each sample was grouped near the response variable and related metabolites in their respective quadrants. On the right part of the plot, OD120 and PR samples were associated with glutamic acid, aspartic acid, 5'-AMP, 5'-GMP, and umami intensity. This aligns with the higher concentration of these compounds observed in OD120 and PR samples (Figure 3.3) and their recognized contribution to umami taste in food systems, as discussed previously. Moreover, FD and VD samples were clustered closely on the left side of the plot, associated with most of the free amino acids and short peptides, indicating an accumulation of these compounds in the samples. Furthermore, antioxidant activities analyzed via both assays were also located in the same quadrant, with FD samples positioned adjacent to ascorbic acid and glutathione, confirming the contribution of these compounds to the

antioxidant activities of FD samples. Additionally, TPC was relatively close to amino acids and peptides, indicating their contribution to this parameter. The correlation observed between antioxidant activities, umami taste quality, and nonvolatile metabolites in the biplot is in alignment with the patterns observed in the earlier discussion of metabolite profiling.
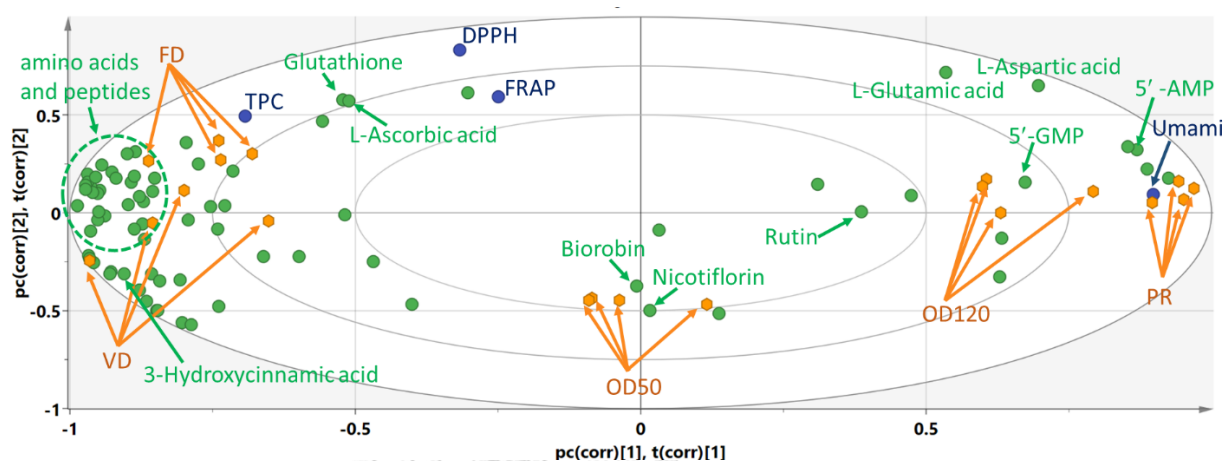
Figure 3.5 Correlation biplot of umami taste, total phenolic content (TPC), antioxidant activity, and metabolite concentrations in chaya leaves, Correlation biplot shows results of PLS analysis and indicates the relationships among the Y-variables (umami taste, TPC, and antioxidant activity analyzed using DPPH and FRAP assays) and the X-variables (relative metabolite concentrations) annotated using ultra-high performance liquid chromatography–quadrupole time-of-flight mass spectrometry.

3.4 Conclusions

An untargeted metabolomics approach was used to investigate the impact of different drying processes on volatile and nonvolatile metabolites in dried chaya leaves. The effects of drying methods, namely FD, VD, OD50, OD120, and PR, on the umami taste, aroma characteristics, and antioxidant properties were examined. Overall, our hypothesis that different drying methods affect the aroma characteristics, umami taste components, and antioxidant properties of chaya leaves, was supported by our findings. HS-GC/MS analysis identified aldehydes as the predominant volatiles in the dried samples. rOAV highlighted 14 key volatile compounds, with 3-methylbutanal showing the highest rOAV and being associated with contributing to a malty and nutty aroma. Chaya leaves subjected to FD showed the second highest rOAV for hexanal, which imparts a green grass–like aroma. However, OD120 and PR drying methods yielded samples with elevated levels of 2-methylbutanal, providing more cocoa- and coffee-like odors. UHPLC–qTOF/MS analysis revealed that OD120 and PR samples exhibited significantly higher relative content of umami-tasting amino acids and 5'-ribonucleotides ($p < 0.05$). The electronic tongue assay confirmed that these samples had the highest umami taste intensity ($p < 0.05$), equivalent to approximately 0.04% (w/v) MSG. FD samples showed the highest antioxidant capacity according to DPPH and FRAP assays results, whereas OD50 samples exhibited the lowest capacity ($p < 0.05$). PLS biplot analysis indicated that L-glutamic acid, 5'-AMP, and 5'-GMP are each positively correlated with umami taste intensity, whereas L-ascorbic acid and glutathione were among key compounds that provided antioxidant activities of chaya leaves, specifically observed in FD samples. Moreover, since amino acids and peptides were within the same quadrant as TPC, DPPH and FRAP, their contribution might not be negligible. In conclusion, high-temperature–short-time drying processes (OD120 and PR) can enhance umami taste and produce higher amount of 2-methylbutanal that may provide more coffee-like aroma to the dried leaves. Conversely, FD better preserved the antioxidant activity of the leaves. These findings provide

valuable insights into the aroma characteristics, umami taste, and antioxidant capacity of chaya leaf under different processing conditions.

Credit authorship contribution statement

NH: conceptualization, methodology, investigation, writing–original draft, AT: methodology, investigation, PP: methodology, investigation, PP: methodology, investigation, AP: data curation, review & editing, NT: data curation, review & editing, US: funding acquisition, project administration, writing–review & editing, conceptualization, data curation, review & editing, SS: funding acquisition, project administration, writing–review & editing, conceptualization, data curation, review & editing

Declaration of competing interests

The authors declare that they have no known competing financial interests or personal relationships that influenced the work reported in this paper.

Acknowledgements

CHAPTER IV
CONCLUSIONS AND FUTURE WORKS

4.1 Conclusions

The identification of key umami substances and the effect of different drying methods on volatile and nonvolatile metabolites, umami taste intensity, and antioxidant capacity of chaya leaves were studied. The results of the study supported the hypothesis that free amino acids and short peptides are the key umami substances in fresh Chaya leaf, and that different drying methods affect the nonvolatile and volatile profiles, umami taste components, and antioxidant properties of chaya leaves.

A multiplatform metabolomics approach was used, including UHPLC–qTOF/MS, GC–MS, and HCTUltra/LC–MS, combined with electronic tongue assay and molecular docking approaches. The result found that amino acids, sugars, nucleotides, organic acids, flavonoids, alkaloids, and peptides varied in concentrations among chaya species and maturation stages of leaves. Regardless of the species, young leaves exhibited the highest umami taste intensity, followed by mature and old leaves, respectively. Consequently, key umami substances in the leaves were identified as L-glutamic acid, 5'-AMP, pyroglutamic acid, quinic acid, trigonelline, Ala-Tyr, Leu-Gly-Pro, and Leu-Asp-Gln, with the last six being the novel umami substances. Additionally, Leu-Gly-Pro exhibited synergism with MSG, as analyzed using the electronic tongue assay. The use of HS-GC/MS analysis showed that aldehydes were the most prevalent volatiles in the dried samples, with 3-methylbutanal (malt-like odor) being the dominant volatile in all samples based on rOAV analysis. High-temperature–short-time drying processes (OD120 and PR) were found to be better suited for increasing the intensity of umami taste and may provide a coffee-like aroma contributed from 2-methylbutanal, while FD was better preserving the antioxidant activity. The findings of this research provide valuable insights based on theoretical evidence into the key umami substances,

nonvolatile and volatile metabolite profile, umami taste intensity, and antioxidant capacity of chaya leaf, which can be beneficial for manufacturing of dried chaya leaf.

4.2 Future works

The present work shows that chaya leaves have a strong umami taste intensity and could be further enhanced by a suitable drying process. As mentioned, chaya is a fast-growing tree resistant to drought and easy to find in the country. Apart from these advantages, its umami quality is expressed without any fermentation process, unlike other umami-rich food ingredients such as cheese, soy sauce, shrimp paste, etc. Therefore, the leaves could potentially be used in various plant-based food products such as patties, nuggets, minced meat, etc. and tested for feasibility. For ease of use and storage, the development of "instant dissolve" chaya leaves powder by spray drying the aqueous leaf extract and their application in a food model could be further pursued. The ultimate goal is to improve the organoleptic and physiochemical properties of savory food products by increasing the intensity of umami taste and antioxidant capacity, respectively, through the use of this economically favorable and natural food ingredient.

REFERENCES

Amin, M. N. G., Kusnadi, J., Hsu, J. L., Doerksen, R. J., & Huang, T. C. (2020). Identification of a novel umami peptide in tempeh (Indonesian fermented soybean) and its binding mechanism to the umami receptor T1R. *Food Chemistry*, *333*, 127411.

Andrianov, A. M., Kornoushenko, Y. V., Karpenko, A. D., Bosko, I. P., & Tuzikov, A. V. (2021). Computational discovery of small drug-like compounds as potential inhibitors of SARS-CoV-2 main protease. *Journal of Biomolecular Structure and Dynamics*, *39*, 5779–5791.

Avila-Ospina, L., Clément, G., & Masclaux-Daubresse, C. (2017). Metabolite profiling for leaf senescence in barley reveals decreases in amino acids and glycolysis intermediates. *Agronomy*, *7*, 15.

Bartoli, C. G., Tambussi, E. A., Diego, F. & Foyer, C. H. (2009). Control of ascorbic acid synthesis and accumulation and glutathione by the incident light red/far red ratio in *Phaseolus vulgaris* leaves. *FEBS Letters*, 583, 118–122.

Bawarskar, H. S., Bawarskar, P. H., & Bawarskar, P. H. (2017). Chinese restaurant syndrome. *Indian Journal of Critical Care Medicine*, *21*(1), 49–50.

Bellisle, F. (1999). Glutamate and the UMAMI taste: sensory, metabolic, nutritional and behavioural considerations. A review of the literature published in the last 10 years, *Neuroscience and Biobehavioral Reviews,* 23, 423–438.

Bhatt, N. M., V. D. Chavada, S., M., & Shrivastav, P. S. (2019). Influence of pH and organic modifiers on the dissociation constants of selected drugs using reversed-phase thin-layer chromatography: Comparison with other techniques and computational tools. *Biomedical Chromatography*, *33*, 4666.

Brand-Williams, W., Cuvelier, M. E. & Berset, C. (1995). Use of free radical method to evaluate antioxidant activity, *LWT*, 28, 25–30.

Chan, E. W. C., Lim, Y. Y., Wong, S. K., Lim, K. K., Tan, S. P., Lianto, F. S. & Yong, M. Y. (2009). Effects of different drying methods on the antioxidant properties of leaves and tea of ginger species, *Food Chemistry*, 113(1), 166–172.

Dando, R., Dvoryanchikov, G., Pereira, E., Chaudhari, N. & Roper, S. D. (2012). Adenosine enhances sweet taste through A2B receptors in the taste bud. *Journal of Neuroscience*, 32(1), 322–30.

Dawidowicz, A. L. & Typek, R. (2017). Transformation of chlorogenic acids during the coffee beans roasting process. *European Food Research and Technology*, 243, 379–390.

Dermiki, M., Mounayar, R., Suwankanit, C., Scott, J., Kennedy, O. B., Mottram, D. S., Gosney, M. A., Blumenthal, H., & Methven, L. (2013). Maximising umami taste in meat using natural ingredients: Effects on chemistry, sensory perception and hedonic liking in young and old consumers. *Journal of the Science of Food and Agriculture*, *93*, 3312–3321.

Dermiki, M., Prescott, J., Sargent, L. J., Willway, J., Gosney, M. A. & Methven, L. (2015). Novel flavours paired with glutamate condition increased intake in older adults in the absence of changes in liking. *Appetite*. 90, 108.

Diaz, C., Purdy, S., Christ, A., Morot-Gaudry, J. F., Wingler, A., & Masclaux-Daubresse, C. L. (2005). Characterization of markers to determine the extent and variability of leaf senescence in Arabidopsis: A metabolic profiling approach. *Plant Physiology*, *138*, 898–908.

Diaz-Mendoza, M., Velasco-Arroyo, B., Santamaria, M. E., González-Melendi, P., Martinez, M., & Diaz, I. (2016). Plant senescence and proteolysis: Two processes with one destiny. *Genetics and Molecular Biology*, *39*, 329–338.

Eberhardt, J., Santos-Martins, D., Tillack, A. F., & Forli, S. (2021). AutoDock Vina 1.2.0: New docking methods, expanded force field, and python bindings. *Journal of Chemical Information and Modeling*, *61*, 3891–3898.

ECHO community. (2006). *Chaya*. Plant Information Sheet [online]. Available from: https://www.echocommunity.org/en/resources/af937e2d-4b83-4da9-ac3f-375c98f167b7

Flaig, M., Qi, S., Wei, G., Yang, X. & Schieberle, P. (2020). Characterization of the key odorants in a high-grade Chinese green tea beverage (*Camellia sinensis*; Jingshan Cha) by means of the sensomics approach and elucidation of odorant changes in tea

leaves caused by the tea manufacturing process. *Journal of Agricultural and Food Chemistry*. 68 (18), 5168−5179.

Gao, B., Hu, X., Li, R., Zhao, Y., Tu, Y., & Zhao, Y. (2021). Screening of characteristic umami substances in preserved egg yolk based on the electronic tongue and UHPLC-MS/MS. *LWT*, *152*, 112396.

Gemert, L. J. *(2011). Compilations of Odour Threshold Values in Air, Water & Other Media and Compilations of Flavour Threshold Values in Water & Other Media*, 2nd ed.; Leffingwell & Associates Canton: Canton, GA, USA.

Ghasempour, H., Gaff, D., Williams, R. & Gianello, R. D. (1998). Contents of sugars in leaves of drying desiccation tolerant flowering plants, particularly grasses. *Plant Growth Regulation,* 24, 185–191.

Goel, P. & Singh, A. K. (2015). Abiotic Stresses Downregulate Key Genes Involved in Nitrogen Uptake and Assimilation in *Brassica juncea* L. *PLoS ONE,* 10(11), 0143645.

González-Laredo, R. F., Flores De La Hoya, M. E., Quintero-Ramos, M. J., & Karchesy, J. J. (2003). Flavonoid and cyanogenic contents of chaya (spinach tree). *Plant Foods for Human Nutrition*, *58*, 1–8.

Goto, T. K., Yeung, A. W., Tanabe, H. C., Ito, Y., Jung, H. S., & Ninomiya, Y. (2016). Enhancement of combined umami and salty taste by glutathione in the human tongue and brain. *Chemical Senses*, *41*, 623–630.

Green, P. J. (1994). The ribonucleases of higher plants. *Annual Review of Plant Physiology and Plant Molecular Biology*, *45*, 421–445.

Guo, Y., Chen, D., Dong, Y., Ju, H., Wu, C. & Lin, S. (2018). Characteristic volatiles fingerprints and changes of volatile compounds in fresh and dried *Tricholoma matsutake* Singer by HS-GC-IMS and HS-SPME-GC-MS. *Journal of Chromatography B*, 1099, 46–55.

Guo, X., Ho, C.T., Schwab, W. & Wan, X. (2021). Effect of the roasting degree on flavor quality of large-leaf yellow tea. *Food Chemistry*, 347, 129016.

Hassain, M. B, Barry-Byan, C., MartinDiana, A. B & Bruntin, N. P. (2010). Effect of drying method on the antioxidant capacity of six Lamiaceae herbs. *Food Chemistry,* 123, 85–91.

Hayashi, N., Roggang, C., Hidekaz, I., & Tomomi, U. (2008). Evaluation of the umami taste intensity of green tea by a taste sensor. *Journal of Agricultural and Food Chemistry*, *16*, 7384–7387.

Ho, C. T. X. & Zheng, S. Li. (2015). Tea aroma formation, *Food Science and Human Wellness*, 9–27.

Hong, X., Wang, C., Jiang, R., Hu, T., Zheng, X., Huang, J., Liu, Z. & Li, Q. (2022). Characterization of the key aroma compounds in different aroma types of chinese yellow tea. *Foods.*12(1), 27.

Hua, J. & Huang, K. L. (2010). Preparation and characterization of 5'-phosphodiesterase from barley malt rootlets. *Natural Product Communications.* 5(2), 265–268.

Hutasingh, N., Chuntakaruk, H., Tubtimrattana, A., Ketngamkum, Y., Pewlong, P., Phaonakrop, N., Roytrakul, S., Rungrotmongkol, T., Paemanee, A., Tansrisawad, N., Siripatrawan, U. & Sirikantaramas, S. (2023). Metabolite profiling and identification of novel umami compounds in the chaya leaves of two species using multiplatform metabolomics, *Food Chemistry,* 404, 134564.

Jumper, J., Evans, R., Pritzel, A., Green, T., Figurnov, M., Ronneberger, O., Tunyasuvunakool, K., Bates, R., Žídek, A., Potapenko, A., Bridgland, A., Meyer, C., Kohl, S. A. A., Ballard, A. J., Cowie, A., Romera-Paredes, B., Nikolov, S., Jain, R., Adler, J. & Hassabis, D. (2021). Highly accurate protein structure prediction with AlphaFold. *Nature*, *596*, 583–589.

Kobayashi, Y., Habara, M., Ikezazki, H., Chen, R., Naito, Y., & Toko, K. (2010). Advanced taste sensors based on artificial lipids with global selectivity to basic taste qualities and high correlation to sensory scores. *Sensors*, *10*, 3411–3443.

Kongphapa, J., Chupanit, P., Anutrakulchai, S., Cha'on, U., & Pasuwan, P. (2021). Nutritional and phytochemical properties of chaya leaves (Cnidoscolus chayamansa Mc Vaugh) planted in Northeastern Thailand. *Asia-Pacific Journal of Science and Technology*, *27*.

Kunishima, N., Shimada, Y., Tsuji, Y., Sato, T., Yamamoto, M., Kumasaka, T., Nakanishi, S., Jingami, H., & Morikawa, K. (2000). Structural basis of glutamate recognition by a dimeric metabotropic glutamate receptor. *Nature*, *407*, 971–977.

Kuti, J. O., & Konoru, H. B. (2006). Cyanogenic glycosides content in two edible leaves of tree spinach (*Cnidoscolus* spp.). *Journal of Food Composition and Analysis*, *19*, 556–561.

Kuti, J. O. & Torres, E. S. (1996). Potential nutritional and health benefits of tree spinach. *Progress in New Crops*. 516–520.

Lai, Z., Tsugawa, H., Wohlgemuth, G., Mehta, S., Mueller, M., Zheng, Y., Ogiwara, A., Meissen, J., Showalter, M., Takeuchi, K., Kind, T., Beal, P., Arita, M., & Fiehn, O. (2018). Identifying metabolites by integrating metabolome databases with mass spectrometry cheminformatics. *Nature Methods*, *15*, 53–56.

Lemus-Mondaca, R., Ah-Hen, K., Vega-Gálvez, A., Honores, C. & Moraga, N. O. (2016). *Stevia rebaudiana* Leaves: effect of drying process temperature on bioactive components, antioxidant capacity and natural sweeteners. *Plant Foods for Human Nutrition*, 71, 49–56.

Li, X. B., Feng, T., Zhou, F., Zhou, S., Liu, Y. F., Li, W., Ye, R. & Yang, Y. (2015). Effects of drying methods on the tasty compounds of *Pleurotus eryngii. Food Chemistry*. 166, 358–364.

Li, X., Liu, Y. Wang, J. Wang, Y. Xu, S. Yi & J. Li. (2021a). Combined ultrasound and heat pretreatment improve the enzymatic hydrolysis of clam (*Aloididae aloidi*) and the flavor of hydrolysates. *Innovative Food Science & Emerging Technologies*, 67, 102596.

Li, S., Shao, Z., Lu, C., Yao, J., Zhou, Y. & Duan D. (2021b). Glutamate Dehydrogenase Functions in Glutamic Acid Metabolism and Stress Resistance in *Pyropia haitanensis*. *Molecules*. 10, 26, 6793.

Li, W., Zhang, H., Li, X., Zhang, F., Liu, C., Du, Y., Gao, X., Zhang, Z., Zhang, X., Hou, Z., Zhou, H., Sheng, X., Wang, G., & Guo, Y. (2017). Integrative metabolomic and transcriptomic analyses unveil nutrient remobilization events in leaf senescence of tobacco. *Scientific Reports*, *7*, 12126.

Lin, S., Ya-Hsin Hsiao & Po-An Chen. (2022). Revealing the profound meaning of pan-firing of oolong tea – A decisive point in odor fate, *Food Chemistry*, 375,131649.

Liu, J., Liu, M., He, C., Song, H. & Chen, F. (2015). Effect of thermal treatment on the flavor generation from Maillard reaction of xylose and chicken peptide. *LWT,* 64(1), 316–325.

Lioe, H., Apriyantono, A., Takara, K., Wada, K., & Yasuda, M. (2006). Umami taste enhancement of MSG/NaCl mixtures by subthreshold l-α-aromatic amino acids. *Journal of Food Science*, *70*, 401–405.

López Cascales, J. J., Oliveira Costa, S. D., de Groot, B. L., & Walters, D. E. (2010). Binding of glutamate to the umami receptor. *Biophysical Chemistry*, *152*, 139–144.

Masayoshi, A., ShoJi, A. & Manabh, H. (1980). Kinetic studies on decomposition of glutathione. I. Decomposition in Solid State. *Chemical and Pharmaceutical Bulletin*, 28, 514–520.

Mattar, T. V., Gonçalves, C. S., Pereira, R. C., Faria, M. A., de Souza, V. R., & Carneiro, JdD. S. (2018). A shiitake mushroom extract as a viable alternative to NaCl for a reduction in sodium in beef burgers: A sensory perspective. *British Food Journal*, *120*, 1366–1380.

Moura, L., Silva, N., Lopes, T. D. P., Benjamin, S. R., Brito, F. C. R., Magalhães, F. E. A., Florean, E. O. P. T., de Sousa, D. O. B., & Guedes, M. I. F. (2018). Ethnobotanic, phytochemical uses and ethnopharmacological profile of genus *Cnidoscolus* spp. (Euphorbiaceae): A comprehensive overview. *Biomedical Pharmacotherapy*, *109*, 1670–1679.

Nguyen, N. T., Nguyen, T. H., Pham, T. N. H., Huy, N. T., Bay, M. V., Pham, M. Q., Nam, P. C., Vu, V. V., & Ngo, S. T. (2020). Autodock Vina adopts more accurate binding poses but Autodock4 forms better binding affinity. *Journal of Chemical Information and Modeling*, *60*, 204–211.

Olsson, M. H., Søndergaard, C. R., Rostkowski, M., & Jensen, J. H. (2011). PROPKA3: Consistent treatment of internal and surface residues in empirical pKa predictions. *Journal of Chemical Theory and Computation*, *7*, 525–537.

Oruna-Concha, M. J., Methven, L., Blumenthal, H., Young, C., & Mottram, D. S. (2007). Differences in glutamic acid and 5′-ribonucleotide contents between flesh and pulp

of tomatoes and the relationship with umami taste. *Journal of Agricultural and Food Chemistry*, *55*, 5776–5780.

Pang, Z., Zhou, G., Chong, J., & Xia, J. (2021). Comprehensive meta-analysis of COVID-19 global metabolomics datasets. *Metabolites*, *11*, 44.

Peleg, H., & Noble, A. C. (1998). Effect of viscosity, temperature and pH on astringency in cranberry juice. *American Journal of Enology and Viticulture*, *59*, 210–221.

Pettersen, E. F., Goddard, T. D., Huang, C. C., Couch, G. S., Greenblatt, D. M., Meng, E. C., & Ferrin, T. E. (2004). UCSF Chimera—A visualization system for exploratory research and analysis. *Journal of Computational Chemistry*, *25*, 1605–1612.

Raigond, P., Singh, B., Dhulia, A., Chopra, S. & Dutt, S. (2015). Flavouring compounds in Indian potato snacks. *Journal of Food Science and Technology*, 52, 8308–14.

Ramos-Gómez, M., Figueroa-Pérez, M., Guzmán-Maldonado, H., LoarcaPina, G., Mendoza, S., Quezada- Tristan, T. & Reynoso-Camacho, R. (2017). Phytochemical profile, antioxidant properties and hypoglycemic effect of chaya (*Cnidoscolus chayamansa*) in stzinduced diabetic rats. *Journal of Food Biochemistry*, 41, 12281.

Rodrigues, L. G. G., Mazzutti, S., Siddique, I., da Silva, M., Vitali, L., & Ferreira, S. R. S. (2020). Subcritical water extraction and microwave-assisted extraction applied for the recovery of bioactive components from Chaya (*Cnidoscolus aconitifolius* Mill.). *Journal of Supercritical Fluids*, *165*, 104976.

Rosado-Souza, L., David, L. C., Drapal, M., Fraser, P. D., Hofmann, J., Klemens, P. A. W., Ludewig, F., Neuhaus, H. E., Obata, T., Perez-Fons, L., Schlereth, A., Sonnewald, U., Stitt, M., Zeeman, S.C ., Zierer, W., & Fernie, A. R. (2019). Cassava metabolomics and starch quality. *CurrentProtocols in Plant Biology*, *4*, 20102.

Ross-Ibarra, J., & Molina-Cruz, A. (2002). The Ethnobotany of Chaya (*Cnidoscolus aconitifolius* ssp. *aconitifolius* Breckon): A nutritious maya vegetable. *Economic Botany*, *56*, 350–365.

Scalone, G. L. L., Cucu, T., De Kimpe, N., & De Meulenaer, B. (2015). Influence of free amino acids, oligopeptides, and polypeptides on the formation of pyrazines in Maillard model systems. *Journal of Agriculture and Food Chemistry,* 63(22), 5364–5372.

Seo, W. H. & Hyung, H. B. (2009). Characteristic aroma-active compounds of korean perilla (*Perilla frutescens* Britton) Leaf. *Journal of Agricultural and Food Chemistry,* 57 , 11537–11542.

Shen, Q., He, Z., Ding, Y. & Sun, L. (2023). Effect of Different Drying Methods on the Quality and Nonvolatile Flavor Components of *Oudemansiella raphanipes*. *Foods*, 12, 676.

Shiga, K., Yamamoto, S., Nakajima, A., Kodama, Y., Imamura, M., Sato, T., Uchida, R., Obata, A., Bamba, T., & Fukusaki, E. (2014). Metabolic profiling approach to explore compounds related to the umami intensity of soy sauce. *Journal of Agricultural and Food Chemistry*, *62*, 7317–7322.

Smit, B. A., Engels, W.J. & Smit, G. (2009). Branched chain aldehydes: production and breakdown pathways and relevance for flavour in foods. *Applied Microbiology and Biotechnology,* 81, 987–999.

Spurvey, S., Pan, B. S. & Shahidi, F. (1998). *Flavour of shellfish.* In: Flavor of Meat, Meat Products and Seafood, 2nd ed. (ed. F. Shahidi), 159–196.

Sugisawa, H., Edo, H. (1966). The thermal degradation of sugars I. Thermal polymerization of glucose. *Journal of Food Science,* 31, 561–565.

Sun, Y., Donghong L. & Xingqian, Y. (2015). Effects of drying methods on phytochemical compounds and antioxidant activity of physiologically dropped un-matured citrus fruits, *LWT - Food Science and Technology,* 60, 1269–1275.

Sun, P., Xu, B., Wang, Y., Lin, X., Chen, C., Zhu, J., Jia, H., Wang, X., Shen, J. & Feng, T. (2022). Characterization of volatile constituents and odorous compounds in peach (*Prunus persica* L.) fruits of different varieties by gas chromatography–ion mobility spectrometry, gas chromatography–mass spectrometry, and relative odor activity value. *Frontier in Nutrition*, 9, 965796.

Swain, T. & Hillis, W. E. (1959). The phenolic constituents of Prunus domestica I—the quantitative analysis of phenolic constituents, *Journal of Science of Food and Agriculture*, 10, 63–68.

Thomas, H., Ougham, H. J., Wagstaff, C., & Stead, A. D. (2003). Defining senescence and death. *Journal of Experimental Botany*, *54*, 1127–1132.

Tian, Y. T., Zhao, Y. T., Huang, J. J., Zeng, H. L. & Zheng, B. D. (2016). Effects of different drying methods on the product quality and volatile compounds of whole shiitake mushrooms. *Food Chemistry*, 197, 714–722.

Tian, M., Fang, B., Jiang, L., Guo, H. & Cui J. Y. (2015). Structure-activity relationship of a series of antioxidant tripeptides derived from β-Lactoglobulin using QSAR modeling. *Dairy Science and Technology*, 176, 1815–1833.

Triba, M. N., Le Moyec, L., Amathieu, R., Goossens, C., Bouchemal, N., Nahon, P., Rutledge, D. N., & Savarin, P. (2015). PLS/OPLS models in metabolomics: The impact of permutation of dataset rows on the K-fold cross-validation quality parameters. *Molecular Biosystems*, *11*, 13–19.

USAID. (2013). Chaya - Technical Bulletin #92 [online], Available from: https://pdf.usaid.gov/pdf_docs/PA00K93C.pdf [accessed 29 January 2021].

Wang, K., Zhuang, H., Bing, F., Chen, D., Feng, T., & Xu, Z. (2021). Evaluation of eight kinds of flavor enhancer of umami taste by an electronic tongue. *Food Science and Nutrition*, *9*, 2095–2104.

Webb, J., Bolhuis, D. P., Cicerale, S., Hayes, J. E., & Keast, R. (2015). The relationships between common measurements of taste function. *Chemosensory Perception*, *8*, 11–18.

Wen, X., Wen, L., Wu, L., Wanchao, C., Zhong, Z., Di, W., & Yan, Y. (2022). Quality characteristics and non-volatile taste formation mechanism of *Lentinula edodes* during hot air drying, *Food Chemistry,* 393, 133378.

Williams, P., & Norris, K. (1987). *Near infrared technology in the agricultural and food industries* (pp. 143–167). American Association of Cereal Chemists.

Wingler, A., & Roitsch, T. (2008). Metabolic regulation of leaf senescence: Interactions of sugar signaling with biotic and abiotic stress responses. *Plant Biology*, *10*, 50–62.

Xu, H. X. & Chen, J. W. (2011). Commercial quality, major bioactive compound content and antioxidant capacity of 12 cultivars of loquat (*Eriobotrya japonica* Lindl.) fruits. *Journal of the Science of Food and Agriculture,* 91, 1057–1063.

Xu, Y., Xiao, Y., Lagnika, C., Song, J., Li, D. & Liu, C. (2020). A comparative study of drying methods on physical characteristics, nutritional properties and antioxidant capacity of broccoli, *Drying Technology*, 38, 1378–1388.

Xue, W. F., Szczepankiewicz, O., Thulin, E., Linse, S., & Carey, J. (2009). Role of protein surface charge in monellin sweetness. *Biochimica et Biophysica Acta (BBA) – Proteins and Proteomics*, 1794, 410–420.

Yang, J., Huang, Y., Cui, C., Dong, H., Zeng, X., & Bai, W. (2021). Umami-enhancing effect of typical kokumi-active γ-glutamyl peptides evaluated via sensory analysis and molecular modeling approaches. *Food Chemistry*, 338, 128018.

Yang, L., Dai, B., Ayed, C., & Liu, Y. (2019). Comparing the metabolic profiles of raw and cooked pufferfish (Takifugu flavidus) meat by NMR assessment. *Food Chemistry*, *290*, 107–113.

Yamaguchi, S., Yoshikawa, T., Ikeda, S., & Ninomiya, T. (1971). Measurement of the relative taste intensity of some l-amino acids and 5′-nucleotides. *Journal of Food Science*, *36*, 846–849.

Ye, F., Qiao, X., Gui, A., Wang, S., Liu, P., Wang, X., Teng, J., Zheng, L., Feng, L. & Han, H. (2021). Metabolomics provides a novel interpretation of the changes in main compounds during black tea processing through different drying methods. *Molecules.* 26, 6739.

Yi, C., Li, Y., Zhu, H., Liu, Y. & Quan, K. (2021). Effect of *Lactobacillus plantarum* fermentation on the volatile flavors of mung beans. *LWT*, 146, 111434.

Yu, Z., Kang, L., Zhao, W., Wu, S., Ding, L., Zheng, F., Liu, J., & Li, J. (2021). Identification of novel umami peptides from myosin via homology modeling and molecular docking. *Food Chemistry*, *344*, 128728.

Zeki, Ö. C., Eylem, C. C., Reçber, T., Kır, S., & Nemutlu, E. (2020). Integration of GC–MS and LC–MS for untargeted metabolomics profiling. *Journal of Pharmaceutical and Biomedical Analysis*, *190*, 113509.

Zhang, L., Dong, X., Feng, X., Ibrahim, S. A., Huang, W. & Liu, Y. (2021). Effects of Drying Process on the volatile and non-volatile flavor compounds of *Lentinula edodes. Foods,* 10, 2836.

Zhang, Z., Elfalleh, W., He, S., Tang, M., Zhao, J., Wu, Z., Wang, J. & Sun, H. (2018). Heating and cysteine effect on physicochemical and flavor properties of soybean peptide Maillard reaction products, *International Journal of Biological Macromolecules,* 120, 2137–2146.

Zhang, L., & Peterson, D. G. (2018). Identification of a novel umami compound in potatoes and potato chips, *Food Chemistry*, *240*, 1219–1216.

Zhang, Y., Venkitasamy, C., Pan, Z., Liu, W., & Zhao, L. (2017). Novel umami ingredients: Umami peptides and their taste. *Journal of Food Science*, *82*, 16–23.

Zhang, M., Xing, S., Fu, C., Fang, F., Liu, J., Kan, J., Qian, C., Chai, Q. & Jin, C. (2022). Effects of drying methods on taste components and flavor characterization of *Cordyceps militaris. Foods*, 11, 3933.

Zhao, C. J., Schieber, A., & Gänzle, M. G. (2016). Formation of taste-active amino acids, amino acid derivatives and peptides in food fermentations – A review. *Food Research International*, *89*, 39–47.

Zheng, X. Q., & Ashihara, H. (2004). Distribution, biosynthesis and function of purine and pyridine alkaloids in Coffea arabica seedlings. *Plant Science*, *166*, 807–813.

Zhou, J., Chan, L., & Zhou, S. (2012). Trigonelline: A plant alkaloid with therapeutic potential for diabetes and central nervous system disease. *Current Medicinal Chemistry*, *19*, 3523–3531.

Zhu, M., Li, N., Zhao, M., Yu, W., & Wu, J. L. (2017). Metabolomic profiling delineate taste qualities of tea leaf pubescence. *Food Research International*, *94*, 36–44.

Zou, T. B, He, T. P., Li, H. B., Tang, H. W. & Xia, E. Q. (2016). The Structure-Activity Relationship of the Antioxidant Peptides from Natural Proteins. *Molecules*. 21, 72.

APPENDIX

Appendix A: Metabolite Profiling and Identification of Novel Umami Compounds in the Chaya Leaves of Two Species using Multiplatform Metabolomics

Table A1 Correlation analysis of the compounds detected in both ultra-high performance liquid chromatography–quadrupole time-of-flight mass spectrometry and gas chromatography–mass spectrometry analyses. The young, mature, and old leaf samples of *Cnidoscolus chayamansa* (three-lobed leaves) and *Cnidoscolus aconitifolius* (five-lobed leaves) (3Y,3M, and 3O and 5Y, 5M, and 5O, respectively).

Compound	Platform	Mean value of normalized peak area						Correlation coefficient
		3Y	3M	3O	5Y	5M	5O	
L-Lysine	UHPLCqTOF/MS	1.67	0.26	1.22	2.08	0.51	1.40	**0.84**
	GC/MS	0.69	0.20	0.80	0.68	0.22	0.59	
L-Glutamine	UHPLCqTOF/MS	3.56	0.64	0.51	2.19	0.51	0.48	**0.95**
	GC/MS	0.72	0.21	0.27	0.39	0.12	0.05	
L-Serine	UHPLCqTOF/MS	0.46	0.55	0.47	0.42	0.43	0.36	**0.76**
	GC/MS	0.27	0.32	0.27	0.27	0.13	0.13	
L-Glutamic acid	UHPLCqTOF/MS	6.22	3.89	1.75	7.38	5.09	2.31	**0.93**
	GC/MS	1.34	0.74	0.44	1.11	0.90	0.44	
L-Aspartic acid	UHPLCqTOF/MS	0.72	0.67	0.57	0.84	0.67	0.79	**0.67**
	GC/MS	0.29	0.22	0.19	0.33	0.18	0.21	
L-Proline	UHPLCqTOF/MS	1.12	0.26	1.25	2.36	0.79	1.49	**0.76**
	GC/MS	0.11	0.05	0.13	0.12	0.08	0.10	
L-Valine	UHPLCqTOF/MS	2.26	0.62	2.63	3.58	1.70	2.97	**0.82**
	GC/MS	0.21	0.09	0.34	0.25	0.13	0.23	
L-Tyrosine	UHPLCqTOF/MS	14.37	4.22	16.61	17.04	7.13	16.91	**0.90**
	GC/MS	0.33	0.10	0.47	0.30	0.15	0.35	
L-Isoleucine	UHPLCqTOF/MS	20.21	6.01	19.18	22.44	9.95	19.93	**0.77**
	GC/MS	0.33	0.12	0.44	0.35	0.14	0.29	
L-Phenylalanine	UHPLCqTOF/MS	38.92	11.53	42.09	45.02	17.87	41.78	**0.89**
	GC/MS	0.42	0.13	0.65	0.41	0.17	0.48	
Sucrose	UHPLCqTOF/MS	4.17	12.17	5.64	4.31	12.82	7.60	**0.75**
	GC/MS	6.92	8.55	5.81	7.99	9.54	7.98	
Tryptophan	UHPLCqTOF/MS	1.45	1.31	8.84	9.73	3.12	10.48	**0.81**
	GC/MS	0.08	0.05	0.15	0.09	0.05	0.14	
Quinic acid	UHPLCqTOF/MS	3.01	0.60	0.05	2.24	1.06	0.19	**0.96**

	GC/MS	1.98	0.71	0.21	1.99	1.32	0.53	
Ascorbic acid	UHPLCqTOF/MS	0.69	1.03	1.26	3.21	1.88	2.29	**0.56**
	GC/MS	0.16	0.27	0.11	0.41	0.28	0.12	

Table A2 Mean of normalized peak area of annotated metabolites used in the heatmap as analyzed by ultra-high performance liquid chromatography–quadrupole time-of-flight mass spectrometry. The young, mature, and old leaf samples of *Cnidoscolus chayamansa* (three-lobed leaves) and *Cnidoscolus aconitifolius* (five-lobed leaves) (3Y, 3M, and 3O and 5Y, 5M, and 5O, respectively).

Annotated compound	Mean value of normalized peak area					
	3Y	3M	3O	5Y	5M	5O
L-Lysine	1.66	0.25	1.21	2.07	0.50	1.40
L-Arginine	9.67	2.52	4.99	9.37	7.34	5.46
L-Pyroglutamic acid	1.96	0.79	0.39	1.56	0.87	0.30
L-Glutamine	3.56	0.64	0.51	2.19	0.51	0.47
L-Glutamic acid	6.22	3.89	1.75	7.38	5.09	2.31
L-Tyrosine	14.37	4.22	16.61	17.04	7.13	16.96
L-Isoleucine	20.21	6.01	19.18	22.44	9.95	19.95
L-Phenylalanine	38.92	11.53	42.09	45.02	17.87	41.70
L-Proline	1.12	0.26	1.25	2.36	0.79	1.49
L-Valine	2.26	0.62	2.63	3.58	1.70	2.97
L-Tryptophan	1.45	1.31	8.84	9.73	3.12	10.47
N6-Acetyl-L-lysine	13.14	3.41	11.12	15.66	4.13	10.18
gamma-Glu-Val	6.98	4.01	5.83	8.06	2.58	5.16
gamma-Glu-Leu	11.95	3.08	12.22	12.19	3.15	10.64
gamma-Glu-Phe	3.93	0.54	4.90	4.42	0.33	3.23
Glutathione	0.44	3.96	1.93	18.62	14.75	4.06
Ile-Ser	5.15	1.87	4.57	4.15	1.55	3.42
Ser-Leu	9.39	2.62	8.14	7.58	1.88	5.12
Ala-Ile	5.34	3.31	4.57	5.15	1.62	4.67
Ala–Tyr	1.98	0.36	0.87	2.03	0.37	0.38
Thr-Phe	1.73	0.33	1.42	1.79	0.28	0.93
Leu-Ser	3.42	0.86	3.94	4.49	0.74	3.02
Leu-Asn	4.44	1.28	5.60	5.69	1.17	3.96
Val-Gln	2.04	0.34	2.04	3.77	0.94	2.63
Leu–Gly–Pro	2.22	n.d.	n.d.	2.04	0.21	0.00
Glu-Ile-Val	2.51	1.16	3.26	2.89	0.60	2.90
Leu-Leu-Asn	2.54	1.58	2.71	2.89	1.72	2.77
Leu–Asp–Gln	1.65	n.d.	0.79	1.67	0.00	0.00
Sucrose	4.17	12.17	5.64	4.31	12.82	7.60
5′-AMP	1.70	0.63	0.00	1.81	0.81	0.00

Adenine	2.21	1.04	2.06	3.08	1.54	2.19
cAMP	2.03	0.00	0.63	7.91	0.86	2.63
Guanosine	17.02	5.18	23.18	26.76	9.80	16.24
Guanine	6.28	1.73	8.50	3.95	3.47	5.87
cGMP	2.86	n.d.	1.78	13.01	1.43	3.99
Asperulosidic acid	9.69	1.64	5.67	13.30	4.74	10.87
4-Hydroxycinnamic acid	2.20	0.75	3.64	3.38	1.30	3.27
Quinic acid	3.01	0.60	0.05	2.24	1.06	0.19
Nopalinic acid	0.43	0.29	0.94	0.62	0.82	0.52
Trigonelline	10.88	4.37	5.12	11.04	7.17	7.86
Moschamine	1.07	0.00	0.81	1.24	n.d.	0.24
Hyoscyamine	0.68	0.12	0.67	0.93	n.d.	0.75
Indoline	11.94	2.82	13.50	14.74	4.56	12.62
Clovin	1.07	1.01	1.53	4.27	1.37	1.42
Nicotiflorin	1.12	0.69	1.21	29.51	20.06	28.75
Robinin	18.08	19.85	28.25	11.43	4.37	5.46
Rutin	3.58	1.10	0.68	6.19	2.00	0.54
Biorobin	26.20	4.72	2.51	5.75	1.08	0.96
Linamarin	8.83	7.71	0.53	6.07	17.02	3.65
Glucolepidiin	3.87	2.29	0.29	3.26	3.12	1.91

n.d.: not detected

Table A3 Mean of normalized peak area of annotated metabolites used in the heatmap as analyzed by gas chromatography–mass spectrometry. The young, mature, and old leaf samples of *Cnidoscolus chayamansa* (three-lobed leaves) and *Cnidoscolus aconitifolius* (five-lobed leaves) (3Y, 3M, and 3O and 5Y, 5M, and 5O, respectively).

Annotated compound	Mean of normalized peak area					
	3Y	3M	3O	5Y	5M	5O
L-Alanine	0.63	0.32	0.66	0.57	0.39	0.60
L-Lysine	0.69	0.18	0.80	0.68	0.22	0.59
L-Leucine	0.16	0.03	0.15	0.16	0.03	0.13
L-Valine	0.21	0.09	0.34	0.25	0.13	0.23
L-Isoleucine	0.33	0.12	0.44	0.35	0.14	0.29
L-Proline	0.11	0.01	0.12	0.12	0.06	0.10
L-Glycine	0.38	0.11	0.41	0.35	0.13	0.30
L-Serine	0.55	0.60	0.72	0.51	0.43	0.44
L-Threonine	0.46	0.19	0.52	0.45	0.31	0.41
L-Tyrosine	0.33	0.10	0.47	0.30	0.15	0.35
L-Methionine	0.03	0.00	0.02	0.03	0.00	0.02
L-Aspartic acid	0.29	0.22	0.18	0.33	0.18	0.21
L-Glutamic acid	1.34	0.74	0.44	1.11	0.90	0.44
L-Phenylalanine	0.42	0.13	0.65	0.41	0.17	0.48
Homoserine	0.18	0.04	0.26	0.13	0.02	0.12
L-Glutamine	0.72	0.21	0.26	0.39	0.12	0.00
L-Tryptophan	0.08	0.02	0.13	0.09	0.02	0.14
L-Ornithine	0.04	0.00	0.02	0.01	0.01	0.02
4-Aminobutanoic acid	0.64	0.61	1.16	0.63	0.83	1.05
D-Arabinose	0.07	0.04	0.20	0.10	0.04	0.14
Xylitol	0.01	0.03	0.08	0.01	0.03	0.54
D-Fructose	3.26	0.81	2.82	3.08	1.51	2.41
D-Glucose	5.63	1.98	3.63	5.53	4.20	4.12
D-Altrose	2.20	0.53	1.65	2.27	1.60	4.13
D-Allose	0.12	0.12	0.00	0.09	0.076	0.09
L-(+)-Threose	0.04	0.00	0.01	0.03	0.01	0.03
Sucrose	6.92	8.55	5.81	7.99	9.54	5.85
1,5-Anhydroglucitol	0.71	0.37	0.38	0.62	0.49	0.45
Lactic acid	0.09	0.08	0.11	0.10	0.11	0.08
Phosphoric acid	0.33	0.06	n.d.	0.30	0.06	0.02
Succinic acid	0.22	0.06	0.05	0.24	0.13	0.11
Glyceric acid	0.13	0.18	0.20	0.12	0.16	0.15
2-Butenedioic acid	0.27	0.00	0.06	0.25	0.11	1.44
Malic acid	3.11	2.16	3.15	3.39	3.94	4.52
Glutaric acid	0.09	0.05	0.01	0.03	0.05	0.06

Shikimic acid	0.17	0.03	0.03	0.22	0.06	0.27
Citric acid	1.12	1.68	2.61	1.24	1.62	1.16
Quinic acid	1.98	0.71	0.21	1.99	1.32	0.46
D-Gluconic acid	0.06	0.04	0.09	0.10	0.07	0.10
Galactaric acid	1.01	0.19	0.14	0.81	0.23	0.21
cis-Coutaric acid	0.22	0.15	0.11	0.18	0.21	0.31
Ascorbic acid	0.13	0.26	0.08	0.39	0.24	0.13
2,3,4-Trihydroxybutyric acid	0.27	0.24	0.15	0.31	0.42	0.24
D-Myo-Inositol	0.07	n.d.	n.d.	0.07	0.00	0.04
3-Pyridinol	0.11	0.15	0.16	0.12	0.15	0.38
Glycerol	1.00	0.70	1.01	1.02	0.82	1.20
Stearic acid	1.54	1.50	1.73	1.58	1.09	1.56
Palmitic acid	1.21	1.18	1.36	1.22	1.14	0.92
Propanoic acid	0.01	0.02	0.02	0.01	0.01	0.02
Oleamide	0.09	0.08	0.04	0.10	0.08	0.10

n.d.: not detected

Table A4 Model diagnostic of partial least square regression using a cross-validation test

Analytical platform	Number of components*	RMSECV	R^2X	R^2Y	Q^2
GC-MS	2	0.894	0.371	0.989	0.924
UHPLC–qTOF/MS	2	0.986	0.285	0.951	0.910
HCTUltra/LC–MS	4	1.364	0.482	0.990	0.907

*Optimum number of components provides a minimum value of the root mean square error estimated from cross-validation (RMSECV).

จุฬาลงกรณ์มหาวิทยาลัย

CHULALONGKORN UNIVERSITY

Table A5 Umami taste intensity of the potent umami compounds was analyzed with an electronic tongue. The mean values were calculated from four measurements (n = 4).

Sample	Umami taste intensity*
0.75 mM MSG	2.67 ± 0.03^b
0.75 mM 5′-AMP	3.74 ± 0.04^a
0.75 mM LGP	1.59 ± 0.0^f
0.75 mM LDQ	2.21 ± 0.05^e
0.75 mM AY	2.31 ± 0.01^d
0.75 mM Pyroglutamic acid	1.40 ± 0.03^g
0.75 mM Quinic acid	1.42 ± 0.09^{gh}
0.75 mM Trigonelline	0.77 ± 0.06^i

Different superscript letters indicate significant differences ($p < 0.05$) among samples by Duncan's test.

Table A6 Umami taste intensity of a binary mixture of potent umami compounds and monosodium glutamate at an equivalent molarity analyzed with an electronic tongue. The expected umami taste intensity was summed from the umami intensity of each compound indicated in Table A5. The expected umami taste intensity was summed from the umami intensity of each compound indicated in Table A5.

Sample	Umami taste intensity		
	Expected	Actual	Actual - Expected
0.75 mM MSG	-	2.67 ± 0.03	-
1.5 mM MSG	-	5.34 ± 0.05^c	-
0.75 mM MSG + 0.75 mM 5′-AMP	6.41	7.06 ± 0.02^a	0.65
0.75 mM MSG + 0.75 mM LGP	4.26	6.16 ± 0.19^b	1.90
0.75 mM MSG + 0.75 mM LDQ	4.88	4.95 ± 0.15^e	0.07
0.75 mM MSG + 0.75 mM AY	4.98	4.47 ± 0.16^f	-0.51
0.75 mM MSG + 0.75 mM Pyroglutamic acid	4.07	4.35 ± 0.04^{fg}	0.28
0.75 mM MSG + 0.75 mM Quinic acid	4.09	5.24 ± 0.03^d	1.15
0.75 mM MSG + 0.75 mM Trigonelline	3.44	4.04 ± 0.23^h	0.60

Different superscript letters indicate significant differences ($p < 0.05$) among samples by Duncan's test.

Figure A1 Sampling of chaya leaves (*Cnidoscolus aconitifilus*: a five-lobed leaves) at Krathum Baen District, Samut Sakhorn Province, Thailand.
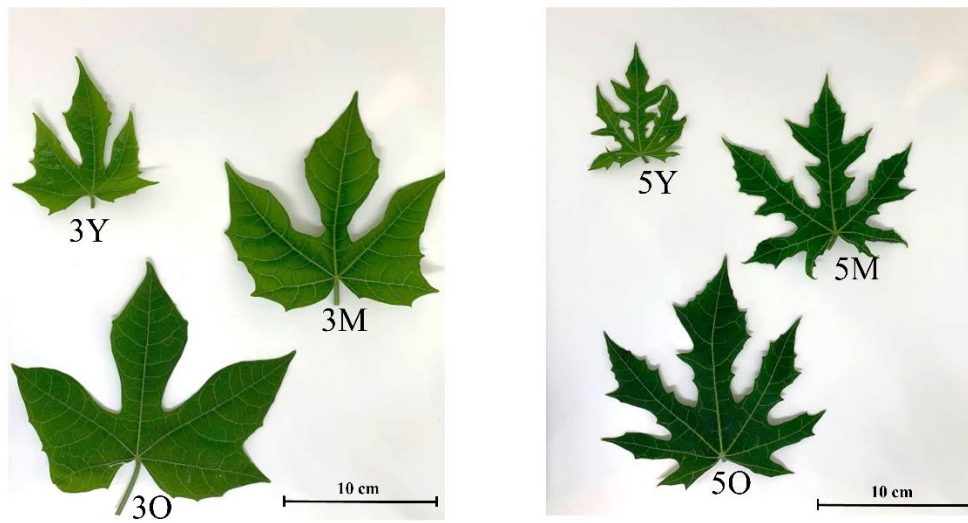
Figure A2 Young, mature, and old leaves of *Cnidoscolus chayamansa*: three-lobed leaves (3Y, 3M, and 3O) and young, mature, and old leaves of *Cnidoscolus aconitifilus*: five-lobed leaves (5Y, 5M, and 5O), respectively.
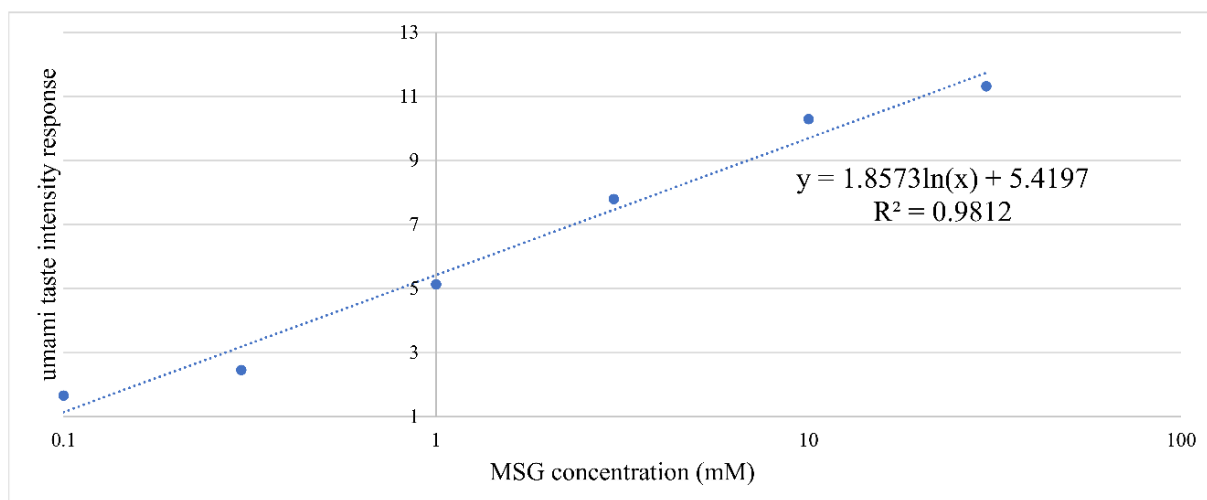
Figure A3 Standard curve of umami taste intensity measured by an electronic tongue
(TS-5000Z taste sensing system). The umami taste intensity values were obtained
from monosodium glutamate concentrations ranging 0.1–50 mM.
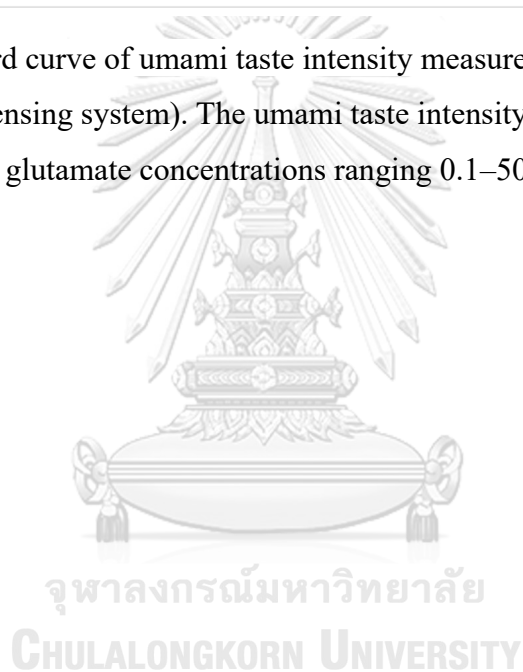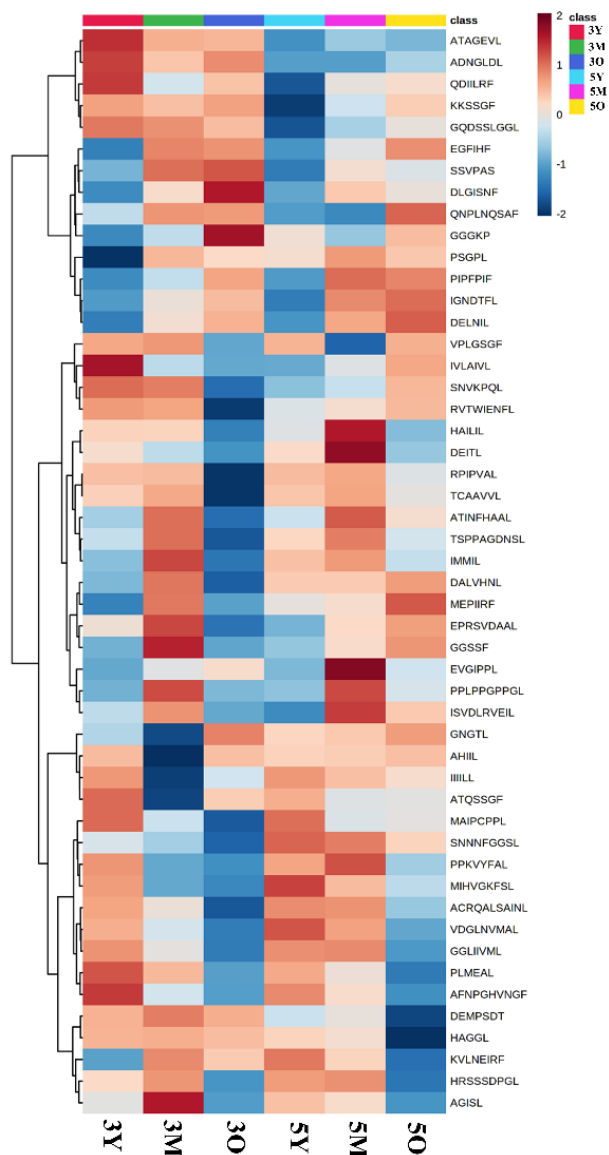
Figure A4 Heatmap visualization of the top 50 annotated metabolites based on the relative abundance from high-capacity ultra-ion trap/liquid chromatography–mass spectrometry among chaya leaf samples (n = 4) at different leaf maturation stages and species. The color in the heatmap indicates the relative fold change of each metabolite between groups, with red and blue colors expressing higher or lower abundances, respectively.

(A)

(B)

(C)
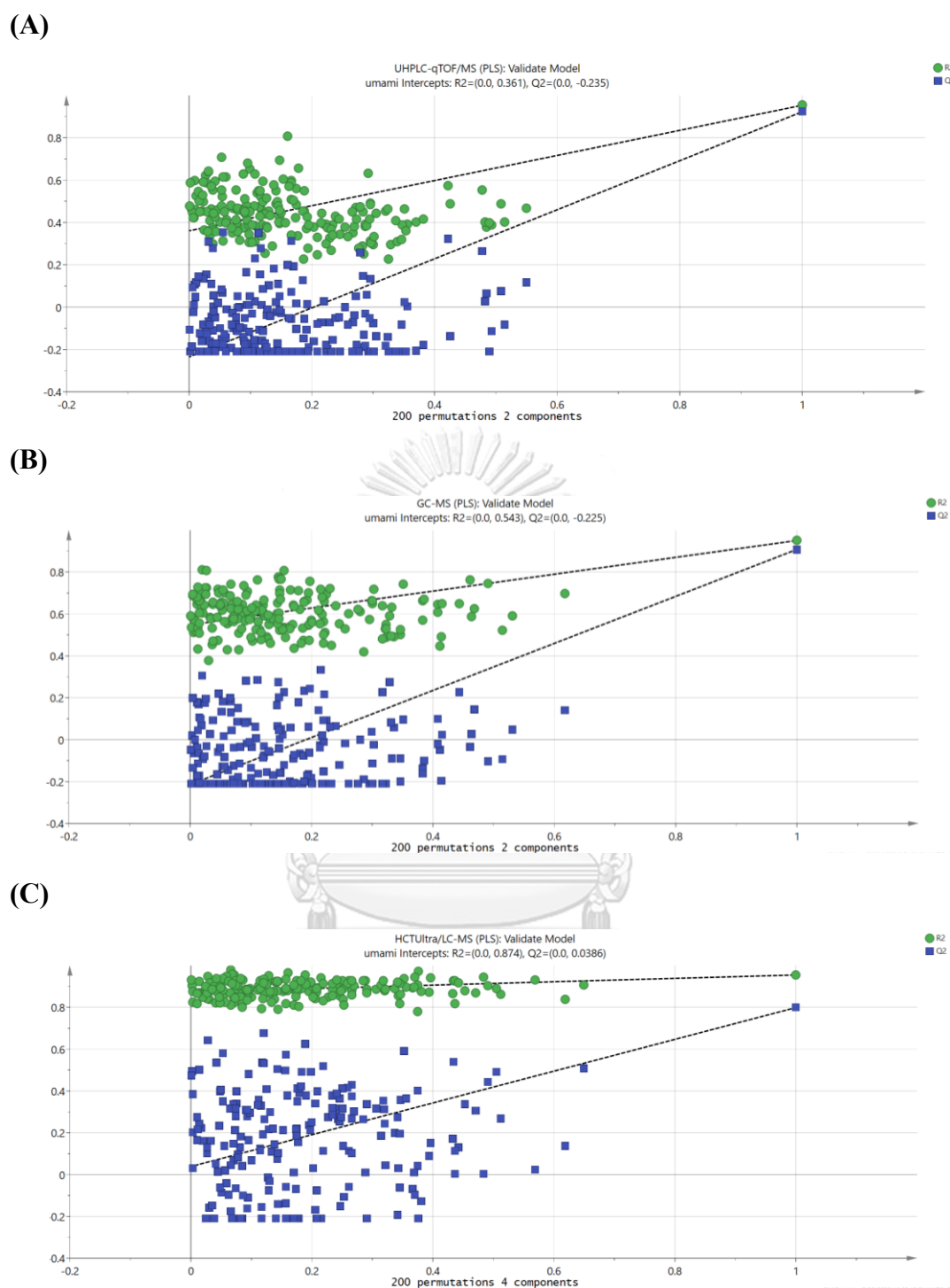
Figure A5 Permutation test of partial least square regression obtained from ultra-high performance liquid chromatography–quadrupole time-of-flight mass spectrometry (R^2 intercept = 0.361, Q^2 intercept = −0.235) (A), gas chromatography–mass spectrometry (R^2 intercept = 0.543, Q^2 intercept = −0.225), (B) and high-capacity ultra-ion

trap/liquid chromatography–mass spectrometry (R^2 intercept = 0.874, Q^2 intercept = 0.0386) (C).
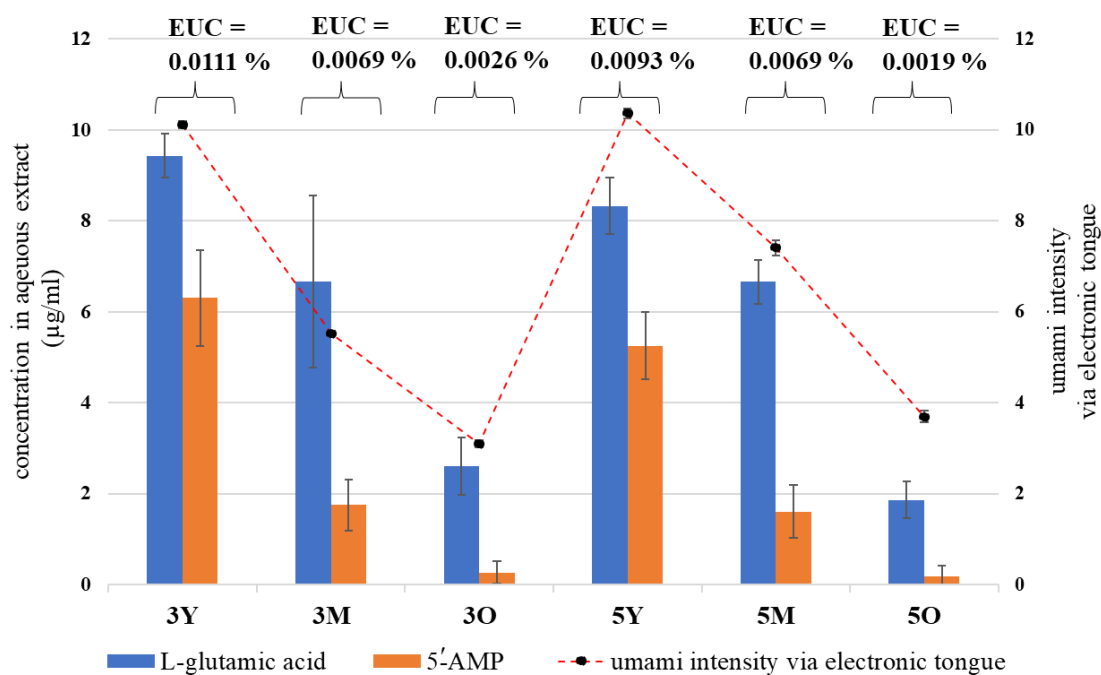
Figure A6 Mean values of L-glutamic and 5′-AMP concentration (primary y-axis) in chaya leaf aqueous extracts used in the electronic tongue analysis and their umami intensity values (secondary y-axis). The equivalent umami concentration (EUC; % monosodium glutamate) of each sample was calculated from the concentration of L-glutamic acid and 5′-AMP. The EUC value of all samples was lower than the monosodium glutamate recognition threshold (4 mM or 0.07% w/w).

(A)
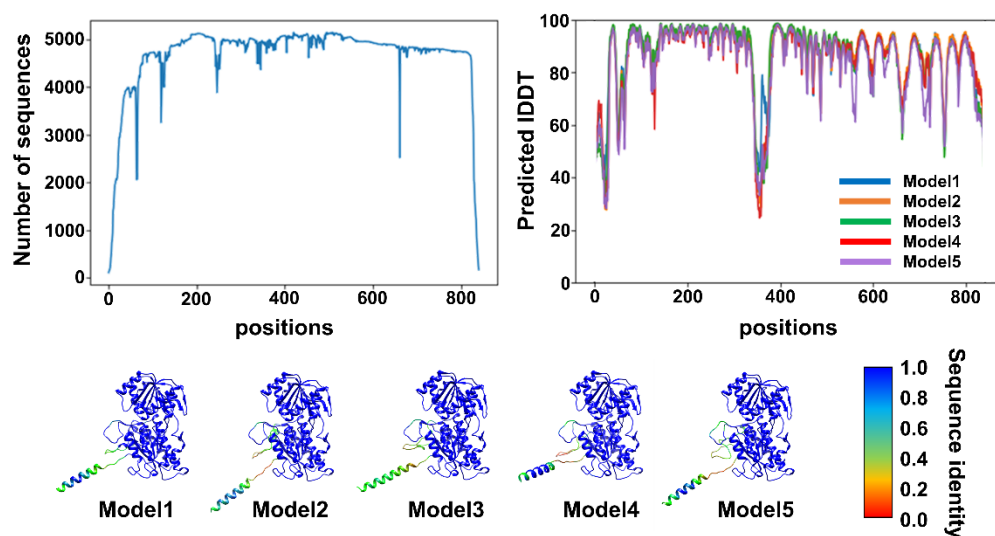
(B)
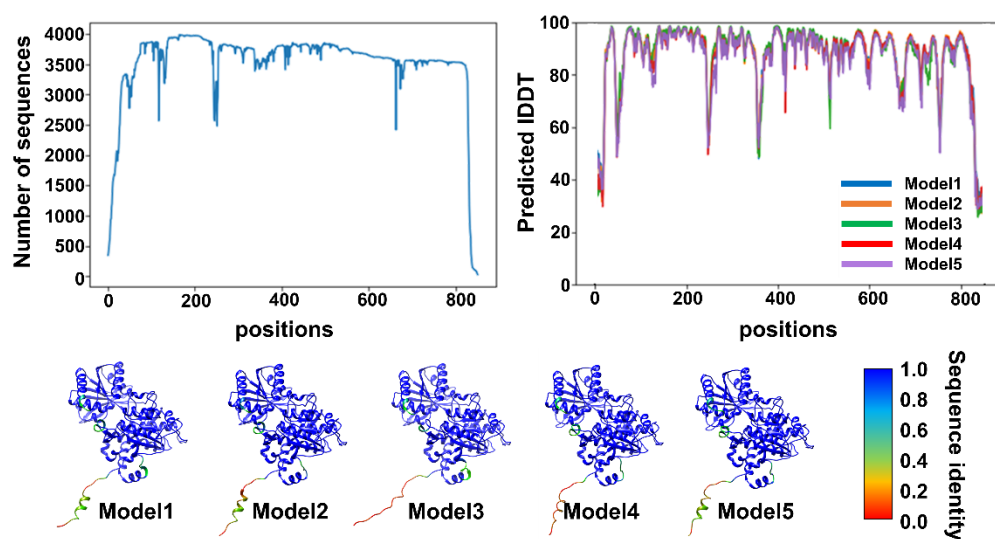
Figure A7 The 3-dimensional structures of taste receptor type 1 member 1 (A) and taste receptor type 1 member 3 (B) predicted by AlphaFold2.
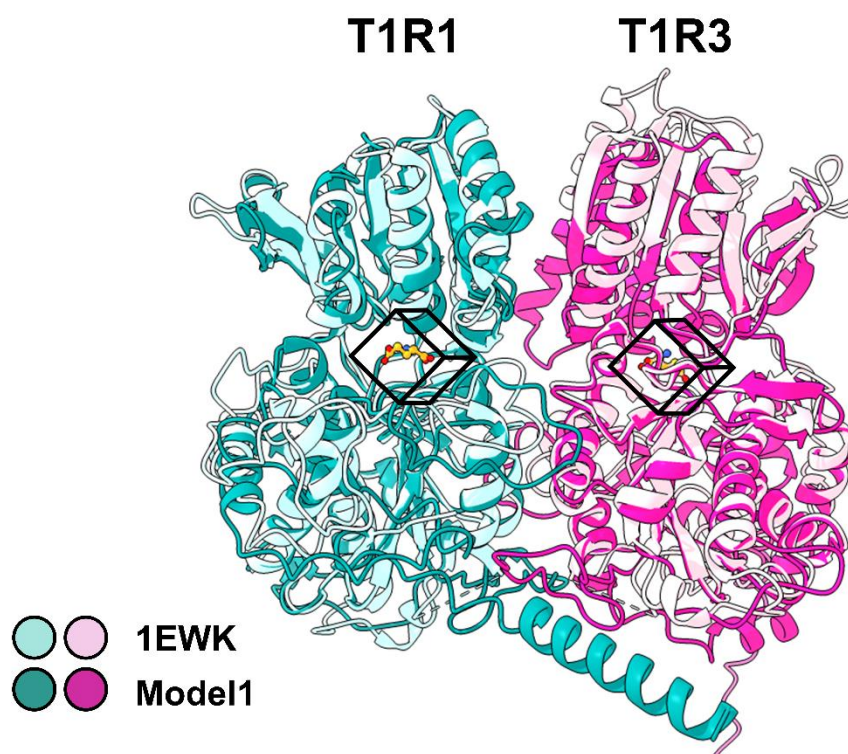
Figure A8 Superimposition of the template of the closed–open state of metabotropic glutamate receptor 1/L-glutamate complex (PDB: 1EWK) consisting of taste receptor type 1 member 1 (T1R1) in the closed conformation (light cyan) and taste receptor type 1 member 3 in the open conformation (light pink) and the 3-dimensional predicted structure obtained from AlphaFold2 (taste receptor type 1 member 1: deep cyan, and taste receptor type 1 member 3: deep pink) visualized with the University of California at San Francisco Chimera package.
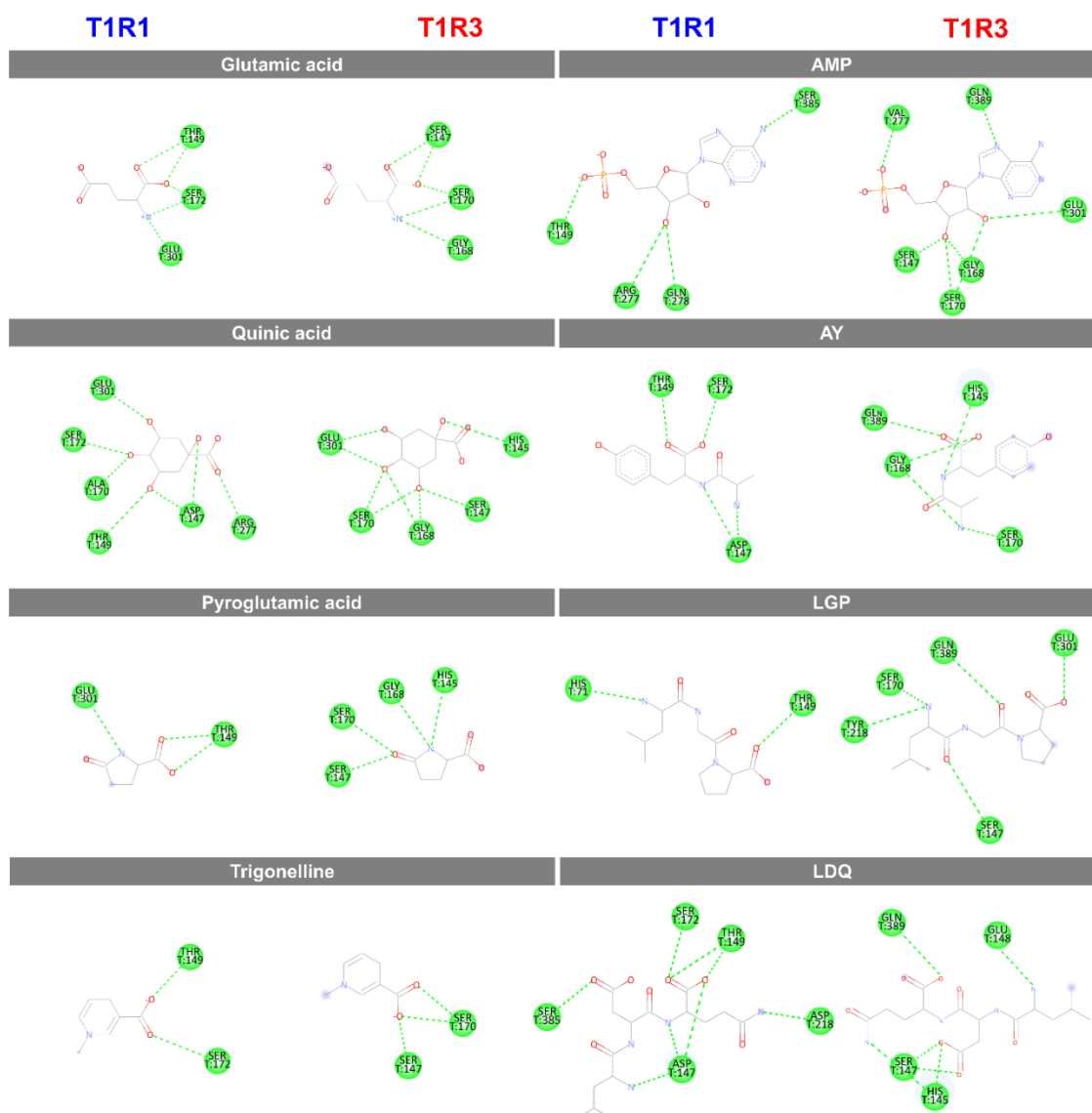
Figure A9 2-dimensional binding interaction of umami ligands with the active site residues of the closed conformation of taste receptor type 1 member 1 (left) and the open conformation of taste receptor type 1 member 3 (right). The dashed line represents a hydrogen bond between ligands and T1R1/T1R3 residu

Appendix B: Unraveling the Effects of Drying Techniques on Chaya Leaves: Metabolomics Analysis of Nonvolatile and Volatile Metabolites, Umami Taste, and Antioxidant Capacity

Table B1 Annotation data for volatile metabolites from HS-GC/MS analysis.

Category	Compound	Threshold[a] (ug/kg, ppb)	RT[b] (min)	RI$_t$[c]	RI$_c$[d]	SI[e]	Formula	Mass fragment
Alcohol	1-Penten-3-ol	400	4.23	723	680	83	$C_5H_{10}O$	84,71,57,55,29
	(R,R)-Butane-2,3-diol	20000	6.68	743	790	95	$C_4H_{10}O_2$	90,75,57,45,29
	(Z)-3-Hexen-1-ol	70	6.73	849	841	90	$C_6H_{12}O$	82,67,55,41,31
	4-Vinylguaiacol	0.4	12.51	1318	1309	93	$C_9H_{10}O_2$	150,135,107, 89,77,63,51
	2-Butyl-1-octanol	N/A	12.59	1327	1360	91	$C_{12}H_{26}O$	113,95,85, 71,57,43, 41,29
	1-Hexadecanol	1100	16.02	1664	1854	97	$C_{16}H_{34}O$	125,111,97, 83,69,55,43,29
Aldehyde	2-Methylpropanal	4.0	2.98	543	543	96	C_4H_8O	72,57,43,41,29
	3-Methylbutanal	1.5	3.89	706	676	98	$C_5H_{10}O$	86,71,58,44,43,41,29
	2-Methylbutanal	12.5	3.98	712	663	98	$C_5H_{10}O$	86,71,58,57,41,29
	Pentanal	12	4.43	733	707	95	$C_5H_{10}O$	58,44,41,29
	Hexanal	4.5	6.20	819	806	95	$C_6H_{12}O$	85,72,56,44,41
	2-Hexenal	30	7.07	868	820	96	$C_6H_{10}O$	97,83,69,55,41,29
	Heptanal	30	7.80	911	905	96	$C_7H_{14}O$	80,60,57,44,41,29
	Octanal	0.7	9.17	1008	1005	95	$C_8H_{16}O$	84,82,56,43,41
	Nonanal	1.4	10.36	1107	1104	94	$C_9H_{18}O$	95,70,57,43,41,29
	2,6,6-Trimethyl-1-cyclohexene-1-carboxaldehyde	5	11.64	1229	1204	87	$C_{10}H_{16}O$	152,137,123,109,95.8167,43,41,29
Ketone	2-Butanone	7000	3.12	671	655	92	C_4H_8O	72,57,43,38,29
	2,3-Butanedione	20	3.21	676	691	91	$C_4H_6O_2$	86,72,57,43,41,29
	1-Hydroxy-2-Propanone	80000	5.20	769	698	95	$C_3H_6O_2$	74,61,43,31,29
	Heptane-2,3-dione	N/A	6.66	845	869	93	$C_7H_{12}O_2$	85,72,57,43,31,29
	2-Heptanone	140	7.52	893	898	94	$C_7H_{14}O$	114,99,85,71,58,43,41,29
	1-(2-Furanyl)-1-propanone	N/A	7.55	895	977	80	$C_7H_8O_2$	124,109,95,81,57,43,41,29
	3-(Hydroxy-phenyl-methyl)-2,3-dimethyl-octan-4-one	N/A	8.62	968	984	81	$C_{17}H_{26}O_2$	114,95,85,71,58,43,41,29
	6-Methyl-5-hepten-2-one	50	8.92	989	938	94	$C_7H_{14}O$	108,93,71,69,43,41,29
	2,2,6-Trimethylcyclohexanone	310	9.59	1043	1086	87	$C_9H_{16}O$	140,127,111,97,82,69,55,41,29
	2,3-Dihydro-3,5-dihydroxy-6-methyl-4H-Pyran-4-one	35000	10.85	1153	1178	91	$C_6H_8O_4$	144,128,112,101,83,72,56,43,29
Aromatic	Toluene	1000	5.61	788	794	97	C_7H_8	91,71,65,51,39,29
	Ethylbenzene	200	7.18	874	893	92	C_8H_{10}	106,103,91,77,71,65,51,39,31
	o-Xylene	1800	7.32	882	907	94	C_8H_{10}	106,91,77,65,51,39,32
	3,5-Dimethylphenol	5000	8.18	937	1127	89	$C_8H_{10}O$	122,107,91,79,69,39,31
	1,3-bis(1,1-Dimethylethyl)benzene	50	11.89	1254	1334	88	$C_{14}H_{22}$	190,175,159, 147,131,119,105,91,57
	3,5-bis(1,1-Dimethylethyl)phenol	50	14.15	1510	1555	82	$C_{14}H_{22}O$	205,191,177,163,145, 128,115,57,41,29
Heterocyclic	2-Methylfuran	3500	2.75	654	642	90	C_5H_6O	82,81,69, 53,39,29
	2,5-Dimethylfuran	100	4.10	717	703	95	C_6H_8O	98,96,81,65,53,43,39,33
	1-Methyl-1H-pyrrole	48900	4.71	746	677	95	C_5H_7N	81,66,53,39,30
	2,4-Dimethylfuran	N/A	4.71	746	732	88	C_6H_8O	98,96,83,67,41,29
	1-Ethyl-1H-pyrrole	N/A	6.16	817	776	93	C_6H_9N	95,80,67,53,41,29
	2,5-Dimethylpyrazine	1700	7.36	884	894	86	$C_6H_8N_2$	108,91,79,66,43,39,30
	1-Butyl-1H-pyrrole	N/A	8.37	950	975	86	$C_8H_{13}N$	123,108,85,80,68,53,41,29
Ether	Decyl heptyl ether	N/A	11.31	1196	1209	91	$C_{19}H_{40}O$	139,113,98,85,71,57,43,41,29
	Eicosyl octyl ether	N/A	11.82	1247	1292	93	$C_{28}H_{58}O$	168,155,141,127,113,99,85,71,57,43

	Dodecyl heptyl ether	N/A	13.36	1412	1467	93	$C_{19}H_{40}O$	169,154,141,127,112,99,85,71,57,43,31
Others	Diisobutyl cellosolve	90	2.78	655	667	92	$C_{10}H_{22}O_2$	101,86,71,58,43,39,29
	Isobutyronitrile	64	2.83	658	600	95	C_4H_7N	68,42,41,29
	Acetic acid	60000	3.17	674	621	95	$C_2H_4O_2$	60,43,30
	N,N-Dimethylmethylamine	198	4.14	701	703	93	C_3H_9N	58,42,30
	(Z)-3-Hexen-1-ol-formate	N/A	8.05	928	969	95	$C_7H_{12}O_2$	82,67,55,41,29
	Methylhexanoate	87	8.11	932	922	92	$C_7H_{14}O_2$	99,87,74,57,43,41,29
	Limonene	10	9.52	1037	1030	94	$C_{10}H_{16}$	136,121,107,93,79,68,53,39,29
	Triethyl phosphate	N/A	10.52	1122	1122	95	$C_6H_{15}O_4P$	155,127,125,99,91,81,65,45,31,29
	Oxalic acid, dodecyl isohexyl ester	N/A	11.46	1210	1250	86	$C_{20}H_{38}O_4$	111,85,71,57,43,41,29
	Sulfurous acid, butyl heptadecyl ester	N/A	12.44	1310	1333	89	$C_{21}H_{44}O_3S$	111,85,71,57,41,29
	Caryophyllene	64	13.59	1441	1494	94	$C_{15}H_{24}$	161,147,133,120,105,93,79,69,55,41

[a] Threshold of volatile compounds were obtained from a textbook named compilations of odor threshold values in air, water and other media (second enlarged and revised edition)

[b] RT: retention time

[c] RI_t: the theoretical retention index in the NIST17 library

[d] RI_c: the calculated retention index

[e] SI: similarity index (score out of 100)
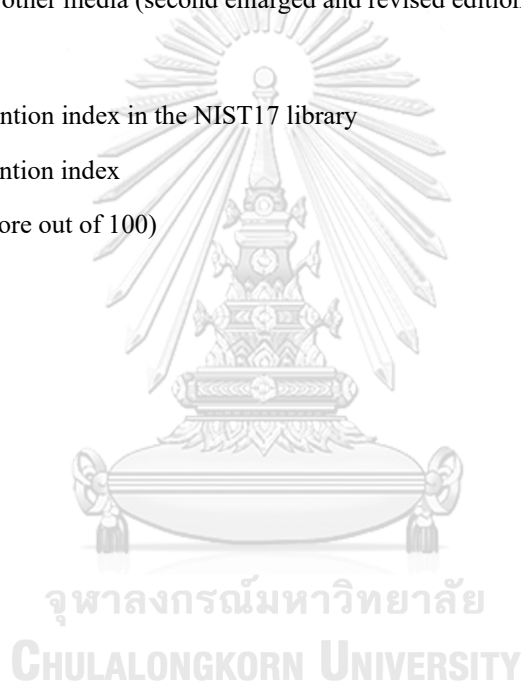
Table B2 Mean value of relative concentration of annotated volatile metabolites analyzed using HS-GC/MS, in chaya leaf samples dried with different drying methods: freeze drying (FD), vacuum drying (VD), oven drying at 50°C (OD50), oven drying at 120°C (OD120) and pan roasting (PR).

Category	Compound	Average relative concentration (ppb)				
		FD	VD	OD50	OD120	PR
Alcohol	1-Penten-3-ol	45.5	0.0	11.5	0.0	0.0
	(R,R)-Butane-2,3-diol	353.5	965.3	224.5	0.0	0.0
	(Z)-3-Hexen-1-ol	170.8	0.0	0.0	53.6	0.0
	4-Vinylguaiacol	0.0	0.0	0.0	0.0	212.0
	2-Butyl-1-octanol	8.4	3.2	7.7	6.1	5.6
	1-Hexadecanol	24.9	0.0	0.0	0.0	0.0
	total	**603.2**	**968.5**	**243.7**	**59.8**	**217.7**
Aldehyde	2-Methylpropanal	1073.7	0.0	834.0	84.6	0.0
	3-Methylbutanal	4364.8	7755.2	7928.1	7092.3	4372.1
	2-Methylbutanal	2295.7	2691.2	4013.1	6695.5	5245.7
	Pentanal	752.4	631.3	970.5	1503.4	1418.0
	Hexanal	1490.7	706.7	1072.1	1024.7	874.3
	2-Hexenal	4062.5	457.1	1368.3	601.3	216.3
	Heptanal	358.9	226.7	410.4	849.1	495.5
	Octanal	166.0	59.0	138.0	80.5	117.1
	Nonanal	367.1	0.0	435.3	0.0	0.0
	2,6,6-Trimethyl-1-cyclohexene-1-carboxaldehyde	29.6	28.6	40.0	40.5	33.9
	total	**14961.4**	**12555.9**	**17209.9**	**17971.9**	**12773.0**
Ketone	2-Butanone	201.8	0.0	165.1	89.4	32.2
	2,3-Butanedione	436.8	0.0	0.0	0.0	0.0
	1-Hydroxy-2-Propanone	66.6	111.6	156.7	269.3	847.8
	Heptane-2,3-dione	0.0	0.0	0.0	12.8	61.0
	Heptan-2-one	0.0	52.9	46.1	288.5	297.2
	1-(2-Furanyl)-1-propanone	42.7	20.1	0.0	0.0	0.0
	3-(Hydroxy-phenyl-methyl)-2,3-dimethyl-octan-4-one	0.0	0.0	0.0	279.5	400.7
	6-Methyl-5-hepten-2-one	177.8	213.3	266.8	290.4	323.7
	2,2,6-Trimethylcyclohexanone	92.1	72.9	0.0	95.6	80.5

	2,3-Dihydro-3,5-dihydroxy-6-methyl-4H-Pyran-4-one	0.0	0.0	0.0	0.0	158.4
	total	**1018.0**	**470.9**	**634.6**	**1325.5**	**2201.4**
Aromatic	Toluene	142.9	236.9	131.7	710.7	1100.0
	Ethylbenzene	1.7	12.5	39.1	58.1	151.1
	o-Xylene	91.8	8.4	55.2	263.9	634.9
	3,5-Dimethylphenol	0.0	0.0	20.1	110.8	140.7
	1,3-bis(1,1-Dimethylethyl)benzene	192.4	152.6	209.0	202.0	168.4
	3,5-bis(1,1-Dimethylethyl)phenol	22.9	21.8	30.4	42.0	46.6
	total	**451.6**	**432.2**	**485.5**	**1387.4**	**2241.7**
Heterocyclic	2-Methylfuran	29.3	0.0	0.0	1.4	93.5
	2,5-Dimethylfuran	58.6	11.6	7.0	2.3	45.7
	1-Methyl-1H-pyrrole	72.4	0.0	0.0	631.5	1896.9
	2,4-Dimethylfuran	171.4	211.1	20.3	62.1	41.6
	1-Ethyl-1H-pyrrole	0.0	0.0	0.0	114.0	525.2
	2,5-Dimethylpyrazine	0.0	0.0	0.0	0.0	386.8
	1-Butyl-1H-pyrrole	0.0	0.0	0.0	0.0	105.2
	total	**331.6**	**222.7**	**27.3**	**811.4**	**3094.8**
Ether	Decyl heptyl ether	30.9	24.2	45.4	38.4	31.0
	Eicosyl octyl ether	50.7	33.4	49.6	59.4	41.9
	Dodecyl heptyl ether	14.0	9.9	11.3	14.0	12.3
	total	**95.6**	**67.5**	**106.3**	**111.7**	**85.2**
Others	Diisobutyl cellosolve	1518.1	0.0	0.0	0.0	0.0
	Isobutyronitrile	0.0	0.0	0.0	387.3	455.7
	Acetic acid	323.4	1328.2	763.3	1205.3	1631.5
	N,N-Dimethylmethylamine	19.5	0.0	0.0	0.0	162.0
	(*Z*)-3-Hexen-1-ol-formate	32.0	0.0	13.0	0.0	0.0
	Methylhexanoate	35.9	0.0	17.5	0.0	0.0
	Limonene	56.3	16.4	0.0	6.8	37.3
	Triethyl phosphate	166.4	137.5	0.0	0.0	0.0
	Oxalic acid, dodecyl isohexyl ester	54.0	44.8	53.1	92.5	117.8
	Sulfurous acid, butyl heptadecyl ester	18.4	8.1	10.5	17.2	20.1
	Caryophyllene	10.9	1.3	14.1	10.2	0.0
	total	**2235.0**	**1536.2**	**871.4**	**1719.5**	**2424.5**

Table B3 Mean odor active values (OAV) of volatile metabolites in chaya leaf samples dried with different methods: freeze drying (FD), vacuum drying (VD), oven drying at 50°C (OD50), oven drying at 120°C (OD120), and pan roasting (PR).

Category	Compound	Threshold[a] (µg/kg ,ppb)	OAV				
			FD	VD	OD50	OD120	PR
Alcohol	1-Penten-3-ol	400	0.1	0.0	0.0	0.0	0.0
	(R,R)-Butane-2,3-diol	20000	<0.1	<0.1	<0.1	0.0	0.0
	(Z)-3-Hexen-1-ol	70	2.4	0.0	0.0	0.8	0.0
	4-Vinylguaiacol	0.4	0.0	0.0	0.0	0.0	530.1
	2-Butyl-1-octanol	N/A	N/A	N/A	N/A	N/A	N/A
	1-Hexadecanol	1100	<0.1	0.0	0.0	0.0	0.0
Aldehyde	2-Methylpropanal	4	268.4	0.0	208.5	21.1	0.0
	3-Methylbutanal	0.2	2909.9	5170.1	5285.4	4728.2	2914.7
	2-Methylbutanal	12.5	183.7	215.3	321.1	535.6	419.7
	Pentanal	12.0	62.7	52.6	80.9	125.3	118.2
	Hexanal	4.5	331.3	157.0	238.3	227.7	194.3
	2-Hexenal	30	135.4	15.2	45.6	20.0	7.2
	Heptanal	30	12.0	7.6	13.7	28.3	16.5
	Octanal	0.7	237.1	84.3	197.2	115.0	167.2
	Nonanal	1.4	262.2	0	310.9	0.0	0.0
	2,6,6-Trimethyl-1-cyclohexene-1-carboxaldehyde	5.0	5.9	5.7	8.0	8.1	6.8
Ketone	2-Butanone	7000	<0.1	0.0	<0.1	<0.1	<0.1
	2,3-Butanedione	20	21.8	0.0	0.0	0.0	0.0
	1-Hydroxy-2-Propanone	80000	0.0	0.0	0.0	0.0	0.0
	Heptane-2,3-dione	N/A	N/A	N/A	N/A	N/A	N/A
	Heptan-2-one	140	0.0	0.4	0.3	2.1	2.1
	1-(2-Furanyl)-1-propanone	N/A	N/A	N/A	N/A	N/A	N/A
	3-(Hydroxy-phenyl-methyl)-2,3-dimethyl-octan-4-one	N/A	N/A	N/A	N/A	N/A	N/A
	6-Methyl-5-hepten-2-one	50.0	3.6	4.3	5.3	5.8	6.5
	2,2,6-Trimethylcyclohexanone	310.0	0.3	0.2	0.0	0.3	0.3
	2,3-Dihydro-3,5-dihydroxy-6-methyl-4H-pyran-4-one	35000	0.0	0.0	0.0	0.0	0.0
Aromatic	Toluene	1000	0.1	0.2	0.1	0.7	1.1
	Ethylbenzene	200	0.0	0.1	0.2	0.3	0.8
	o-Xylene	1800	0.1	0.0	0.0	0.1	0.4
	3,5-Dimethylphenol	5000	0.0	0.0	<0.1	<0.1	<0.1
	1,3-bis(1,1-Dimethylethyl)benzene	50	3.8	3.1	4.2	4.0	3.4
	3,5-bis(1,1-Dimethylethyl)phenol	50	0.5	0.4	0.6	0.8	0.9
Heterocyclic	2-Methylfuran	<0.1	0.0	0.0	0.0	<0.1	0.0
	2,5-Dimethylfuran	0.586	0.6	0.1	0.1	0.0	0.5
	1-Methyl-1H-pyrrole	<0.1	0.0	0.0	0.0	0.0	0.0

	2,4-Dimethylfuran	N/A	N/A	N/A	N/A	N/A	N/A
	1-Ethyl-1H-pyrrole	N/A	N/A	N/A	N/A	N/A	N/A
	2,5-Dimethylpyrazine	0.0	0.0	0.0	0.0	0.0	0.2
	1-Butyl-1H-pyrrole	N/A	N/A	N/A	N/A	N/A	N/A
Ether	Decyl Heptyl ether	N/A	N/A	N/A	N/A	N/A	N/A
	Eicosyl octyl ether	N/A	N/A	N/A	N/A	N/A	N/A
	Dodecyl heptyl ether	N/A	N/A	N/A	N/A	N/A	N/A
Others	Diisobutyl cellosolve	90.0	16.9	0.0	0.0	0.0	0.0
	Isobutyronitrile	64.0	0.0	0.0	0.0	6.1	7.1
	Acetic acid	60000.0	<0.1	<0.1	<0.1	<0.1	<0.1
	N,N-Dimethylmethylamine	198.0	<0.1	0.0	0.0	0.0	0.8
	(Z)-3-Hexen-1-ol-formate	N/A	N/A	N/A	N/A	N/A	N/A
	Methylhexanoate	87.0	0.4	0.0	0.2	0.0	0.0
	Limonene	10.0	5.6	1.6	0.0	0.7	3.7
	Triethyl phosphate	N/A	N/A	N/A	N/A	N/A	N/A
	Oxalic acid, dodecyl isohexyl ester	N/A	N/A	N/A	N/A	N/A	N/A
	Sulfurous acid, butyl heptadecyl ester	N/A	N/A	N/A	N/A	N/A	N/A
	Caryophyllene	64.0	0.2	<0.1	0.2	0.2	0.0

[a] Threshold of volatile compounds were obtained from Gemert (2011)

Table B4 Annotation data for nonvolatile metabolites from UHPLC-qTOF/MS analytical platforms

Category	Annotated compound	RT	m/z	Adduct	Formula	Error (mDa)	Mass fragment
Amino acid	L-Arginine	0.758	175.118	[M+H]+	$C_6H_{14}N_4O_2$	1.1521	70.0647, 116.095
	L-Serine	0.776	106.050	[M+H]+	$C_3H_7NO_3$	0.3695	60.0441
	L-Alanine	0.794	90.055	[M+H]+	$C_3H_7NO_2$	-0.0351	90.05499
	L-Asparagine	0.794	133.061	[M+H]+	$C_4H_8N_2O_3$	0.0686	72.0423, 70.0294
	L-Aspartic acid	0.812	134.044	[M+H]+	$C_4H_7NO_4$	0.8842	88.0393, 74.0234, 70.0287
	L-Threonine	0.812	120.066	[M+H]+	$C_4H_9NO_3$	-0.2804	75.0597, 56.0495
	L-Glutamine	0.812	147.077	[M+H]+	$C_5H_{10}N_2O_3$	-0.0814	130.0493, 84.0446, 56.0509
	L-Glutamic acid	0.830	148.061	[M+H]+	$C_5H_9NO_4$	-0.5658	102.0547, 84.0446, 56.0495
	L-Proline	0.940	116.070	[M+H]+	$C_5H_9NO_2$	1.1050	70.0647, 53.0382
	L-Valine	1.147	118.085	[M+H]+	$C_3H_7NO_2$	1.1550	72.0803, 55.0533, 53.0382
	L-Methionine	1.444	150.058	[M+H]+	$C_5H_{11}NO_2S$	0.6260	113.0311, 104.0537, 74.0234, 61.0098, 86.0959, 69.0691, 56.0495
	L-Isoleucine	2.099	132.100	[M+H]+	$C_6H_{13}NO_2$	1.8051	165.0543, 119.0494, 91.0547, 77.0381,
	L-Tyrosine	2.165	182.079	[M+H]+	$C_9H_{11}NO_3$	2.3697	65.0389
	L-Leucine	2.303	132.102	[M+H]+	$C_6H_{13}NO_2$	-0.2949	86.0959, 69.0691, 56.0495 120.0799, 103.0537, 91.0547, 77.0381,
	L-Phenylalanine	5.651	166.083	[M+H]+	$C_9H_{11}NO_2$	3.3550	51.0241
	L-Tryptophan	8.595	205.097	[M+H]+	$C_{11}H_{12}N_2O_2$	0.0541	170.0596, 146.0598, 118.0652, 91.0547
Peptide	Lys-Leu	0.867	260.197	[M+H]+	$C_{13}H_{26}NO_4$	0.1681	147.1121, 130.0869, 84.0799, 69.0676
	Val-Gln	1.063	246.145	[M+H]+	$C_{10}H_{19}N_3O_4$	-0.2675	147.0765, 130.0493, 84.0446, 72.0843, 56.0536
	gamma-Glu-Val	1.374	247.127	[M+H]+	$C_{15}H_{18}O_3$	1.8481	168.9162, 148.061, 102.0547, 84.0466, 72.0803, 55.0547
	Ala-Leu-Val-Ser	1.409	389.239	[M+H]+	$C_{21}H_{34}O_4$	0.0612	371.2284, 260.1967, 215.1374, 130.0869, 84.0816
	Gly-Val	1.444	175.108	[M+H]+	$C_7H_{14}N_2O_3$	-0.3812	72.0803, 57.0588, 55.056
	Glutathione (reduced)	1.621	308.090	[M+H]+	$C_{10}H_{17}N_3O_6S$	0.8827	162.0226, 116.0161, 84.0446
	Val-Ser	1.726	246.145	[M+ACN]	$C_8H_{16}N_2O_4$	-0.2675	143.1188, 83.0625, 72.0818, 55.0574

Category	Name		m/z	[M+H]+	Formula		Fragments
	Arg-Leu	2.038	288.202	[M+H]+	$C_{16}H_{21}NO_2$	1.4161	175.1202, 158.0932, 116.0695, 76.0647
	Leu-Asp	2.234	247.127	[M+H]+	$C_{10}H_{18}N_2O_5$	1.8481	85.0959
	Ile-Gln	2.389	260.161	[M+H]+	$C_{16}H_{21}NO_2$	3.3054	143.1166, 72.0803
	gamma-Glu-Tyr	2.570	311.123	[M+H]+	$C_{14}H_{18}N_2O_6$	3.1043	309.2866, 136.0745, 91.0547
	Ala-Tyr	2.633	253.118	[M+H]+	$C_{27}H_{31}NO_6$	2.7840	136.0745, 119.0474, 107.0469, 91.0547
	Arg-Phe	2.905	322.186	[M+H]+	$C_{15}H_{23}N_5O_3$	1.1660	322.1862, 175.1202, 120.0819, 72.7303
	Gly-Tyr	2.939	239.103	[M+H]+	$C_{11}H_{14}N_2O_4$	0.1334	136.0767, 119.0494, 91.0547, 65.0398
	Ala-Ile	3.111	203.138	[M+H]+	$C_9H_{18}N_2O_3$	1.3189	86.0959, 53.669
	Ile-Glu	3.140	261.144	[M+H]+	$C_{11}H_{20}N_2O_5$	0.5982	148.061, 130.0493, 102.0547, 86.0959
	Glutathione (oxidized)	3.180	307.083	[M+H]+	$C_{15}H_{14}O_7$	-1.4451	179.046, 136.0382, 113.0357, 98.9831, 80.9736
	Val-Val	3.558	217.154	[M+H]+	$C_{10}H_{20}N_2O_3$	0.9690	101.0588, 72.0803, 55.0546
	Gly-Ile	3.597	189.123	[M+H]+	$C_8H_{16}N_2O_3$	0.8688	86.0959, 69.0676
	Leu-Gly-Pro	3.720	286.176	[M+H]+	$C_{18}H_{20}O_2$	4.3554	169.1331, 70.0631
	Thr-Leu	5.651	233.149	[M+H]+	$C_{10}H_{20}N_2O_4$	0.1836	132.1001, 101.0717, 86.0976, 74.0597, 133.0311, 104.0519, 84.0466, 72.0803,
	Val-Met	6.096	249.126	[M+H]+	$C_{12}H_{16}N_4O_2$	-2.2312	55.0587
	Glu-Ile-Ser	6.833	348.176	[M+H]+	$C_{19}H_{22}O_5$	0.3266	173.129, 128.1078, 86.0959
	Leu-Asp-Gln	6.961	375.189	[M+H]+	$C_{15}H_{26}N_4O_7$	-1.0744	357.1733, 183.1144, 61.047
	Leu-Val-Gly	7.785	288.192	[M+H]+	$C_{18}H_{25}NO_2$	-0.5173	185.1646, 158.0909, 86.0959
	Leu-Pro	8.461	229.155	[M+H]+	$C_{11}H_{20}N2O_3$	-0.1310	116.0695, 86.0959, 70.0662
Sugar	Gentiobiose	1.082	381.082	[M+H]+	$C_{12}H_{22}O_{11}$	-1.3785	363.1862, 110.0709
	Sucrose	1.063	365.104	[M+Na]+	$C_{12}H_{22}O_{11}$	1.9322	365.1036, 203.0541, 185.0450
Nucleotide-related	cCMP	1.132	306.047	[M+H]+	$C_9H_{12}N_3O_7P$	1.7628	178.061, 112.0495, 95.0249
	5'-CMP	1.587	324.058	[M+H]+	$C_9H_{14}N_3O_8P$	0.9275	112.0515, 95.0249, 85.0308
	5'-AMP	1.708	348.070	[M+H]+	$C_{10}H_{14}N_5O_7P$	0.1609	136.0617, 119.0354, 97.0282
	5'-GMP	2.304	364.064	[M+H]+	$C_{10}H_{14}N_5O_8P$	-2.0245	152.0588, 135.0328, 110.0344
	Uracil	2.836	113.034	[M+H]+	$C_4H_4N_2O_2$	0.8538	96.0551, 70.0294
	Adenine	4.290	136.062	[M+H]+	$C_5H_5N_5$	0.0716	136.0617, 119.0354, 92.0231, 82.0396, 65.0132

	Adenosine	4.290	268.099	[M+H]+	C$_{10}$H$_{13}$N$_5$O$_4$	4.8303	268.0992, 136.0617, 119.0354, 109.0499, 94.0391
	cAMP	4.630	330.060	[M+H]+	C$_{10}$H$_{12}$N$_5$O$_6$P	-0.1038	330.0599, 202.0729, 136.0617, 119.0354
	Deoxyadenosine	4.728	252.109	[M+H]+	C$_{10}$H$_{13}$N$_5$O$_3$	-0.2843	136.0617, 119.0354, 92.0231
	Guanosine	5.785	284.098	[M+H]+	C$_{10}$H$_{13}$N$_5$O$_5$	0.6450	152.0565, 135.0306, 110.0344, 82.0396, 55.0315
	Guanine	5.797	152.057	[M+H]+	C$_5$H$_5$N$_5$O	0.1862	152.0565, 135.0306, 110.0344, 80.0244, 55.0302
	cGMP	7.834	346.055	[M+H]+	C$_{10}$H$_{12}$N$_5$O$_7$P	0.3765	152.0565, 135.0506, 110.0344, 80.026
Alkaloid	Theobromine	0.867	219.027	[M+H]+	C$_5$H$_{11}$NO$_2$S	4.7709	148.061, 84.0446
	Trigonelline	0.922	138.056	[M+H]+	C$_7$H$_7$NO$_2$	-0.8451	138.0536, 96.0640, 92.0494, 78.0343, 77.0252
Organic acid	Quinic acid	0.993	193.071	[M+H]+	C$_7$H$_{12}$O$_6$	-0.7354	129.0517, 111.0445, 83.0491, 65.0398
	L-ascorbic acid	1.287	177.040	[M+H]+	C$_6$H$_8$O$_6$	-0.4356	111.0058, 95.1024, 85.0274, 67.1083
	3-Hydroxycinnamic acid	2.165	165.054	[M+H]+	C$_9$H$_8$O$_3$	0.3206	119.0474, 91.0547, 77.0381, 51.0214
Flavonoid	Rutin	9.812	611.158	[M+H]+	C$_{12}$H$_{34}$N$_8$O$_{16}$S$_2$	2.3955	465.0986, 303.0487, 229.0465, 153.0212
	Robinin	10.220	741.221	[M+H]+	C$_{33}$H$_{40}$O$_{19}$	3.1555	595.1685, 449.1093, 443.1097, 397.0921, 353.0617, 287.1847, 239.0912, 147.0632, 129.0580
	Biorobin	11.264	595.164	[M+H]+	C$_{27}$H$_{30}$O$_{15}$	1.7467	287.0542
	Nicotiflorin	11.756	595.164	[M+H]+	C$_{27}$H$_{30}$O$_{15}$	1.7467	287.0573

Table B5 Mean value of normalized peak area (n = 4) of annotated metabolites analyzed via ultra-high performance liquid chromatography–quadrupole time-of-flight mass spectrometry in chaya leaves dried using different drying methods: freeze drying (FD), vacuum drying (VD), oven drying at 50°C (OD50), oven drying at 120°C, and pan roasting (PR).

Category	Annotated compounds	Mean value of normalized peak area				
		FD	VD	OD50	OD120	PR
Amino acid	L-Arginine	1.38	1.46	0.94	0.98	0.63
	L-Serine	0.19	0.08	0.08	0.12	0.09
	L-Alanine	0.43	0.75	0.54	0.13	0.09
	L-Asparagine	0.25	0.15	0.30	0.15	0.13
	L-Valine	2.07	2.09	1.99	0.61	0.43
	L-Glutamic acid	1.91	0.51	0.74	1.79	2.08
	L-Aspartic acid	0.47	0.16	0.13	0.69	0.70
	L-Threonine	0.45	0.45	0.45	0.32	0.28
	L-Glutamine	0.66	0.18	0.22	0.22	0.12
	L-Tyrosine	6.25	7.04	5.57	1.06	0.73
	L-Proline	0.88	1.16	0.85	0.28	0.14
	L-Methionine	2.09	2.17	1.04	0.23	0.10
	L-Leucine	5.78	6.49	5.03	1.17	0.74
	L-Phenylalanine	15.30	16.60	12.99	2.59	1.33
	L-Isoleucine	2.89	2.95	3.14	0.90	0.68
	L-Tryptophan	1.69	2.40	2.21	0.47	0.37
Peptide	gamma-Glu-Val	1.67	2.72	0.96	0.55	0.21
	gamma-Glu-Tyr	0.75	0.88	0.29	0.17	0.02
	Glutathione (reduced)	1.83	0.00	0.00	0.00	0.00
	Glutathione (oxidized)	2.28	0.00	3.20	2.69	2.81
	Lys-Leu	1.05	0.78	0.41	0.23	0.06
	Val-Gln	0.80	0.84	0.31	0.09	0.07
	Gly-Val	1.14	0.96	0.48	0.28	0.10
	Arg-Leu	1.75	0.92	0.90	0.49	0.31
	Ala-Tyr	0.70	0.69	0.40	0.42	0.12
	Val-Ser	0.78	0.72	0.60	0.24	0.13
	Arg-Phe	1.08	2.22	0.87	0.41	0.14
	Gly-Tyr	1.02	1.53	0.55	0.25	0.09
	Ala-Ile	4.35	4.00	2.85	2.18	0.81
	Ile-Glu	7.23	7.16	4.00	3.35	1.22
	Gly-Ile	5.27	4.30	2.69	1.61	0.51
	Thr-Leu	1.77	2.48	1.04	0.08	0.20
	Leu-Asp	1.11	1.23	0.73	0.87	0.33
	Val-Val	1.76	1.43	0.69	0.07	0.00
	Ile-Gln	2.11	1.99	1.05	0.68	0.18
	Leu-Pro	1.53	2.40	0.74	0.00	0.00
	Glu-Ile-Ser	1.14	1.25	0.53	0.32	0.00
	Leu-Asp-Gln	0.46	0.55	0.15	0.07	0.00

	Leu-Gly-Pro	0.20	0.21	0.00	0.00	0.00
	Leu-Val-Gly	1.07	1.54	0.40	0.00	0.00
	Ala-Leu-Val-Ser	1.16	1.59	0.68	0.21	0.11
Sugar	Sucrose	0.36	0.25	0.37	0.51	0.60
	Gentiobiose	0.61	3.26	0.50	0.48	5.33
Nucleotide-related	5'-AMP	1.85	0.58	1.97	6.77	5.08
	5'-CMP	0.22	0.73	0.20	0.17	0.05
	5'-GMP	0.50	0.92	0.57	1.35	0.68
	cAMP	5.53	7.47	4.40	0.63	1.08
	cCMP	0.75	0.97	0.42	0.10	0.14
	cGMP	5.12	6.33	2.98	0.24	0.74
	Adenine	1.55	2.33	2.12	1.14	0.46
	Adenosine	17.82	20.57	18.21	14.21	9.89
	Deoxyadenosine	0.90	0.96	0.37	0.19	0.11
	Guanine	4.15	7.84	6.91	0.81	0.12
	Guanosine	8.58	14.84	13.74	2.74	1.88
	Uracil	0.82	1.19	1.01	0.22	0.20
Alkaloid	Trigonelline	5.02	3.76	5.12	3.92	4.97
	Theobromine	0.60	0.45	0.42	0.22	0.28
Organic acid	Quinic acid	0.54	0.58	0.67	0.64	0.66
	L-ascorbic acid	0.78	0.00	0.00	0.00	0.00
	3-Hydroxycinnamic acid	1.37	2.03	1.33	0.23	0.15
Flavonoid	Rutin	0.24	0.24	0.11	0.21	0.25
	Robinin	4.51	4.11	4.50	4.11	2.63
	Biorobin	1.08	0.89	1.26	1.11	0.90
	Nicotiflorin	1.19	0.94	1.66	1.31	0.92

Table B6 Pearson's correlation analysis for total phenolic content (TPC) and
antioxidant activities analyzed using the DPPH and FRAP assays.

variables	TPC	DPPH	FRAP
TPC	1		
DPPH	0.54	1	
FRAP	0.44	0.99	1

Figure B1 Representative images of chaya leaf samples dried using different methods: freeze drying (FD), vacuum drying (VD), oven drying at 50ºC (OD50), oven drying at 120ºC (OD120), and pan roasting (PR).
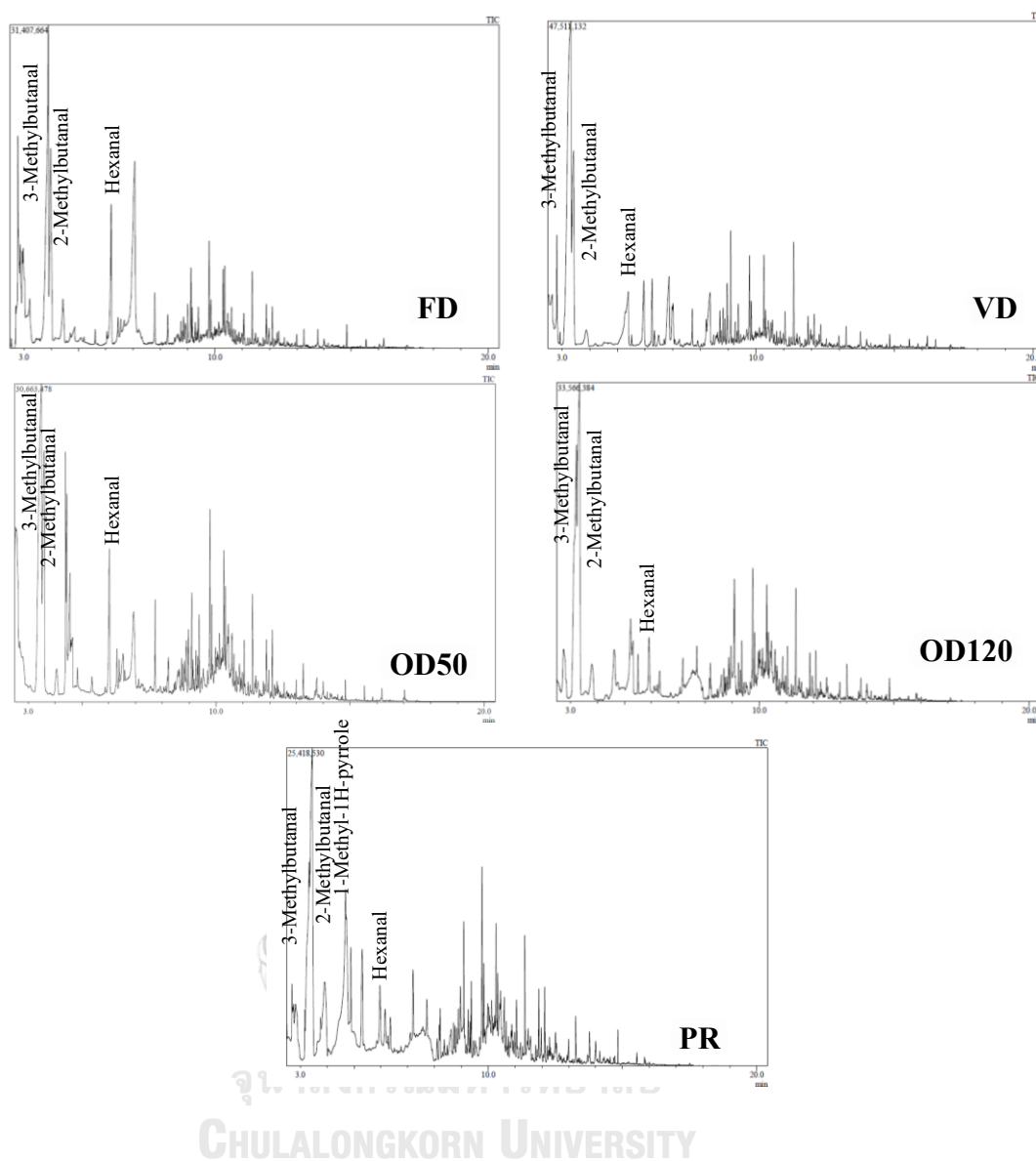
Figure B2 HS-GC/MS total ion chromatograms of chaya leaves dried using different drying methods: freeze drying (FD), vacuum drying (VD), oven drying at 50ºC (OD50), oven drying at 120ºC (OD120), and pan roasting (PR).
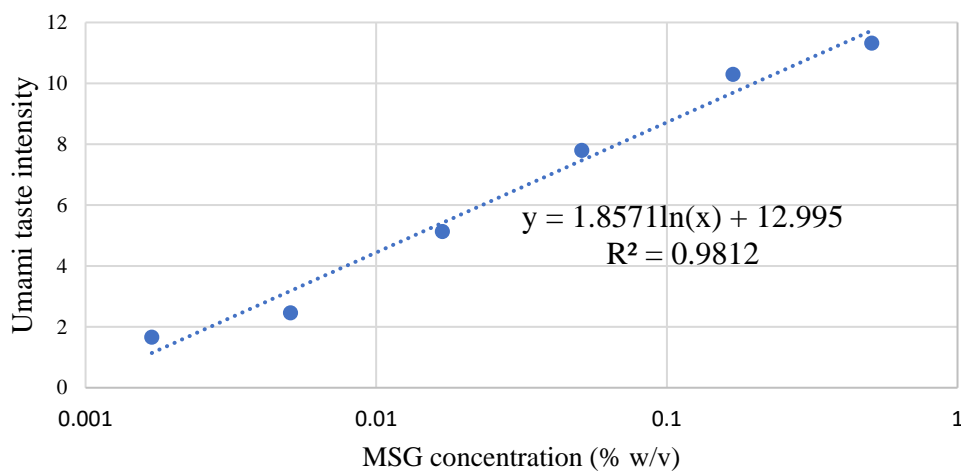
Figure B3 Standard curve of umami taste intensity measured using an electronic tongue (TS-5000Z Taste Sensing System). Umami taste intensity values were obtained from MSG concentrations of 0.1–30 mM [0.0017–0.5073% (w/v)].

REFERENCES

VITA

NAME   Nuti Hutasingh

DATE OF BIRTH   21 June 1994

PLACE OF BIRTH   Bangkok, Thailand

INSTITUTIONS ATTENDED   Chulalongkorn University
AgroParisTech
TU Dublin
Lund University

HOME ADDRESS   363, Ladprao 101, Khlongchaokunsingh, Wangthonglang, Bangkok, 10310

PUBLICATION   Hutasingh, N., Chuntakaruk, H., Tubtimrattana, A., Ketngamkum, Y., Pewlong, P., Phaonakrop, N., Roytrakul, S., Rungrotmongkol, T., Paemanee, A., Tansrisawad, N., Siripatrawan, U. & Sirikantaramas, S. (2023). Metabolite profiling and identification of novel umami compounds in the chaya leaves of two species using multiplatform metabolomics, Food Chemistry, 404, 134564.

AWARD RECEIVED   2022: Winner, 1st Place, APEC Future Food for Sustainability 2022 (from 2018 contestants)
2022: Audience Winner & Runner up, Famelab International 2022 (Science communication contest)
2022: Winner, 1st Place, Famelab Thailand 2022 (Science communication contest)
2021: Winner, 1st Place, Proveg Asean Food Innovation Challenge 2021 (International)
2021: The Most Outstanding Graduate Student of Chulalongkorn University
(นิสิตดีเด่นระดับบัณฑิตศึกษา จุฬาลงกรณ์มหาวิทยาลัย ประจำปีการศึกษา 2564)
2017-2019: Recipient of Erasmus Mundus full Scholarship
2016: 1st Place in FoSTAT-Nestle Quiz Bowl (200+ competitors)
2015: The Most Outstanding Undergraduate Student of Chulalongkorn University
(นิสิตดีเด่นระดับปริญญาตรี จุฬาลงกรณ์มหาวิทยาลัย ประจำปีการศึกษา 2564)
2015: The Most Outstanding Student of Faculty of Science
(นิสิตระดับปริญญาตรีดีเด่น รางวัลจุลมงกุฎ เกียรติภูมิวิทยา ประจำปีการศึกษา 2558)
2012-2016: Recipient of Professor Tab Scholarship, the scholarship awarded to students with the highest academic performance in 4 years of undergraduate degree